R.P.I. Technical Report MP-25

A Progress Report for
July 1, 1971 to December 31, 1971

ANALYSIS AND DESIGN OF A CAPSULE LANDING SYSTEM AND SURFACE VEHICLE CONTROL SYSTEM FOR MARS EXPLORATION

National Aeronautics and Space Administration

Grant NGL 33-018-091

Submitted by the Special Projects Committee

D.K. Frederick
P.K. Lashmet
G.N. Sandor
C.N. Shen
E.J. Smith
S.W. Yerazunis

School of Engineering
Rensselaer Polytechnic Institute

ABSTRACT

Investigation of problems related to control of a mobile planetary vehicle according to a systematic plan for the exploration of Mars has been undertaken. Problem areas receiving attention include: overall systems analysis; vehicle configuration and dynamics; toroidal wheel design and evaluation, on-board navigation systems; satellite-vehicle navigation systems; obstacle detection systems; terrain sensing, interpretation and modeling; computer simulation of terrain sensor-path selection systems; and chromatographic systems design concept studies. The specific tasks which have been undertaken are defined and the progress which has been achieved during the period July 1, 1971 to December 31, 1971 is summarized. Projections of the work to be undertaken in certain areas during the period December 31, 1971 to June 30, 1972 are included.

TABLE OF CONTENTS

Analysis and Design of a Capsule Landing System and Surface Vehicle Control System for Mars Exploration

I. Introduction

Current national goals in space exploration include a detailed study and examination of the planet Mars. The effectiveness of Mars exploration missions would be enhanced according to the extent to which the investigative devices which are landed are mobile, to the range of their mobility, and to the ability to control their motion. In order to achieve basic mission objectives, and beyond that, to maximize the return on the commitment of resources to the mission, formidable technical problems must be resolved. The major factor contributing to these problems is the round trip communications time delay between martian and earth control stations which varies from a minimum of about 9 minutes to a maximum of 25 minutes. This time delay imposes stringent requirements on the vehicle, on its control and communication systems and on those systems included on board to make the scientific measurements, in terms of their ability to function autonomously. These systems must be able to operate with a high degree of reliability and must be capable of calling for earth control under appropriate circumstances.

A number of important problems originating with these factors and relating directly the basic mission objectives of an unmanned exploration of Mars have been and are currently being investigate' by a faculty-student project team at Rensselaer Polytechnic Institute with the support of NASA NGL-33-018-091.

This progress report describes the tasks which have been undertaken and documents the progress which has been achieved in the interval July 1, 1971 to December 31, 1971.

II. Definition of Tasks

The delay time in round trip communication between Mars and Earth gives rise to unique problems relevant to martian and/or other planetary explorations. All phases of the mission from landing the capsule in the neighborhood of a desired position to the systematic traversing of the surface and the attendant detection, measurement, and analytical operations must be consummated with a minimum of control and instruction by earth based units. The delay time requires that on board systems capable of making rational decisions be developed and that suitable precautions be taken against potential catastrophic failures. Four major task areas, which are in turn divided into appropriate sub-tasks, have been defined and are listed below.

A. Vehicle Configuration, Control, Dynamics, Systems and Propulsion. The objectives of this task are to investigate problems related to the design of a roving vehicle for Mars exploration with respect to configuration; motion and attitude control; obstacle avoidance; control, information and power systems; and propulsion systems. In addition, the design concepts must accommodate the equipment and instruments required to automate the vehicle and to perform the scientific objectives of the mission.

B. General Systems Analysis. The objective of this task is to develop a framework within which decisions in design involving conflicting requirements can be made rationally and in the context of the whole system and mission. Relationships between alternative mission profiles and specifications and weight, energy and space allocation and management will be sought.

C. Surface Navigation and Path Control. Once the capsule is landed and the roving vehicle is in an operational state, it is necessary that the vehicle can be directed to proceed under remote control from the landing site to specified positions on the martian surface. This task is concerned with the problems of terrain modeling, path selection and navigation between the initial and terminal sites when major terrain features precluding direct paths are to be anticipated. On board decision making capability must be designed to minimize earth control responsibility except in the most adverse circumstances.

D. Chemical Analysis of Specimens. A major objective of martian surface exploration will be to obtain chemical, biochemical or biological information. Most experiments proposed for the mission require a general duty, chromatographic separator prior to chemical analysis by some device. The objective of this task is to generate fundamental data and concepts required to optimize such a chromatographic separator according to the anticipated mission.

III. Summary of Results

Task A. Vehicle Dynamics, Collapsibility and Deployment, Wheel Design, Control and Propulsion

During the past period, a new phase in the development of the RPI-MRV vehicle has been initiated. The first generation model has been completed and tested, Ref. 1. This test series and investigations under Subtask A.2, Collapsibility and Deployment, has revealed deficiencies in the original design. The primary deficiency is the suspension system which produces poor angular payload isolation and makes collapsibility virtually impossible. In addition, the spring rates of the wheels and suspension were too large. A new suspension system is being designed and reported under Subtask A.1. The spring rates will be adjusted in accordance with the results of a mathematical simulation to be initiated February 15, 1972.

More emphasis is being placed on the characteristics of the martian environment. Lunar terrain appears to be a close approximation of the martian surface except for the presence of an atmosphere which may involve winds producing deep sand or dust drifting. The performance of the RPI-MRV under such conditions will be determined by tests. The goal of these tests will be to compare the RPI-MRV design with competing vehicle concepts.

Task A.1. Vehicle Dynamics - M. Rodamaker
Faculty Advisor: Prof. G. N. Sandor

The vehicle dynamics tests which were undertaken early in this

reporting period have revealed some serious deficiencies in the original design.

1. Payload isolation has proved to be poor primarily due to the rigid coupling between the payload and the suspension. This coupling was removed and the payload section suspended by a single-shaft axis. Input disturbances to the rear wheels no longer have a direct path to the payload, but are filtered by the intermediate suspension.

2. In order to continue the tilt-back capability, a new suspension would be needed. The best suspension would seem to be a planar four-bar linkage mounted in the longitudinal-vertical plane. Straight-line vertical motion over the normal suspension travel with motion toward the front of the vehicle at the lower limit of travel would be desirable, but difficulties in synthesizing this suspension have obviated its use so far. A compromise has been made which consists of a swing axle mounted in the longitudinal direction. This suspension is called a powered torsion bar and has many advantages over any previous designs in that it can provide a continuously variable ground clearance and c.g. location in addition to performing the tilt-back maneuver. Three-wheel operation can be performed without tilting the payload section, a feature appealing to the navigation task, so this feature has been renamed the shiftback capability. Schematics of this suspension are shown in Figures 1 and 2.

3. An aerodynamic study is underway to determine the effects of the surface winds on vehicle stability. The new suspension has the capability of raising or lowering the payload to provide an optimum trade-off between ground clearance (obstacle negotiation) and wind stability. Thus, ride height could be varied during the mission depending on local weather and terrain conditions. In addition, the risk of a catastrophic failure while performing the shiftback maneuver could be evaluated in terms of overall mission reliability.

4. One apparent disadvantage of the powered torsion bar suspension is that its motion is not straight-line vertical over the normal operating range. This is generally important only in high speed vehicles. Nevertheless, this problem can be alleviated by using the wheels to best advantage. Specifically, the wheel spring constant should be picked to produce a natural frequency slightly above the highest expected input frequency. This will probably occur at about 10 Hz. which is considerably lower than the present value which is approximately 25 Hz. The wheels can thus provide compliance in whatever direction the input occurs. In effect, the wheels become the primary suspension with the suspension action primarily to provide damping and vary the ride height. Tuning the suspension in this way provides optimum payload isolation.

5. It is easy to show that payload isolation of a large mass is more difficult than for a small mass. Therefore, the motors not needed for payload leveling are being moved to positions

FIGURE 1
ADVANTAGES OF POWERED TORSION BAR

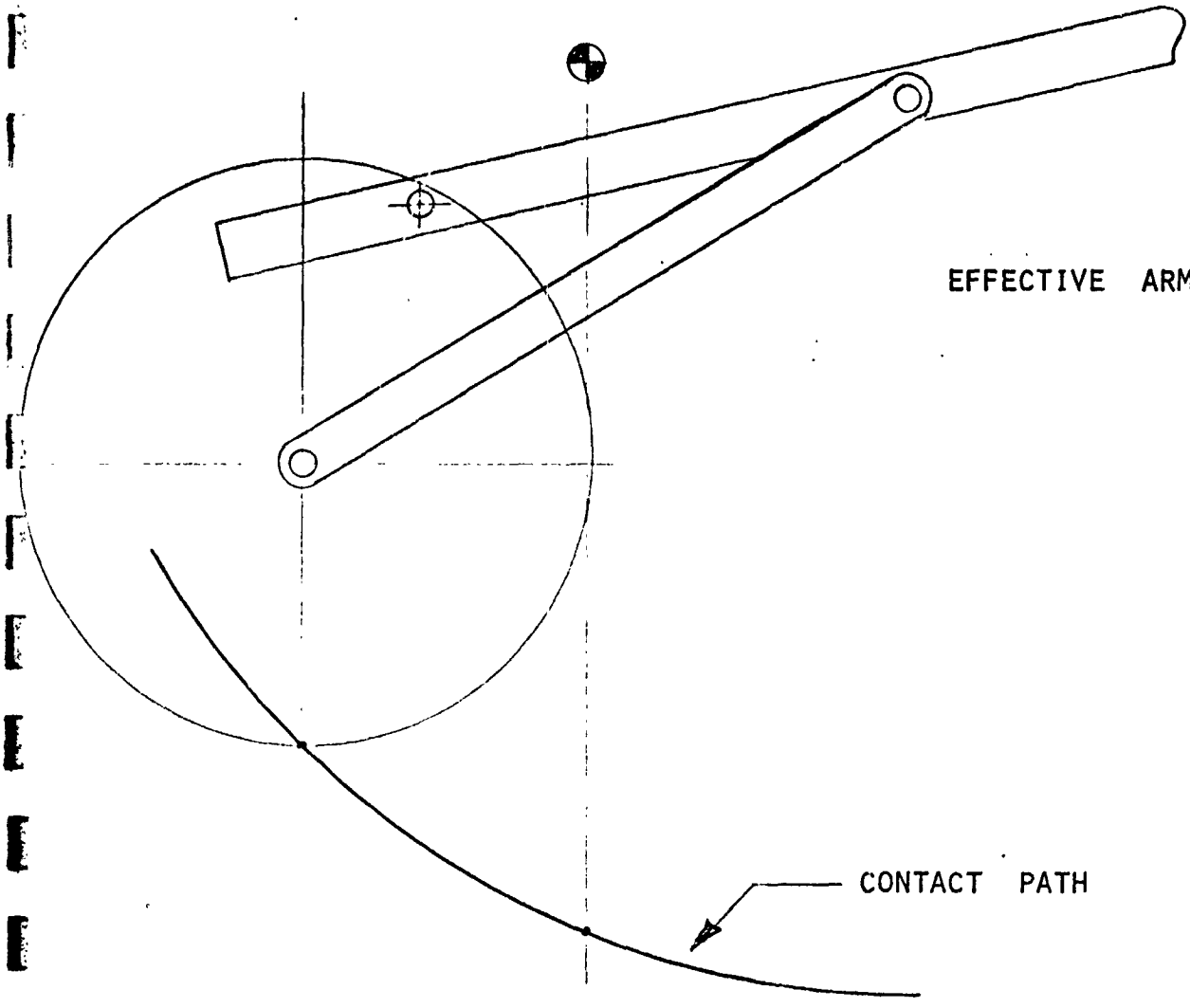

1. VARIABLE GROUND CLEARANCE

2. VARIABLE C.G. POSITION

3. SHIFT BACK CAPABILITY

FIGURE 2

POWERED TORSION BAR

TOP VIEW

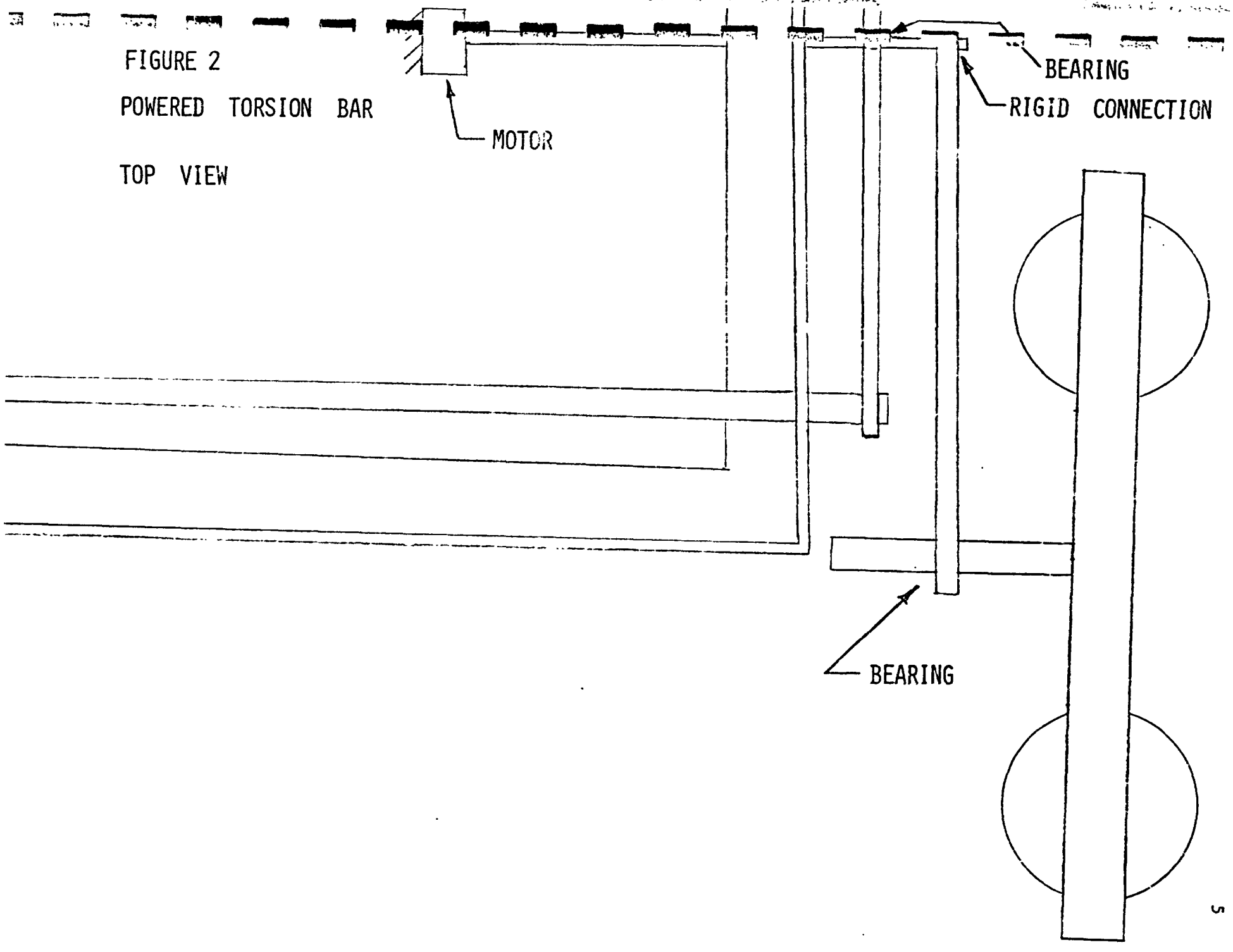

closer to their points of application. The steering motor will be mounted on the steering axis and the drive motors mounted on the vehicle structure but not on the platform. The platform will retain its leveling motor naturally, but will not have to contend with counteracting the torques of the other motors. These modifications should result in better payload isolation for the scale model and, therefore, closer correlation between tests and performance of the full-sized vehicle. It is our intention to provide the best possible performance from the scale model for model to full-size correlation and also for the best presentation of our design in comparison with other proposed designs.

The actual construction of the powered torsion bar suspension is being handled under Subtask A.1.1. February 23 has been set as the completion date for this task. In the meantime, work on a new method for analyzing the toroidal loop wheel is progressing. The method of analysis will be worked out by March 1 at which time it will be programmed for computation under Subtask A.3.c. Starting March 1, a mathematical simulation of the new vehicle will be initiated starting with a two-dimensional bicycle model. The completed vehicle as well as an analysis of the wheel for load versus footprint deflection will be completed by May 15, 1972. At the same time, preliminary results from the vehicle simulation should be forthcoming.

Task A.1.a. Vehicle Model Testing - W. Cobb
Faculty Advisor: Prof. G. N. Sandor

One of the main purposes of constructing a scaled model was to provide for dynamic testing of the proposed design. Preliminary tests were performed during the previous summer with the main conclusion being that design alterations were in order. These have been made, and construction is now in progress. When these changes are incorporated, dynamic testing will again be required with the main purpose being to verify the results of the mathematical simulation so that it can be confidently extended to the full sized vehicle.

Key components of the vehicle model are being studied to insure that they meet the basic functional requirements for a Mars mission. Several features such as suspension, drive motor systems, and the toroidal wheels are being thoroughly analyzed and tests are under preparation for endurance and overload capacity.

To begin the testing, the model's response to simulated road wave inputs was measured. By applying a sinusoidal displacement input to the rear wheels natural frequencies of the structure were identified. However, because of nonlinearity of the shaker, frequency limitation of the photographic data acquisition technique, and hysteresis in the suspension travel, these experiments resulted in very little usable data. The basic test procedure is shown in Figure 3, followed by results from the early test series.

Fig. 3

ORIGINAL TEST SETUP

STANDARD* VEHICLE

ELECTROMAGNETIC SHAKER

PHOTOGRAPHIC TRACKING/RECORDING

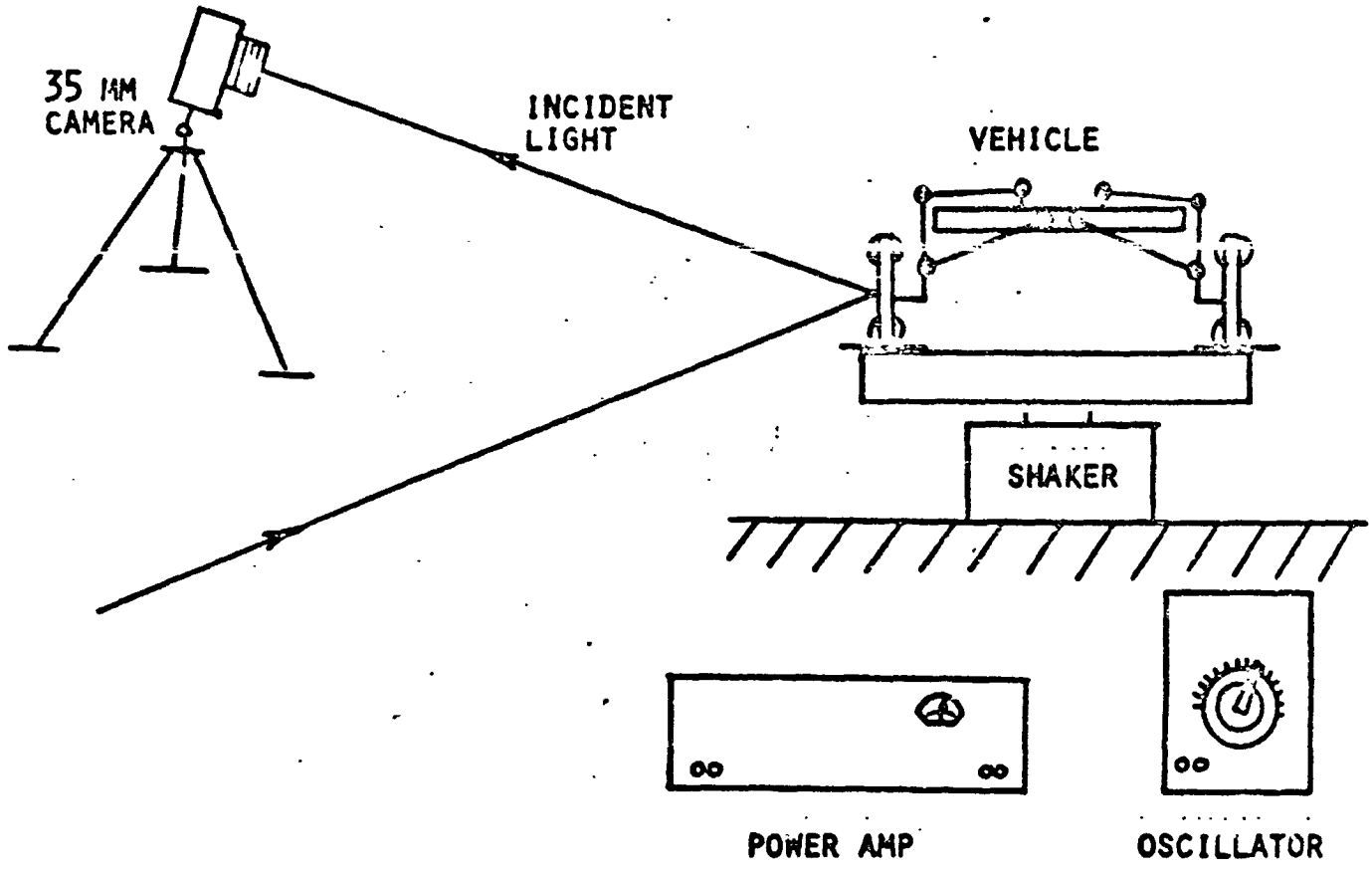

* RPI MRV AS OF SEPT. 71

The dynamic testing of the scaled vehicle will be resumed as soon as the improved model, now under construction, is ready. In the improved model, excessive rear suspension will be eliminated, and the softer wheels of the new model will protect the payload from shock more effectively. A new type of damper design will be properly scaled for the softer wheels and suspension.

Using new facilities provided by the Engineering Design Laboratory, reconstruction of the vehicle was undertaken. A quantity of spring steel was obtained in thicknesses ranging from .0026" to .010". A number of wheels, with larger dimensions, were hand built for test purposes. The new wheels deflect a greater amount, and their larger footprint reduces ground contact pressure. By decreasing the ratio of deflection-to-hoop diameter, maximum stress is reduced and reliability is increased.

The increase in softness of the wheels was accomplished by using larger hoops which increases the volume of the wheels. Once the proper wheel deflection characteristics are established with the aid of this model, the wheels of the full-size prototype will be designed to fit within the smaller volume of the original wheels.

In building the model wheels, to save time and eliminate softening of the spring steel caused by spot welding a new technique for the outer rim is attached to the hoops by epoxy cement. The prototype will be spotwelded with heat treatment to insure proper spring tamber.

Three versions of the model wheel were constructed:

1) Rayfield wheel	Thickness = .010"	width of hoop = .25"
2) Modified #1	T = .006"	W = .25"
3) Modified #2	T = .008"	W = .25"

The results of static tests on these wheels is shown on Figure 4. Deflection is plotted against axle load. Data for these curves was obtained by loading the hub with known test weights and measuring deflection of the hub.

Note that the wheels (T = .006, .008) are reasonably linear with load within their intended operating range. For the load ranges of the front and rear wheels, the two modified wheels display a very favorable spring rate constant, Front $K = 2.44 \frac{LB.}{IN.}$ Rear $K = 2.14 \frac{LB.}{IN.}$, as compared to the earlier designs.

The rear suspension is being modified to allow it to contribute to the reduction of body pitching motion. Leaf springs, modified linkages, and torsion bar axles are being considered. Linkage schemes favorable to compact collapsibility requirements will receive highest priority.

FIG. 4

DISPLACEMENT vs. FORCE

FRONT AND REAR WHEELS :

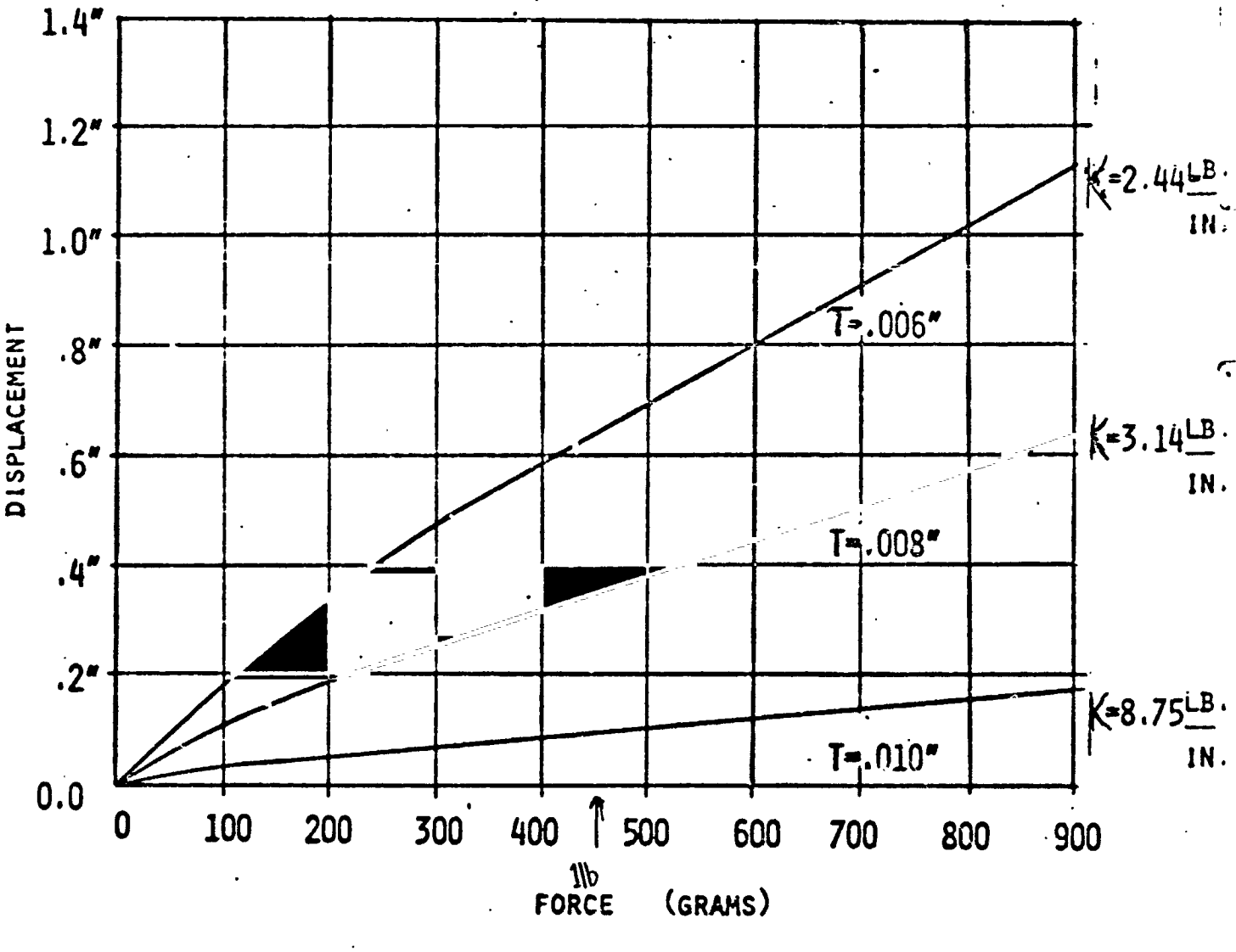

It has been suggested that the tilt-back maneuver can be incorporated into the rear suspension design.

The instruments, with the aid of which the redesigned MRV model will be tested, are also being rebuilt, Figure 5.

The electromagnetic shaker has no usable output below 5 Hz. A slider crank shaker has been built to provide data on vehicle motion in the range of 0.0 to 15 cps. A new addition to the test facilities is a two axis optical tracker, which gives an electrical analog of vertical and horizontal motion of any selected target. Frequency responses as well as the ride quality provided by the wheels and suspension will be rapidly and repeatedly measured.

The principal goal of the dynamic testing is to determine the scale model's steady state response to sinusoidal inputs. Complete response characteristics will be determined before May 15, 1972.

Dynamics testing is a time consuming activity that can be computer simulated. Therefore, dynamic testing is being used to obtain preliminary values for dynamic characteristics and to prove the accuracy of the mathematical simulation. Once the mathematical simulation is verified, no more dynamic testing will be required unless a major vehicle revision is made.

Task A.1.b. Obstacle Negotiation - A. Steinbock
Faculty Advisor: Prof. G. N. Sandor

The objective of this task is to determine the performance of the RPI-MRV in traversing steps, crevasses, slopes and combinations of these three major obstacle types.

Efforts this Fall have been directed towards collecting and collating all previous information and data associated with obstacle negotiation. Other work in this area includes the task of exploring new areas of vehicle stability.

Vehicle stability and obstacle negotiation performance can be considered as a function of the geometries of the vehicle and the terrain surface. For a given surface geometry one can vary the vehicle geometry to achieve the desired performance. Similarly one could set the vehicle geometry and determine its performance on various terrains. The work done on the MRV has utilized both methods.

1. A continuing literature search is being conducted to gather information relating to Martian terrain data, wheel test apparatus, soil properties, and the obstacle negotiation. These references are being used to design and construct the wheel test bin and to find methods of vehicle evaluation as regards to obstacles.

FIG. 5

REVISED TEST SETUP

MODIFIED VEHICLE

- SUSPENSION
- DAMPING
- WHEELS

SLIDER CRANK SHAKER

DUAL-AXIS ELECTRONIC OPTICAL TRACKER

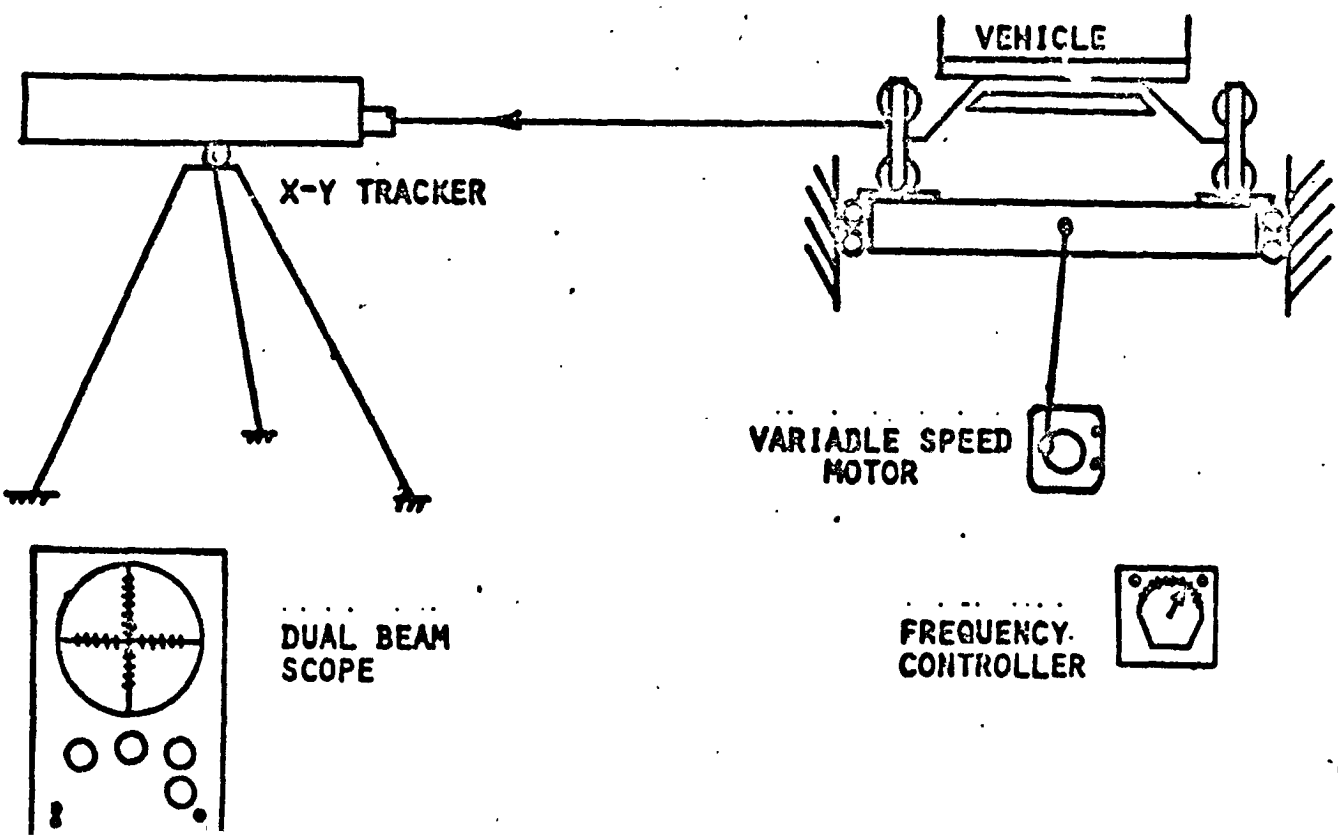

2. All previous works regarding obstacle negotiation has been collected, analyzed and filed. The work collected consists of three computer programs which calculate the required torque at the rear wheels as the vehicle proceeds from the point of contact with the obstacle. The three separate obstacles were:

1) step obstacle

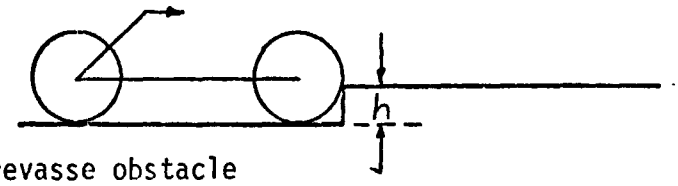

2) crevasse obstacle

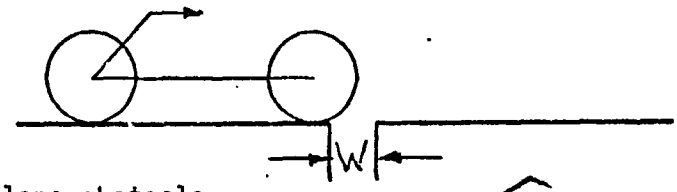

3) slope obstacle

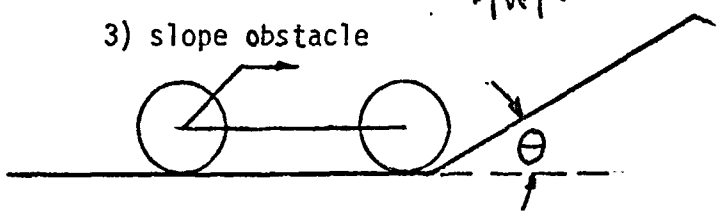

The following graphs have been compiled from the data collected.

Maximum torque vs. a) slope angle
b) step height
c) crevasse width

Torque vs. Distance traveled

a) slope obstacle
b) step obstacle
c) crevasse obstacle

3. A computer program has been developed to evaluate the ground clearance capabilities of the MRV. For example, in going over a ridge, the program compares the vehicle geometry to a set of given terrain geometries and calculates the ridge angle which causes the terrain to contact the vehicle body.

This program has also been written so as to calculate β (maximum) as the vehicle geometry is changed.

The program will soon be debugged, and the data that it will generate will then be tabulated and analyzed with the objective of optimizing the vehicle geometry.

Future work in this area includes:

1. Work will continue on reviewing useful literature regarding wheel testing and obstacle negotiation, including applicable reference texts.

2. The obstacle clearance computer program will be completed. This program will show how the vehicle geometry can be altered to achieve a desired performance.

3. The Mars Roving Vehicle design is still being changed and improved. This will necessitate the reappraisal and possible updating of data to conform to the vehicle's new configuration.

4. Information will be sought on the performance data of the 6-wheeled MRV. A comparison of data will be attempted to show the relative merits of each vehicle.

Task A.1.c. Vehicle Electronics - D. Rosenthal
Faculty Advisor: Prof. G. N. Sandor

The objective of this subtask is to provide Electrical Engineering consultation with the vehicle group, and to design and construct any required electronics equipment. Presently, the assignments include the design of a power supply for the various drive mechanisms, construction of a satisfactory leveling device to include the level sensor and the instrumentation of the full size wheel tester.

Investigation of power amplifiers for use as power supplies for the drive motors has yielded a possibility offering performance superior to the original Hewlett-Packard units used originally. This alternative became a possibility when an encapsulated integrated power amplifier in three different ranges of power output became available from a Japanese firm, Sanko. This means that temperature stability will be guaranteed and the need for operational amplifiers will be eliminated. Delivery of these units is expected in February.

Some of the zener diodes used in the curve shaping assembly of the electronic differential system have not yet arrived as they are special order items, but final delivery is expected by March 1. Velocity feedback for each wheel by means of tachometers

has been considered but weight considerations make this impossible. Furthermore, non-linearities in the input signal would still be present. For this reason the concept of an open-loop control system is being retained.

If tests with the Sanko power amplifiers work out as expected, they will also be used for the steering, leveling, and suspension tilting motors, each with an appropriate feedback: position feedback for suspension, tilting and steering functions and an on-off type signal showing whether or not an error exists and in which direction it exists for the leveling system if the mercury switch sensors are used.

One concept presently being studied for use as a leveling sensor is a relatively large diameter wheel with a shaft and bearing passing through it a small distance from its geometric center of gravity. This is equivalent to a physical pendulum having a long period and therefore a long length but in a much more compact form. By increasing the period of oscillation, the dynamic errors due to vehicle movements may be decreased to an acceptable level. Refinement to make an even better sensor is of little use at this time due to the dynamics of the rest of the leveling system. If a better vertical sensor were needed, a gyro pendulum, Ref. 2, could be employed but although the design parameters will be determined by the present task force, the actual construction of such a device is beyond the technical facilities available at RPI at this time.

To utilize the disk-type sensor, a potentiometer could be used to measure the angle between the sensor's nominal vertical axis and that of the platform. A motor mounted on the platform and exerting torque against the body would be used to drive this angle to zero.

The primary goal of work in the coming semester will be to aid in the completion of an improved dynamic model, scheduled for demonstration on February 24. Before that date a suspension motor will be added with the attendant feedback electronics and the steering and drive motors will be relocated. In addition, considerable help will be rendered in connection with the instrumentation of the wheel tested, to be completed by March 31. The rest of the semester will be devoted to instrumentation of the newly completed dynamic model.

Task A.2. Collapsibility, Stowage and Deployment - T. Janes
Faculty Advisor: Prof. G. N. Sandor

One of the main performance requirements set for the RPI-MRV is that it can carry a larger scientific payload than the competing vehicle designs. If the RPI-MRV would have to fit within the inside

dimensions of the Viking capsule in the vehicle's normal operating configuration (without folding), then the overall dimensions would become so small that the size of the payload would be severely limited. Therefore, subtask A.2 has been initiated to find the most efficient and reliable method of collapsing the vehicle, stowing and protecting it during the flight to Mars and finally deploying the vehicle into its mission configuration in conjunction with the landing sequence. The performance requirements for each of the three parts of the overall subtask are outlined below.

1. Collapsibility - The collapsed configuration of the MRV must be compact enough to effectively utilize the space available in a Viking capsule; must maintain a proper center-of-gravity and minimize the complexity of the collapse operation. The collapse scheme must not limit the dynamic performance of the vehicle.

2. Stowage - Use available anchor points inside the capsule, so as to shelter the vehicle and its scientific payload from the acceleration and shock of launch, landing and possible meteor impact. The stowed position must be compatible with the landing scheme that will be used.

3. Deployment - The vehicle must be unfolded from its stowed launch configuration into its normal operating configuration. This unfolding must be automatic and reliable and should also require as little extra hardware as possible to maintain the high payload fraction of the MRV.

The RPI-MRV offers a unified payload volume available for scientific instrumentation which is greater than the combined payload volume of the three-section six-wheeled vehicle proposed elsewhere. While the three sections of the latter vehicle are collapsed upon one another, the payload package for the RPI-MRV remains unchanged for launch, and only the suspension is collapsed.

Several alternatives were considered for the collapsed configuration including one which would stow the wheels above the vehicle in the dome of the capsule. However, landing the vehicle on its own wheels will avoid the necessity of additional landing gear structure and thus improve payload fraction. This can be accomplished in either of two ways:

1. collapse the suspension to place the wheels under the body.

2. decrease the width of the vehicle.

Placing the wheels under the body in the collapsed configuration would allow the vehicle to unfold once the bottom section of the Viking aeroshell was dropped. A landing upon the wheels could then be accomplished. A rear suspension capable of folding the wheels under the body is presently under investigation.

Decreasing the width of the body was also considered but set aside because it would adversely affect the dynamic performance.

Upon completion of a satisfactory rear suspension design, the advantages for collapsing in wheels above or below the payload will be reconsidered with the objective of achieving satisfactory landing configuration.

The present investigation is expected to yield a workable collapsibility scheme for the vehicle. Feedback based on this study will be used in the design of a payload section. This new payload section will be shaped so as to better utilize the inner space of a Viking Capsule. The development of a good collapsibility scheme will be taken into account in future design changes of the payload section.

Task A.2.a. Physical Construction of Collapsibility Hardware - G. Szatkowski
Faculty Advisor: Prof. G. N. Sandor

Work on the collapsibility scheme began this past summer under subtask A.2. It became immediately apparent that models of both the capsule and vehicle would greatly speed development of a workable collapsibility scheme as well as provide a convincing demonstration of the feasibility of the proposed scheme.

The purpose of this subtask is to construct any hardware considered necessary by project management. A clear Viking aeroshell and a balsa wood vehicle model were constructed.

Since full detail as found on the .184 dynamically scaled model was not needed, a smaller scale could be chosen. For convenience, a scale of .092, one half the scale of the dynamic model, was selected for both the capsule and vehicle.

Actual construction of the scaled vehicle was fairly simple since the dimensions could be measured from the dynamic model. The chassis and body sections were fabricated from standard balsa stock while the wheels were represented by cylindrical cones made from heavy cardboard.

Construction of a clear Viking Aeroshell proved more difficult. A special clear vinyl of 1/16" thickness was found which could be molded at temperatures as low as 200°F. In this case a wood model of the Viking Aeroshell would suffice. A cylinder of glued laminations was made and then

turned on a lathe to finish the capsule model. The vinyl was then heated by an industrial heat gun and stretched over the mold in two separate sections.

This subtask has been essentially completed, and has been turned over to the respective investigators who will make the final modifications necessary for utilization in their development work connected with the vehicle design.

Task A.3 Wheel Design

Task A.3.a. Grouser Design - C. Klette
Faculty Advisor: Prof. G. N. Sandor

The RPI toroidal loop wheel is actually a self-contained design project aside from the rest of the vehicle. As such, its performance may be considered by itself as compared with wheels from other vehicle designers. The wheels are the only components that come in direct contact with the planet surface. The nature of this contact is the subject of this investigation. Few analytic studies are applicable to this problem, so most of the work will involve physical testing of the full size wheel.

Primary on the list of objectives for optimizing the wheel design is the construction of a 2/5 size wheel testing device. This scale was chosen for the sake of economy and lab space utiliziation in establishing wheel design parameters by observation of comparative performance. This device will be used to determine wheel characteristics such as load vs deflection characteristics under various combinations of cant angle, speed and controlled slip. Predetermined slip is enforced by means of driving the wheel and the carriage independently of one another. A variety of soil and terrain simulations will be tried. The wheel test apparatus will be a simplified scale model of the test facility at Vicksburg, Mississippi and the tests run will be similar to the tests to be conducted there on the full size wheel. Optimal traction using different grousers will be analyzed via controlled slip tests. The cohesion, friction angle, and dampness of the soil will be varied to provide a wide variety of soil conditions. Slope capabilities of the wheel on various soils will be determined by wheel torque studies.

With this scaled-down wheel testing device, information will be obtained to verify or revise the work done by the analytic groups involved in the theoretical analysis of the wheel. The construction of the wheel testing device has already begun and it is scheduled to be completed by March 1.

According to Ref. 3, lunar mare soil is a close approximation to the martian soil. The soil values used by the Vicksburg Station for lunar soil are: 37° friction angle, 1.6 g/cm^3 density, and a cohesion of .05 psi to .20 psi. These are the conditions to be approximated in the soil test

bin. In view of the limited availability of materials in this area, a fine grade of sand will have to suffice for test soil instead of sand obtained from Yuma, Arizona that Vicksburg used as their approximation of lunar soil.

The wheel testing apparatus will allow comparison tests among various wheel rims and grousers to optimize traction characteristics, load distribution and footprint of the wheel. The footprint characteristic data will be incorporated in the computer program for the force distribution in the wheel. Actual wheel loading conditions on the martian surface can be approximated by various cant angles and load values simulating martian gravity. With this test program the wheel design will be optimized in preparation for possible future tests on a full size wheel at the Vicksburg facility.

Task A.3.b. Hinge Design - L. Cuprys
Faculty Advisor: Prof. G. N. Sandor

A study of the hinge has been initiated for several reasons: 1) it is the weak link of the wheel and therefore it must be designed to be reliable under all applied loads; 2) its performance and flexibility are needed for the analytical wheel model; 3) fatigue characteristics must be known because of the extended mission on Mars.

In one conceptual model, the maximum stress was predicted from standard beam theory,

$$\sigma = \frac{M_1 C_1}{I_1} + \frac{M_2 C_2}{I_2} + \frac{F_3}{A_0} \qquad (1)$$

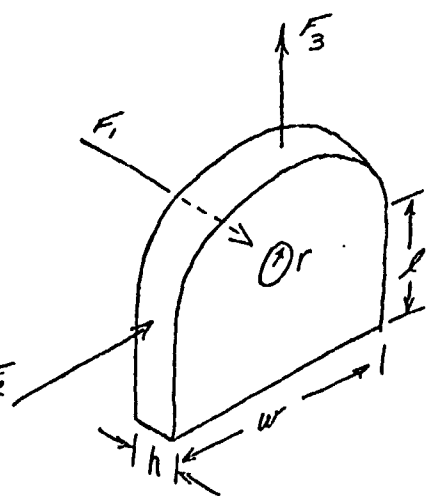

$$\frac{h^2(w^2\sigma_m)}{5F} - h\left(\frac{6F_2 l}{w-r} + \frac{w^2 F_3}{w-r}\right) - 6F_1 l w = 0 \qquad (2)$$

It should be noted that the equation (2) is a function of the two critical dimensions of the hinge: the width, w and the thickness, h. By varying w and solving for h, a family of curves results for various constant safety factors.

A similar analysis has been performed for the flexible hinge.

$$\sigma = \frac{M_1 C_1}{I_1} + \frac{M_2 C_2}{I_2} + \frac{F_3}{A_0} \qquad (3)$$

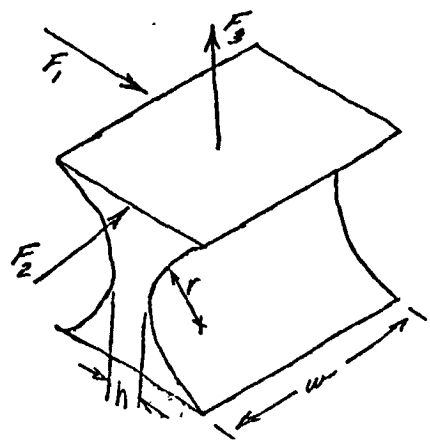

$$h^2\left(\frac{w^2\sigma_m}{S.F.}\right) - h(6F_2r + wF_3) - 6F_1rw = 0 \qquad (4)$$

The same family of curves applicable to the flexible hinge may be drawn from equation (4). It is interesting to note that equations (2) and (4) predict both tensile and compressive stresses depending on whether the tensile or compressive yield strength is used.

The flexibility of the hinge was the next consideration. Obviously, this only applies to the flexible hinge. For this analysis the wheel hoop is considered rigid and the rim can be considered a series of rigid segments. A distributed load on the rim can be represented by a single force "L". The moments and shear stress can then be written:

$$M_{Z1} = (L\cos\theta)\ (7) \qquad (5)$$

$$M_{Z2} = (L\sin\theta)(\cos\theta)\ (2r-x) \qquad (6)$$

$$V = \frac{dM_Z}{dx} = (L\sin\theta)\ (\cos\theta) \qquad (7)$$

Again using standard beam theory, a differential equation for the deflection of the hinge can be written:

$$\frac{d^2v}{dx^2} = \alpha_0 \frac{d}{dx}\left(\frac{V}{GA}\right) - \frac{M_Z}{EI} \qquad (8)$$

A single integration yields the angle of deflection θ.

$$\frac{dv}{dx} = \tan\theta = -\frac{14rL\cos\theta}{EI} - \frac{4rL\sin\theta\cos\theta}{EI} + \frac{4r^2L\sin\theta\cos\theta}{EI} \qquad (9)$$

$$\frac{19050}{L} I = -\cos^2\theta\left(\frac{7}{\sin\theta} + 1.375\right) \qquad (10)$$

Equation (10) was solved using an iterative scheme on the computer. The flexibility can then be defined:

$$FLEX = \frac{\theta}{M}$$

This analysis is valuable in that, equation (4) sets a range of values for the dimensions of the hinge. Once the desired flexibility is set, equations (10) and (11) pick a point in that range representing the proper hinge dimensions.

There are two basic assumptions made in this analysis.

1. the height of the hinge is assumed to be constant.

2. materials are assumed to follow Hooke's Law.

It should be noted that polyurethane is visco-elastic with stress and flexibility depending not only on the forces and the modulus but also on the rate at which the forces are applied. Therefore, research is now in progress on the visco-elastic properties of the hinge. A fatigue study is being studied using the hinge tester built last year and is scheduled to be completed by June 1972. The main thrust of Task A.3 will be the development of the scaled-down wheel tester which is due to be completed by March, 1972.

Task A.3.c. Wheel Analysis - J. Kobus
Faculty Advisor: Prof. G. N. Sandor

Before September 1971, the selection of a candidate wheel for RPI's Mars roving vehicle had been narrowed to a toroidal multi-hoop elastic metal wheel. The distinct advantages of this wheel are clearly outlined in Ref. 4.

A mathematical model of the wheel is being developed to aid in determining footprint vs load characteristics, power dissipation, life expectancy, interaction with vehicle suspension, and in the selection of materials.

The computer program developed earlier, Ref. 4, proved to be too costly to run because of its length and complexity. Just one run of this program involves the calling of numerous subroutines thousands of times and costs hundreds of dollars. Drastic modification of this program was investigated, but was found to be difficult. One serious drawback of this program lies in the excessive iteration scheme. Therefore, a new mathematical model and computer program are being developed and should be operational by March 15, 1972.

The new approach consists of writing simpler programs that give a good approximation to the true solution of the load-deflection and footprint characteristics. By assuming first a relatively stiff wheel rim and then an extremely flexible rim, an envelope within which the true solutions lie is identified. MARSFOOT, the stiff rim program, utilized an observation made of the existing MRV model wheels: most of the load appeared to be born by deflection of only the bottommost hoops and the lower rim. A simple geometric loading technique yielded a series of footprint diagrams, such as Figure 6, for various normal loading conditions, various hoop numbers, and various normal and transverse spring constants of the hoops. Likewise the flexible rim program, MARSFLEX, gave fair results assuming exclusive load-bearing responsibility for the bottommost hoops. Figure 7 shows the similarity of the footprints for the above two extreme assumptions, reasonably close to the observed model wheel deflections. In both cases, transverse deflections of the hoops were virtually negligible in comparison to normal deflections. With this program, for approximately 2 minutes of running time on an IBM 360 Model 50, approximate footprints are known which can be used to further refine the program.

The refinement is now under investigation utilizing expressions for changes in stored internal energy with a change in applied load to the various individual members composing the wheel. The improved program will attempt to eliminate the gross linearizations and geometric simplifications which may be introducing some error in MARSFOOT and MARSFLEX. Determining the pattern of stored internal energy will delineate the shape of the wheel and location of extreme stresses. Also, initial fatigue life studies are possible for various duty cycles that a typical wheel may encounter. This way material selection will be facilitated.

Complications have arisen in modeling the outer rim exactly. Various techniques have been explored, including Fourier cosine series and similar geometric triangulation but did not turn out to be promising, and therefore work is continuing in the direction of finite element techniques.

Recently, detailed information concerning the work of Grumman Aerospace Corp. on the design, development and testing of a Lunar roving vehicle wheel has been obtained. Included in this set of data was a comparison of various candidate wheels. (It may be noted that their study called attention to toroidal wheel drawback of particle entrapment and resulting rapid failure propagation, and relatively high weight: a shortcoming that was eliminated by RPI's hinged design). Basic techniques used by Grumann were studied in depth. Of significance is the applicability of

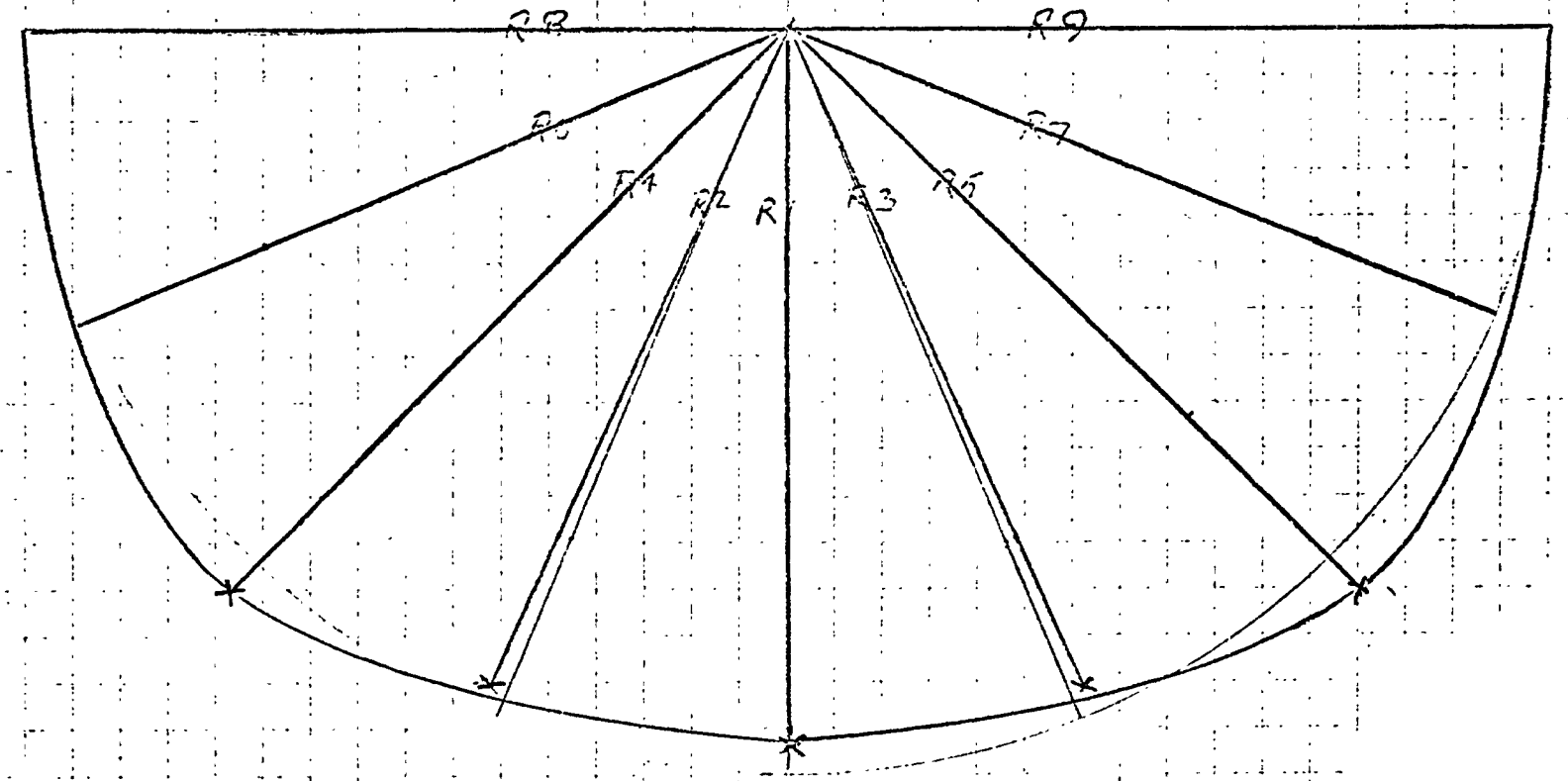

FIG. 6

Footprint Diagram for Relatively Stiff Rim

R_1 = 16 inches, x = 16 spokes

SNØRM = 90 lbs/in., Weight = 150 lbs.

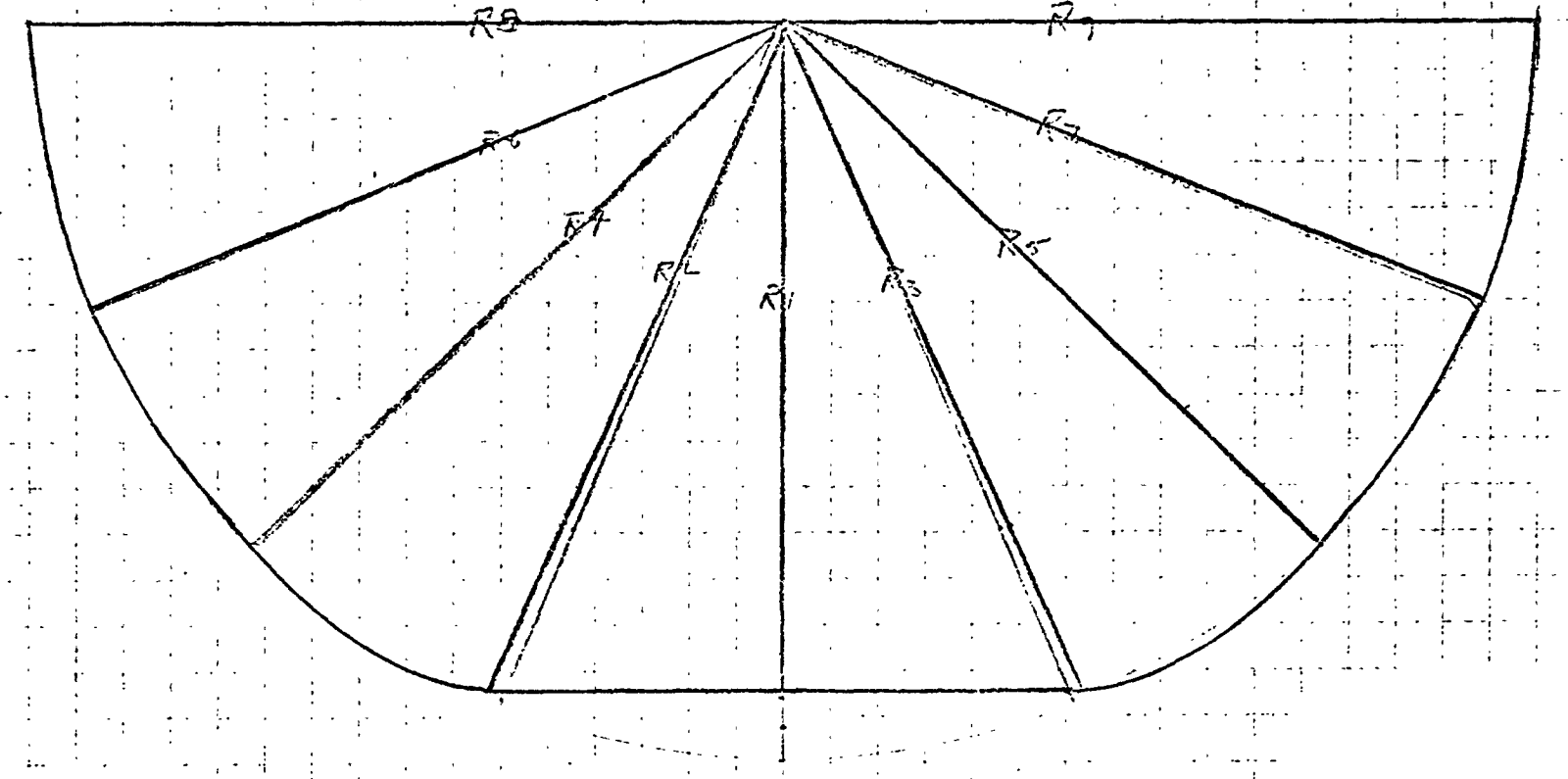

FIG. 7

Footprint Diagram for Flexible Rim

R_1 = 16 inches, x = 16 spokes

SNØRM = 90 lbs/in., Weight = 150 lbs.

their work covering wheel performance and power requirements. This area will be studied further after the completion of the internal energy program, which is expected to be completed by March 15, 1972. Also included in the Grumman report are testing techniques which might be applied to our scale model testing program.

The key fault of toroidal wheels in Grumman's review -- particle entrapment with resulting rapid failure propagation, can be prevented with the use of the flexible-type rim hinge. Referring to Task A.3.b. it is apparent that space for adequate hinge geometry is available but choice of a material that can overcome the embrittlement problem encountered at Martian nighttime temperatures is still unsolved at the present.

Another wheel design trade-off concerns long fatigue life for wheel members versus desired wheel suspension characteristics. Excess flexing of the wheel to obtain a smoother, more stable ride in the Martian temperature environment imposes considerably shorter life to fatigue failure. Tradeoff studies of the problem can proceed when the internal energy program is completed by March 15.

To summarize these points: wheel problem definition on a qualitative level is substantially complete. Exact figures of hoop and rim spring constants, hoop placement and sizing, fatigue life and material choices will be investigated as soon as the new program for modeling the wheel is completed by March 15.

Task B. Systems Analysis

The objective of this task is to develop a framework within which vehicle design decisions involving conflicting requirements can be made. Past work included the identification of the system model, Ref. 5, and formulation of a method to examine design trade-offs by utilizing the model, Ref. 6.

Efforts since July 1, 1971 were divided into several areas:

1. An attempt to solve the optimal system design problem for the present system model.

2. Generation of new system models corresponding to changes in the assumptions made during formulation of the original model.

3. Investigation of the problem of readjusting the system design when changes are made in values of some of the design parameters.

4. Examination of the requirements placed upon and the functions required of the on-board computation and data-handling system.

Task B.1. System Design Optimization for the Original System Model - N. Van Denburg
Faculty Advisor: Prof. E. J. Smith

This task has as its objective the optimization of the design and operational parameters of the original model, Ref. 5. This is being done through the use of mathematical programming techniques of optimizing constrained systems. The system model has several nonlinear relationships inherent in the subsystems, notably the thermal control subsystem where the thermal radiation effects introduce fourth order nonlinearities in several of the system equations of this subsection, and the form of many of these equations is that of a quotient of two fourth order polynomials. The communication subsystem introduces a mild nonlinearity (second order) due to the rate of communication being proportional to the product of the power of the communicator and the area of the antenna. The obstacle avoidance subsystem introduces several terms of exponential and logarithmic form. Another source of nonlinearity is that the weight of the vehicle subsystem is proportional to the wheel base cubed.

The nonlinear nature of this problem leads to the general nonlinear programming (NLP) format. This format is to maximize or minimize some function (the objective function) which evalutes the effectiveness of the resulting system with a given choice of variable parameters. The extremization is subject to various nonlinear inequality constraints of the form $g_i(\underline{x}) \geqslant 0$ and equality constraints of the form $h_i(\underline{x}) = 0$. The iterative scheme is usually based upon a second order gradient method for finding a local (possibly global) maximum or minimum which may or may not be upon a constraint boundary of the feasible set.

The alternative possibility of a closed form solution is considered to be almost impossible due to the extremely complex nature of the problem. For just the unconstrained critical points of the objective function, which is highly nonlinear since it evaluates the total system, one would need to solve a system of twelve tightly linked nonlinear equations in twelve unknowns, a problem which could very well be impossible without resorting to numerical techniques. If one includes all the inequality constraints a closed form solution would involve solving 54 equations in 54 unknowns.

Since the problem can be put into a form which is well adapted to a NLP procedures, Ref, 6, 7, 8, which will include inequalities as well as equalities, it was decided that this would be the best approach. This NLP procedure, Fiacco & McCormick's Sequential Unconstrained Minimization Technique (SUMT), was recently obtained from the Rensselaer Hartford Graduate Center and was originally from Research Analysis Corp., McLean, Va.

As mentioned above, the general NLP format is to maximize or minimize the objective function subject to inquality constraints and equality constraints. In particular, SUMT handles problems of the form:

$$\min. \; F(\underline{x})$$

$$\text{subj. to: } g_i(\underline{x}) \geqslant 0 \qquad i = 1,2,\ldots,M$$

$$g_i(x) = 0 \qquad i = (M+1),\ldots,(M+MZ)$$

This form of the NLP problem statement is put into a form which is adaptable to the techniques of unconstrained minimization through the use of penalty terms which are added to the objective function. This augmented function has the form:

$$P(\underline{x},r) = F(\underline{x}) - r\sum_{i=1}^{n} \ln[g_i(\underline{x})] + \frac{1}{r}\sum_{i=M+1}^{M+MZ}[g_i(\underline{x})]^2$$

Note how the negative logarithmic term increases as one approaches the boundary of the feasible region forcing the minimization technique to stay within the feasible region. This unconstrained problem is solved for a sequence of decreasing r values(i.e., decreasing the weight on the inequality constraints and increasing the weight on the equality constraints) until the convergence criterion is met. One of the problems with this technique is that of local minima, however, the $-r\sum_{i=1}^{n}\ln[g_i(\underline{x})]$ term shapes the surface in such a way that given a sufficiently large initial weight and a reasonably slow reduction in weight on this term the program has more of a probability of converging to the dominant minimum than to any other local minimum. Other problems are those of finding a suitable initial value of r and the problems associated with convergence stopping.

The first try at programming the model and using SUMT to optimize the parameters resulted in a nonconvergent series of points which did not meet the equality constraints, of which there were two from the thermal control subsystem. The system is of order twelve so the first try was a problem in fourteen variables and two equality constraints. It was thought that the elimination of these two equality constraints would aid and speed the solution of the optimization problem. In the process of reworking the system equations one additional term describing the power required to cool the vehicle during the Mars day was added to the equations for the power profiles of the vehicle in the stationary mode and in the roving mode.

The choice of the unknowns was dictated mostly by the form of the equations, however, even here there were problems. It would appear that the form of the equations affects the solution of the NLP problem. So far this has given rise to some problems which have necessitated rearrangement of the programming problem.

The Sequential Unconstrained Minimization Technique finds its own initial feasible point so it is not necessary to be too exact about an initial guess at the parameters which are free. This technique is dependent upon the starting value in that convergence for each value of r to the global minimum is guaranteed for some region of space near the minimum only.

To date the computing has been centered around three areas. First and most basic was the trial of the technique on several practice problems to give the user a feel for how the technique works. Second, was the first effort in programming the original model. This effort

resulted in minor refinements of the model and several improvements to the method of programming the problem. The third area is that of rechecking and rearranging the system equations in such a way as to give a better probability of convergence of the programming problem.

The obvious need is for a solution for the optimal choice of operational and design parameters of the system. A possible intermediate step toward this end might be the taking of analytic first and second partials of the system equations. This step might be taken if the present numerical differencing scheme proves to be unsatisfactory. Results to date have necessitated extensive rearrangement of the system equations which may continue to be required.

After this original system is optimized there will be an additional effort in the direction of optimization of the revised models, Task B.2.

Task B.2. Changing Design-Dependent Assumptions and Remodeling -
Lance Lieberman
Faculty Advisor: Prof. E. J. Smith

In formulating the system model for a semi-autonomous Mars roving vehicle, Ref. 5, it was necessary to make various assumptions in order to constrain the model for solution. Many, if not most, of these assumptions merely entailed fixing parameters and constants at reasonably feasible values; however, several were basic to the entire model, and a change in any one such important concept could necessitate remodeling whole subsystems and their governing equations. It would be unwarranted to take for granted that because the system is modeled around various assumptions, the final model would necessarily ignore other possible variations in design and be limited to these interpretations; further, there is no reason to accept these assumptions as the most efficient or desirable for the mission, in terms of technology or cost. It thereby becomes obvious that the model must be flexible enough to accept major changes in design-dependent assumptions. By remodeling the entire system of equations, as necessary, to represent a partially altered vehicle, the effect on the various parameters can be examined and the overall changes in the model can be noted. A significant rise in the objective function, for example, could indicate a more efficient system and might be cause for further investigations in the same direction.

The first study performed in this direction was the addition of an active, stationary orbiter linking the rover with the earth ground station resulting in a remodeling of the communications subsystem.

In the original system model, a direct, two-way vehicle-earth communication link was assumed. The addition of an active, stationary relay orbiter at an approximate altitude of forty-thousand kilometers (24-thousand miles) above the Martian surface has several immediately discernable advantages; not only does it cut down necessary communications power on-board the vehicle, allowing a decrease in necessary power allotment to the communications subsystem and/or an increase in the data rate, but it has the additional desirable advantage of allowing vehicle-orbiter communication at more evenly spaced times, and

subsequent relaying to earth during an increased time period -- at all times with proper orientation of the orbiter.

The assumptions and fixing of parameter values made in formulating this remodeling are as follows:

1. The carrier is X-band microwaves of wavelength 3.3×10^{-2} meters, as before.

2. The orbiter antenna is a parabolic dish of diameter d = 8 meters.

3. The rover antenna is a parabolic dish; $\Delta\theta = 1^{o}$, $\Delta\theta$ being the antenna pointing error.

4. Uplink parameters are negligible.

5. Transmitter r.f. efficiency is e = 20%.

6. The worst case link distance of 5.7×10^{11} meters is used.

7. Equivalent system noise temperature is $T_n = 30^{o}K$.

8. The communication efficiency $(B_o/B) = 5\%$.

9. The space loss attenuation $L_p = 3.98 \times 10^{-17}$ for the orbiter at forty-thousand kilometers.

10. While it is not in the scope of the study to specify parameters for the orbiter's earth-link communication system, it seems reasonable to assume that the basic system chosen for the rover's direct earth link would be equally suitable for the orbiter's link. This does not, however, enter into the rover's equations.

The generation of new equations is not necessary to accomplish the desired modeling modification. Equation (1)

$$W_{com} = 0.59\ P_i + 2.0\ D^2_{com} + 39.0 \text{ kgm} \qquad (1)$$

for the weight of the communications package and equation (2)

$$V_c = (8.3 \times 10^{-4})P_i + (4.8 \times 10^{-2})\ m^3 \qquad (2)$$

for its electronics volume remain the same, since the graphs from which they were obtained were linearized in the correct region. Equation (3) however, linking the data rate with the antenna diameter and the transmitter power input, will change due to variations in the constants of the equations from which it was derived, as follows.

Signal power at the receiver must be large enough to overcome the noise. This may be given by

$$P_r = P_t G_t L_p G_r$$

where

P_r is received signal power,
P_t is transmitted signal power,
G_t is transmitting antenna gain,
L_p is the space loss attenuation,
and G_r is the receiving antenna gain.

These can be replaced with

$$P_t = eP_i = .20P_i$$

$$G_t \approx .54\left(\frac{\pi}{\lambda}\right)^2 D_{com}^2 = (4.88 \times 10^3)\, D_{com}^2$$

$$L_p = 3.98 \times 10^{-17}$$

$$G_r \approx .54\left(\frac{\pi d}{\lambda}\right)^2 = 3.13 \times 10^3$$

Substituting, received power is found to be

$$P_r = (1.22 \times 10^{-10})\, P_i D_{com}^2 . \qquad (A)$$

Now, an additional restriction on PCM systems is

$$P_r \geqslant 10^{-23}\, (B/B_o)\, T_n R_{com},$$

where

B/B_o is the inverse of communication efficiency,
T_n is the system noise equivalent temperature, ^oK,
and R_{com} is the data rate in bits/sec.

Inserting values we obtain

$$P_r \geqslant 6.0 \times 10^{-21}\, R_{com} . \qquad (B)$$

Combining equations (A) and (B) and solving for the data rate, the result is:

$$R_{com} \leq (2.04 \times 10^{10})\, P_i D_{com}^2 . \qquad (3)$$

Clearly, for a transmitter of only a few watts and a rover parabolic dish of reasonable size the data rate can be made extremely high. This indicates that the main effect of placing a relay orbiter between rover and earth is the effective elimination of restriction on data rate. By eliminating equation (3) from the model completely, values of P_i and D_{com} can be determined during optimization and a data rate later selected on the basis of existing units and desired specifications.

Since a limiting equation on data rate has been eliminated, it is necessary to remove, at least for a first optimization run, all terms in the system depending upon R_{com}, so that the system solution will not optimize the variable at an unreasonably large value. (After running the model on the computer and obtaining approximate numbers for P_i and D_{com}, estimates of R_{com} can be made and the terms reinserted). This change affects only three equations in Ref. 5:

--in equation (39), the indicated terms will be removed.

$$E_{st} = \left\{P_{nav} + P_{cp} + \left[\frac{3\times10^6}{R_{com}T_{sci}}\right]P_t + P_{scia}\right\}\left\{T_{sci}S_{sci}V_f T_{rov}\right\}$$

--in equation (5), for T_{sci}, can be eliminated since the removal of the communications terms makes it equal to equation (4), for T_{esci}.

--in equation (40), for the objective function, the denominator term T_{sci} should be replaced with T_{esci}.

Obviously, other factors will change slightly as well. Available communications time will increase, for example; however, this should not alter the accuracy of the system equations, since the change is not appreciable, and the benefits will not always be available. The rover only transmits while stopped for that purpose, and while it could now transmit during formally 'dead' periods (due to earth-mars blackout), it is unlikely that earth-station controllers would have the vehicle perform science or maneuvers during periods of such limited 'visibility' and control.

It might be further noted that the orbiter need not have a directional antenna, such as the assumed parabolic dish. An omnidirectional antenna of gain 1 (zero db) would do just as well, since this would effect only the eliminated equation (3) and would still not warrant its insertion -- in that case the upper limit for R_{com} would decrease by three orders of magnitude from that calculated in equation (C).

In the direction of future endeavors, the model will be modified for changes in other basic assumptions. One particularly interesting facet of this will be the change from our presently modeled four-wheel vehicle to a six-wheel, triple-compartment vehicle. While data is still being compiled for this study, it is already evident that major mathematical variations and additions will be necessary in many of the subsystem designs. Results of this analysis should prove quite interesting and helpful in future work.

Task B.3. Accessory Optimal Solutions for State Perturbations -
Carl Pavarini
Faculty Advisor: Prof. E. J. Smith

Consider the situation where an optimal design vector has been determined for a given mathematical model of a system (see Tasks B.1 and B.2). Suppose that one (or more) of the components of the vectors

that is the design parameters, must be adjusted. This may be due to factors not considered in the model:

a. Although the model equations are continuous, perhaps it is not feasible to design for the true optimal value of a parameter (e.g., if the optimal solution requires a communication data rate of 1.347 K, it may be more reasonable to use a 1.5 K value for hardware design)

b. Perhaps an outside constraint is added (e.g., the optimal solution requires the vehicle to climb slopes now considered too hazardous in terms of wheel slippage considerations)

c. It may be advantageous to use a certain piece of off-the-shelf hardware, and its design values may not coincide with the determined optimal values.

In any of these cases, it would be desirable to know how to readjust the values of the design parameters that were unperturbed by the required change in order to maintain the optimal property of the solution.

The task of this sensitivity analysis, then, is to determine the optimal manner in which to adjust these design parameters relative to the initial perturbation. Work done to date considers the problem when one parameter undergoes a required perturbation by some "small" amount. Linearization techniques are employed to reduce the general nonlinear optimization problem to a set of linear inequalities, thus much reducing the complexity of the problem as compared to the original system optimization. The sensitivity approach has the advantage that it is no longer necessary to resolve the nonlinear optimization problem each time a design parameter (state) is perturbed.

Mathematical Analysis of the Problem

The original system design optimization problem has been cast in the form:

$$\max \quad f(x)$$

$$\text{subject to} \quad g_i(x) \geq 0 \quad i=1,2,\ldots,r$$

$$h_j(x) = 0 \quad j=1,2,\ldots,s$$

where x is the n-dimensional vector of design parameters and f and all the g_i and h_j are, in general, nonlinear functions of the components of x.

The optimal solution (x^*) is known by solution of the original problem. Of the r inequality constraints one or more may be active (i.e., equal to zero) at x^*. Appending these to the s h_j's gives a set of m equality relations at x^*, where $m < n$, which now will be denoted $h_j, j=1,2,\ldots,m$.

A necessary condition at the optimal solution is the LaGrange condition

$$F(x^*) = \nabla f(x^*) + \nabla H^T(x^*)\,\lambda^* = 0$$

where

$$\nabla f_i = \frac{\partial f}{\partial x_i}$$

$$\nabla H_{ij} = \frac{\partial h_i}{\partial x_j}$$

∇H is an m x n matric

and λ is an m vector of LaGrange multipliers.

Since x^* is known, the problem of finding the λ^* vector is the solution of n linear equalities. However, since x^* is found by iterative search, the LaGrange condition equations may not be accurately satisfied and it may be necessary to solve for λ^* in a least-squares sense.

If x_1 (the first component of x) is to be perturbed,

$$x_1' = x_1^* + \delta x_1 .$$

At the new optimal (x') the LaGrange condition must also hold:

$$F(x') = \nabla f(x') + \nabla H^T(x')\,\lambda' + \gamma \begin{pmatrix} 1 \\ 0 \\ \vdots \\ 0 \end{pmatrix} = 0$$

where γ is a new LaGrange multiplier, and the vector $\begin{pmatrix} 1 \\ 0 \\ \vdots \\ 0 \end{pmatrix}$ is the gradient of the new constraint on x_1.

A Taylor first-order expansion of F(x) about x* yields

$$F(x') \approx F(x^*) + DF(x^*)(x' - x^*)$$

where DF denotes differentiation. Note that $x' - x^* = \delta x$. Expanding,

$$F(x') \approx F(x^*) + \left[\frac{\partial}{\partial x_i}\nabla f\right]^* \delta x + \nabla H^T(x^*)\left[\frac{\partial \lambda}{\partial x_i}\right]^* \delta x$$

$$+ \lambda^* \left[\frac{\partial}{\partial x_i}\nabla H\right]^* \delta x + \left(\frac{\partial \gamma}{\partial x_i}\right)\begin{pmatrix} 1 \\ 0 \\ \vdots \\ 0 \end{pmatrix}^T \delta x \qquad (1)$$

where the notation $\left[\frac{\partial}{\partial x_i}\right]$ is a gradient operation which transforms a vector to a matrix and a matrix to a three-dimensional array.

In (1), there n equations. There are n unknowns in δx, nm unknowns in $\left[\frac{\partial \lambda}{\partial x_i}\right]$ and n unknowns in $\left(\frac{\partial \nu}{\partial x_i}\right)$ for a total of $n(m+2)$ unknowns. However, solving for all of these unknowns is not necessary for determining the readjustments δx_i, $i=2,\ldots,n$. Matrix algebra manipulation allows the following reductions:

$$\left[\frac{\partial \lambda}{\partial x_i}\right]\delta x \Longrightarrow \begin{pmatrix} \frac{\partial \lambda_1}{\partial x_1} \\ \vdots \\ \frac{\partial \lambda_m}{\partial x_1} \end{pmatrix} \delta x_1$$

$$\left(\frac{\partial \nu}{\partial x_i}\right)\begin{pmatrix} 1 \\ 0 \\ \vdots \\ 0 \end{pmatrix}^T \delta x \Longrightarrow \left(\frac{\partial \nu}{\partial x_1}\right)\begin{pmatrix} 1 \\ 0 \\ \vdots \\ 0 \end{pmatrix}\delta x_1$$

Since interest is in the n-1 readjustments, define

$$\eta = \begin{pmatrix} 1 \\ \eta_2 \\ \vdots \\ \eta_n \end{pmatrix} \qquad \text{so that } \delta x = \eta \delta x_1$$

and equation (1) becomes

$$\left[\frac{\partial}{\partial x_i}\nabla f\right]^* \eta + \nabla H^T(x^*)\frac{\partial \lambda}{\partial x_1} + \lambda^*\left[\frac{\partial}{\partial x_i}\nabla H\right]^* \eta + \frac{\partial \nu}{\partial x_1}\begin{pmatrix} 1 \\ 0 \\ \vdots \\ 0 \end{pmatrix} = 0 \qquad (2)$$

where

$$\left\{\lambda^T\left[\frac{\partial}{\partial x_i}\nabla H\right]\right\}_{ij} = \sum_{k=1}^{m} \lambda_k \frac{\partial^2 h_k}{\partial x_i \partial x_j}$$

There remain n linear equations, and there are n+m unknowns (n-1 η's, m from $\left(\frac{\partial \lambda}{\partial x_1}\right)$, and $\frac{\partial \nu}{\partial x_1}$, a scalar).

Another m equations can be obtained from the linearized constraints

$$\nabla H(x^*)\eta = 0 \qquad (3)$$

which requires that the new optimal point satisfies a linear approximation to the constraints about the original optimal solution. The readjustments are calculated from

$$\delta x_i = \eta_i \delta x_1$$

Results Obtained

Because the technique of the previous section utilizes linear approximations both to the LaGrange condition and the constraint equalities, and because the solution x* may be only an approximation to the actual solution to the original problem, the values of the readjusting parameters ηi, i-2,...,n are only estimates. However, is it hypothesized that since the system model itself is by nature inexact, the values of η obtained will give a good "feel" as to the sensitivities of the design parameters to a change in any one of them. This remains to be demonstrated for the actual system model, although it has been true for various smaller-dimensional test problems.

The method requires that all constraints be considered as strict equalities. When an active inequality is treated as a strict equality for purposes of analysis, this, in effect, requires the inequality to also be active at the new solution, x'. This assumption may not be valid, especially when two or more inequalities are active at x*. Therefore, as a check, it is advisable to treat different combinations of the active inequalities as equalities for several runs of the problem. In addition, if the new solution x violates any inequality that was not treated as active at the adjusted solution, that inequality should be treated as active, and the problem resolved.

For simple problems (those where the true solution is observable, and calculations can be done by hand) the method has been effective in finding the readjustment parameters accurately.

Extension of the present effort will be in the following areas:

a. testing of the method with more complex problems (saddle points, ridges, linearly dependent constraints, higher dimensionality, extremely nonlinear functions)

b. investigation of the inequality problem to attempt to determine a better way to resolve the active-inactive problem

c. establishing sufficiency conditions for the method

d. allowing more than one parameter to be initially varied.

Task B. 4 Computation and Data-Handling Subsystem - Donald Meagher
Faculty Adviser: Prof. E. J. Smith

The objective of this task is to develop a framework within which the function of the Computation and Data-Handling Subsystem can be defined and its organization and operation specified. This analysis requires the determination of various characteristics of the other subsystems and vehicle operational requirements.

An Overview of the Approach

The approach which has been pursued consists of making certain general assumptions concerning the subsystems and the modes of vehicle operation followed by their definition and analysis according to the following criterion:

1. Subsystems
    a. Function
    b. Control Requirements
    c. Data I/O
    d. Computation Requirements
    e. Timing Constraints
    f. Servicing Interrupts
2. Modes of Vehicle Operation
    a. Vehicle Function
    b. Subsystem Utilization
    c. Control Programs
    d. Emergency Servicing

Concurrent with these efforts, a study of existing computer systems has been undertaken in the areas of hardware, performance, organization, and control techniques. The analysis of existing computers in terms of hardware and performance is an attempt to obtain an estimate of the computational capabilities (in terms of additions per second per kg., for example) which could be expected of the technology in which the MRV Computer would be implemented. The analysis of the organization of existing computer systems and the control techniques utilized by them is useful in determining a possible model upon which to base the design. By modeling the design according to existing practice, much of the initial effort is eliminated, and in addition it may be possible to use the mathematical techniques developed for the optimization of the model.

Subsystems

The following is an overview of the subsystems:

1. Computation and Data-Handling Subsystem
    a. CCS-Command Computer Subsystem: The CCS performs computations, makes decisions and issues commands.
    b. FDS-Flight Data Subsystem: The FDS organizes and coordinates the data produced by the vehicle subsystems.
    c. DSS-Data Storage Subsystem: The DDS provides large scale data storage. It is assumed that most, if not all, of this data is eventually to be transmitted to Earth.

2. Communications

   a. Low Gain: This system provides one way low speed engineering and status information to Earth.

   b. High Gain: This system provides high speed two way communications while the vehicle is stopped.

3. Science

   a. TV Cameras (2)
   b. Optical Activity Test
   c. GC-MS
   d. Radioisotope growth test
   e. Turbidity and pH growth test
   f. Calorimetric
   g. Sound detection
   h. Magnetic properties
   i. Seismometry
   j. Meteorology
   k. Soil Moisture
   l. Surface Gravity
   m. ABL

4. Power Generation and Storage

5. Thermal Control

6. Navigation

7. Obstacle Avoidance

8. Vehicle Structure

Modes of Vehicle Operation

Four modes of vehicle operation have been defined. They are the following:

1. Roving Modes, Fig. 8: The function of the vehicle in the Roving Modes is to transport the Science Subsystem across the surface of Mars. A routing algorithm residing in the core memory of the CCS is provided with a current destination (updated from Earth during science stop), the current position of the vehicle (updated by the Navigation Subsystem), and a map of the terrain (provided by the long-range Obstacle Avoidance Subsystem). The algorithm issues commands to the Vehicle Structure Subsystem, which causes the vehicle to seek its destination. When the destination is reached, or a problem arises which the algorithm is unable to cope with, control is restored to the decision making section of the CCS which calls for further action.

ROVING MODE

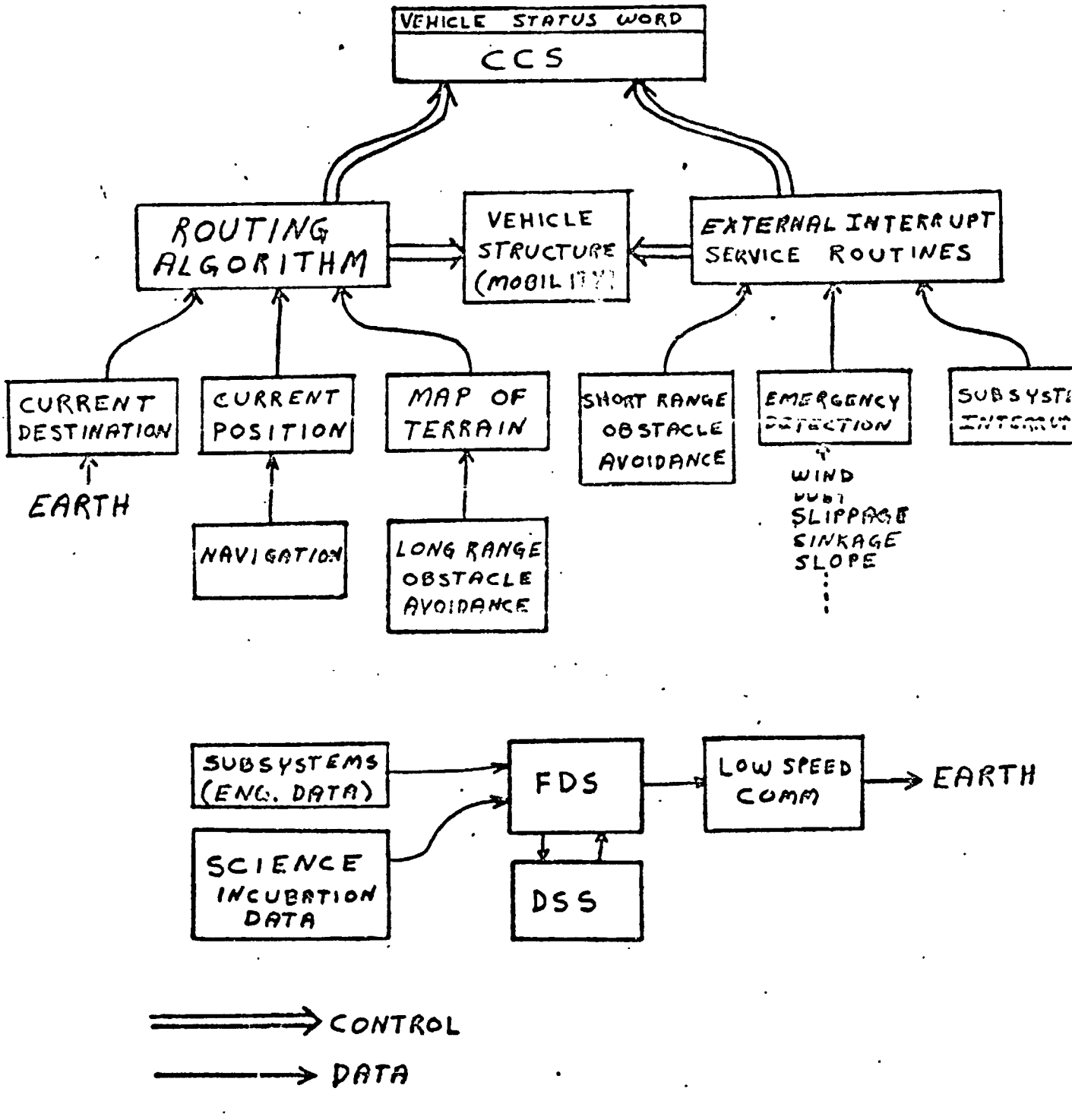

FIG. 8

The External Interrupt Service section of the CCS will handle emergencies and external interrupts on a priority basis. The subsystem engineering data and the science incubation data, if any, is stored in the DDS for later transmission to Earth. A small amount of engineering and status information is transmitted back to Earth via the low-speed communication subsystem.

2. Science Mod, Fig. 9: The vehicle is stationary during the Science Mode. The first priority is to establish two-way high speed communications with Earth. The Science Control Program will then control the performance of the scientific experiments.

3. Recharge Mode, Fig.10: The Recharge Mode is entered when not enough power is available in the batteries for continuation of the Roving or Science Modes. All unnecessary systems are shut down until enough energy has been stored by using the RTG's to charge the batteries to continue.

4. Idle Mode, Fig. 11: The Idle Mode is entered when it will not be possible to establish communications with Earth, should an emergency arise. A timer will signal the programmed mode to be entered at the appropriate time.

System Model

The upper half of Figure 11 shows a typical organizational structure for a mini-computer system. The Processor communicates with the core memory over the Memory Bus. Control is exerted over external devices and information is passed both ways between the Processor and external devices via the Input/Output Bus. Special external devices an communicate with the core memory directly on a cycle stealing basis.

The lower diagram shows the application of the above structure to the problem at hand. The external devices are replaced by vehicle subsystems. Data from the subsystems is fed directly into the FDS, external to this diagram.

Future Work

The immediate goal of this task is the derivation of at least a simplified definition of subsystem control I/O. The analysis of vehicle operation and subsystem data processing requirements is continuing along with the study of existing computer systems.

The long range goal of this task is the determination of a detailed model of the computer, structure and organization, architecture, and physical characteristics. The model could eventually be programmed on a mini-computer, such as the Interdata-4. A hardware realization could be constructed from this implementation with a relatively small expenditure of effort. An I/O Bus would be extended to a working model of the vehicle structure. Sensing circuits in the model would be required only for those functions to be implemented, such as mobility control.

SCIENCE

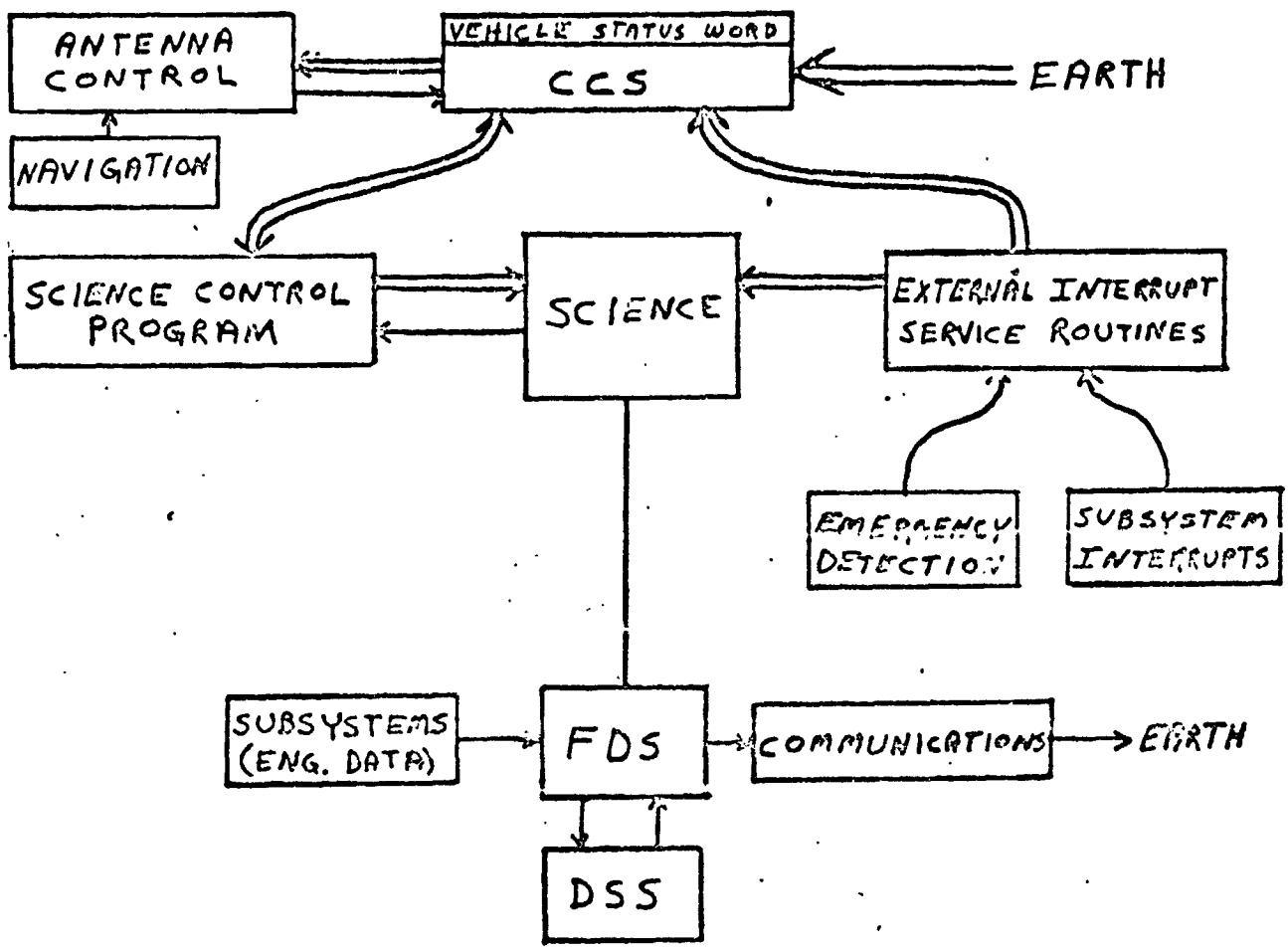

FIG. 9

RECHARGE

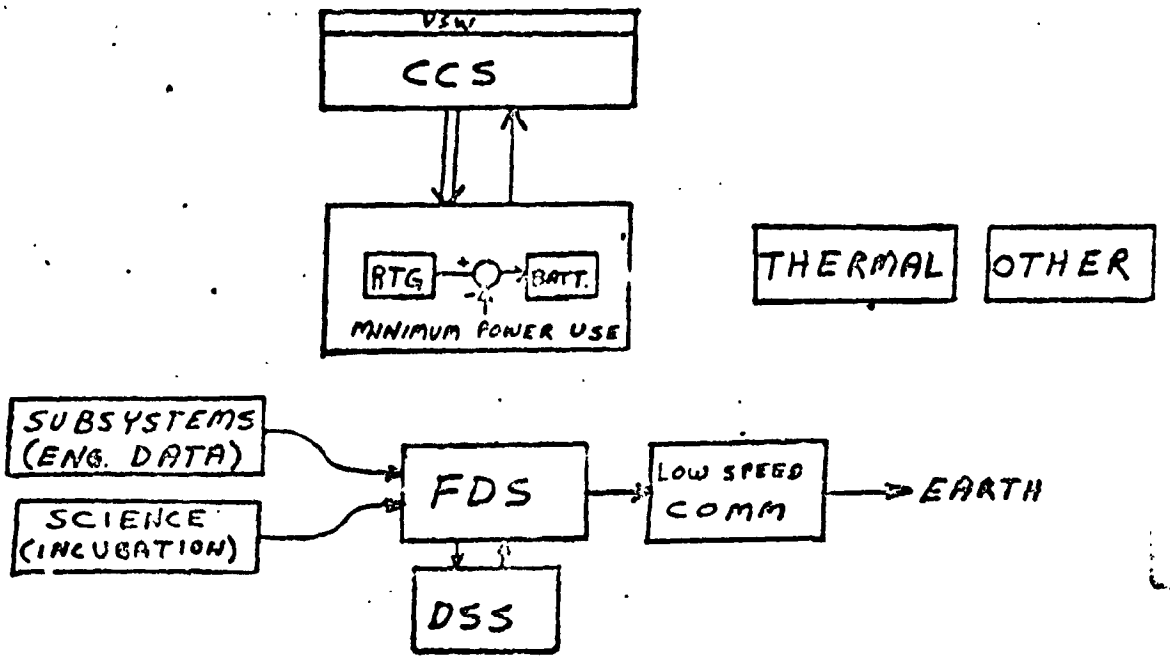

IDLE

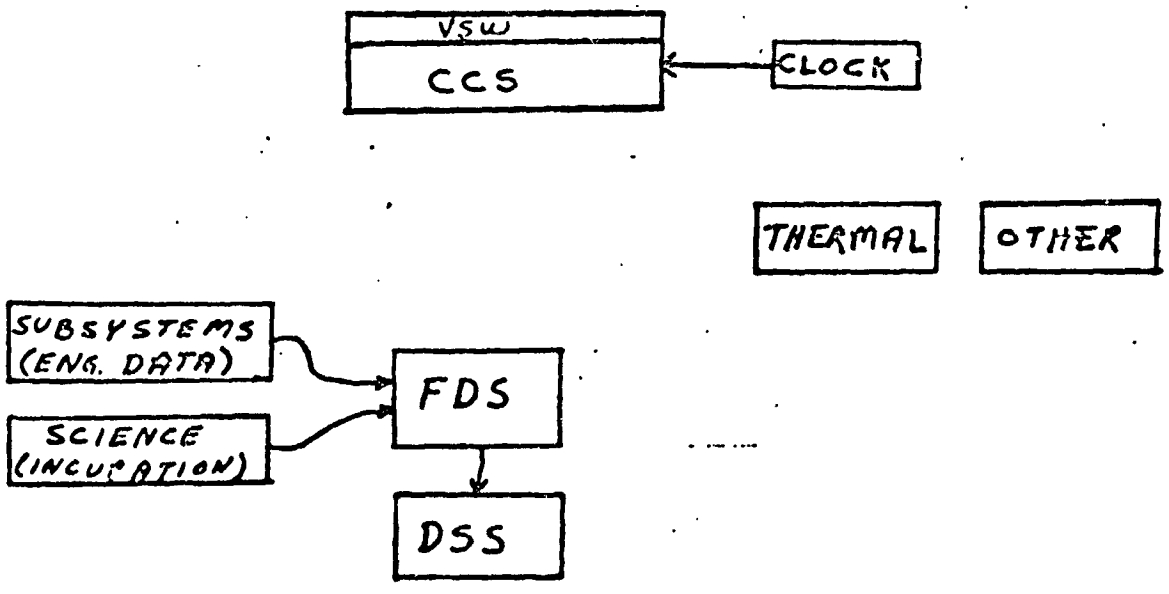

FIG. 10

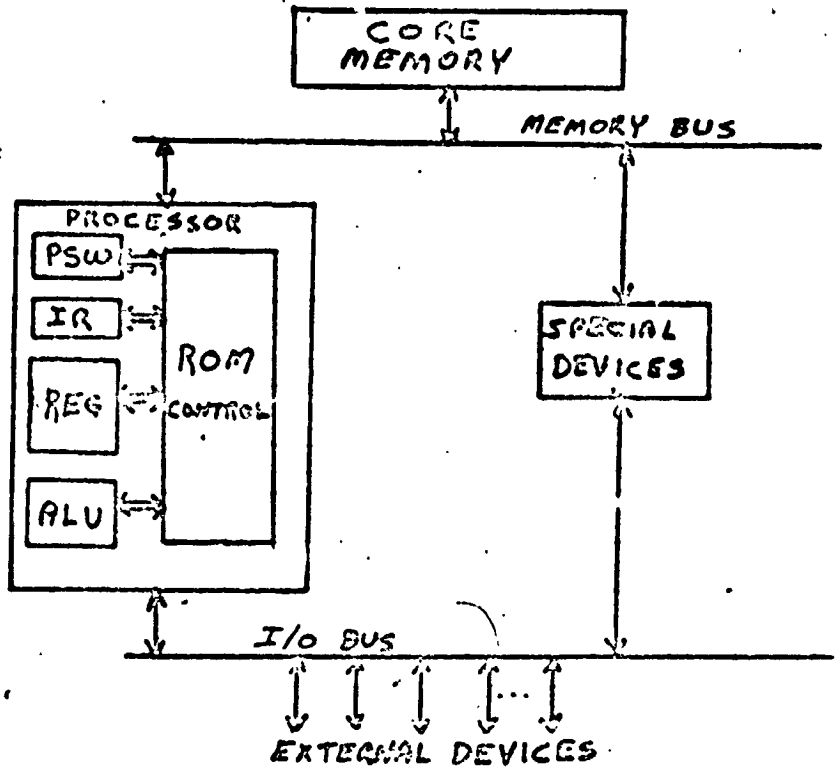
CORE MEMORY
MEMORY BUS
PROCESSOR
PSW
IR
REG
ALU
ROM
CONTROL
SPECIAL DEVICES
I/O BUS
EXTERNAL DEVICES

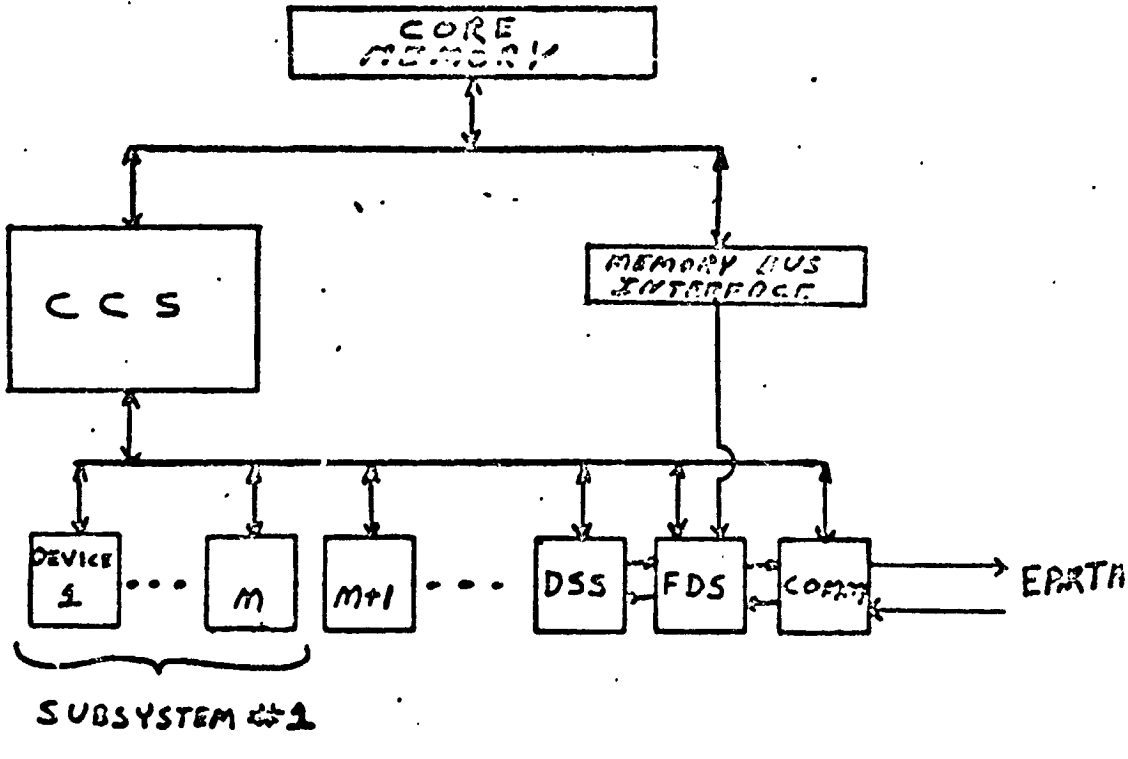
CORE MEMORY
CCS
MEMORY BUS INTERFACE
DEVICE 1
M
M+1
DSS
FDS
COMM
EARTH
SUBSYSTEM #1

FIG. 11

Task C. Navigation, Terrain Modeling and Path Selection

The mission plan to undertake a systematic exploration of Mars requires that the roving vehicle can be instructed to proceed under remote control from its landing site to a succession of desired locations. This objective requires that the vehicle possess the capabilities: of sensing and interpreting the terrain to provide the information required by a path selection system, of selecting paths with due regard to safety and other considerations, and of knowing its location and that of its destination. Tasks relating to these objectives have been defined and are under active study. The progress achieved to date is described in the sections immediately following.

Task C.1. Navigation Systems

The aim of the navigation task is to provide a continuous record of the position of the vehicle as it explores the Martian surface. It was decided to break this objective down into two main types of navigation systems. The Vehicle Navigation System provides a continuous estimate of the vehicle's position. However, this estimate contains some error which grows with time. The Satellite Navigation System provides a more accurate estimate of the vehicle's position at discrete instances of time. These are then used to correct the error in The Vehicle Navigation System.

Past work reported in Ref. 9 included star tracking and local vertical detection systems. During the past period, emphasis has been directed to optimization of satellite orbital parameters and to problems related to range measurements and satellite tracking.

Task C.1.a. Satellite Navigation System - Ronald E. Janosko
Faculty Advisor: Prof. C. N. Shen

In the last progress report covering this area of investigation, Ref. 9, the basic satellite navigation system was derived. This proposed system used three scalar measurements of the distance from the rover to the satellite to locate the rover. Using these distance measurements, ρ_i, three equations of the form

$$\rho_i^2 = (\bar{x} - \bar{s}_i)^T(\bar{x} - \bar{s}_i) \qquad i = 1, 2, 3$$

were able to be formed and solved for $\bar{x}$, the rover location, if the satellite locations, $\bar{s}_i$, were known. At that time an error analysis was also performed. The object of this analysis was to find the mean squared error in locating the rover as a function of the mean squared error in the distance measurements and in the prediction of the satellite positions.

It was noted at that time that the mean squared error in locating the rover was a function of the measurement geometry. Since that report this task has concerned itself with properly identifying the error sources in the measurements involved and with determining

the optimal measurement geometry. The optimal measurement geometry being defined as that geometry which reduces the mean squared location error to a minimum.

Referring to Fig. 12 we can briefly review the problem formulation. A more complete derivation is contained in Ref. 9, 10. First it is assumed that the satellite orbit is circular and in the plane of the Mars equator. If the satellites are separated by an angular distance α then the three satellite locations can be given by:

$$\bar{S}_i^T = (R+A)(0, \cos E_i, \sin E_i) \; ; \; E_1 = \alpha \, , E_2 = 0 \; E_3 = \alpha \tag{1}$$

The rover is to be located in the plane of the I_1 and I_2 axes, thus

$$\bar{x}^T = R(\sin\gamma, \cos\gamma, 0) \tag{2}$$

From equations (1) and (2), the distances that are measured can be given by

$$\rho_i = \sqrt{R^2 + (R+A)^2 - 2R(R+A)\cos\gamma\cos E_i} \tag{3}$$

In the above equations A represents the altitude of the orbit above the Mars surface, R is the radius of Mars, and γ is the distance that the rover is above the orbital plane.

If $\widetilde{\Delta\rho^2}$ is the mean squared error in measuring the distance ρ and

$$B^T = \left[(\bar{x}-\bar{S}_1), (\bar{x}-\bar{S}_2), (\bar{x}-\bar{S}_3)\right] \tag{4}$$

with

$$\bar{\rho}^T = [\rho_1, \rho_2, \rho_3] \tag{5}$$

then the mean squared error in locating the satellite is given by

$$mse = \bar{\rho}^T B^{-1^T} B^{-1} \bar{\rho} \, \widetilde{\Delta\rho^2} \tag{6}$$

which is a function of the variables A, α, γ, and β. Where β is the angular distance from the subsatellite point on the surface of Mars from which the satellite can be seen for a 45 degree from vertical restriction on the look angle

SPECIFIC GEOMETRY

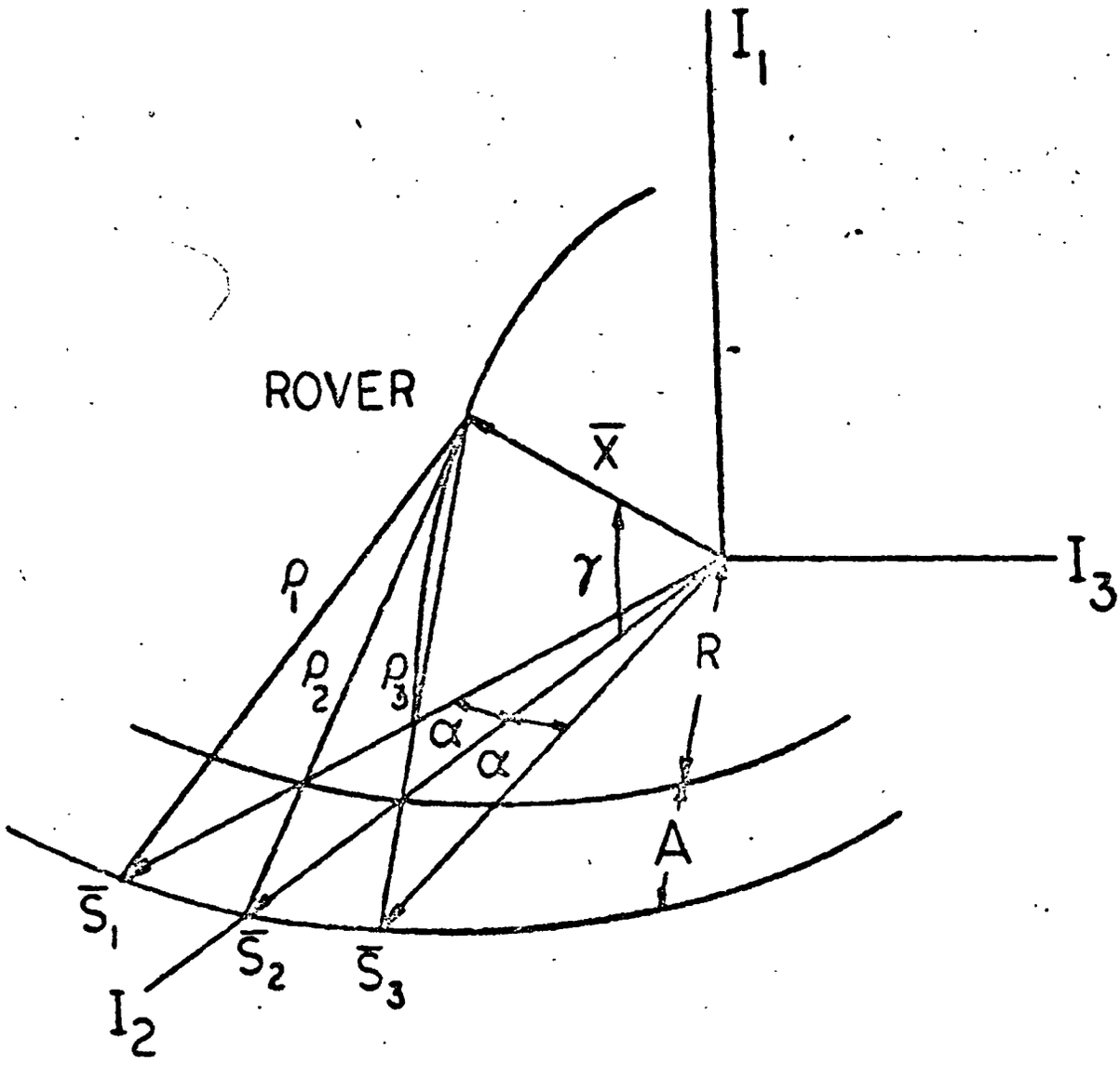

FIG. 12

Equation (6) is to be minimized with respect to the variables A, α, β, and γ. Unfortunately the problem is not so simple as a pure minimization problem for certain constraints must be met by the variables at the solution point. The geometric constraints were derived in the last report and in Ref. 10 and are simply repeated here for completeness. They can be written as

$$\cos\beta - \sin\beta \geq R/(R+A) \tag{7}$$

$$\cos\gamma \cos\alpha \geq \cos\beta \tag{8}$$

$$A \geq A_{min} \tag{9}$$

$$A \leq A_{max} \tag{10}$$

Where equations (7) and (8) were rewritten as inequalities instead of equalities as in Ref. 9 to more accurately represent the problem.

The constraints that have to do with using a laser range finder to measure the distances between the rover and the satellite are given below. Their formulation is considerably different than previously reported because of some inaccurate choice of parameters. As before the power received by the detecter, P_r, must be greater than or equal to the minimum power detectable, P_{min}, or

$$P_r \geq P_{min} \tag{11}$$

Also if P_t is the power transmitted, and P_T is the power incident on the target area, A_T, then

$$\frac{P_r}{P_T} \propto \frac{A_T}{\pi(\tilde{\rho}\,\theta_t)^2} \tag{12}$$

Likewise letting A_r be the receiver area

$$\frac{P_r}{P_T} \propto \frac{A_r}{\pi(\tilde{\rho}\,\theta_r)^2} \tag{13}$$

Where in equations (12) and (13), θ_t and θ_r are the beam divergence angles of the transmitted and reflected beams respectively, and $\tilde{\rho}$ is the average distance between the rover and the satellite. Equations (11), (12) and (13) can be combined to yield

$$P_r = \eta \frac{\phi_a^2 \phi_T A_r A_T P_T}{\pi^2 \theta_r^2 \theta_T^2 \tilde{\rho}^4} \tag{14}$$

where η is the optical efficiency of the system, ϕ_a is the one way atmospheric power transmissivity, and ϕ_r is the efficiency of the reflector. It should be mentioned that it has been assumed that a retroflector is used as the target area on the satellite.

The mean squared measurement error can be approximated by

$$(\Delta\tilde{\rho}^2)^{1/2} = \frac{Kc}{2b}\left[\frac{1}{2(S/N)}\right]^{1/2} \tag{15}$$

which is from Ref. 11. From Ref. 12, we can also find that

$$(S/N) = \frac{\frac{q\eta}{h\nu}P_r}{4bq\left[1 + P_B/P_r + \left[\frac{I_d}{P_r}\right]\left[\frac{h\nu}{q\eta}\right]\right]} \tag{16}$$

Thus the mean squared distance measurement error can be related to the distance measured by equations (14), (15) and (16) which then can be related to the variables A, α, β and γ by equation (3) where

$$\tilde{\rho} = (\rho_1 + \rho_2 + \rho_3)/3 \tag{17}$$

The remaining laser constraint is used to guarantee that the time between sightings is greater than the minimum time needed between laser pulses. Setting the minimum time at 1 sec. the time constraint can be given as

$$1 \leq \frac{\alpha(A+R)^{3/2}}{207} \tag{18}$$

which is from Ref. 13 and holds for a circular orbit.

All of the parameters chosen for the minimization are given in Table I which lists the symbol for the parameter, the equation it is used in, the parameter name and the value chosen and where applicable the reference that the value was taken from.

The minimization of equation (6) was performed for two cases. Case 1 subjected to mirimization to only the constraints given by equations (7) thru (10), that is the case of constant mean squared range error. Case 2 subjected the minimization to equations (7) thru (10) and equations (14) thru (18). The results for both cases are presented in Table II.

After the optimal measurement geometry was determined it was decided to study the visibility requirements. That is, it was felt that the orbit should be further specified so that the rover would be able to see that satellite for a large portion of the orbit. Referring to Fig. 13, it is possible to derive simplified criteria for the visibility

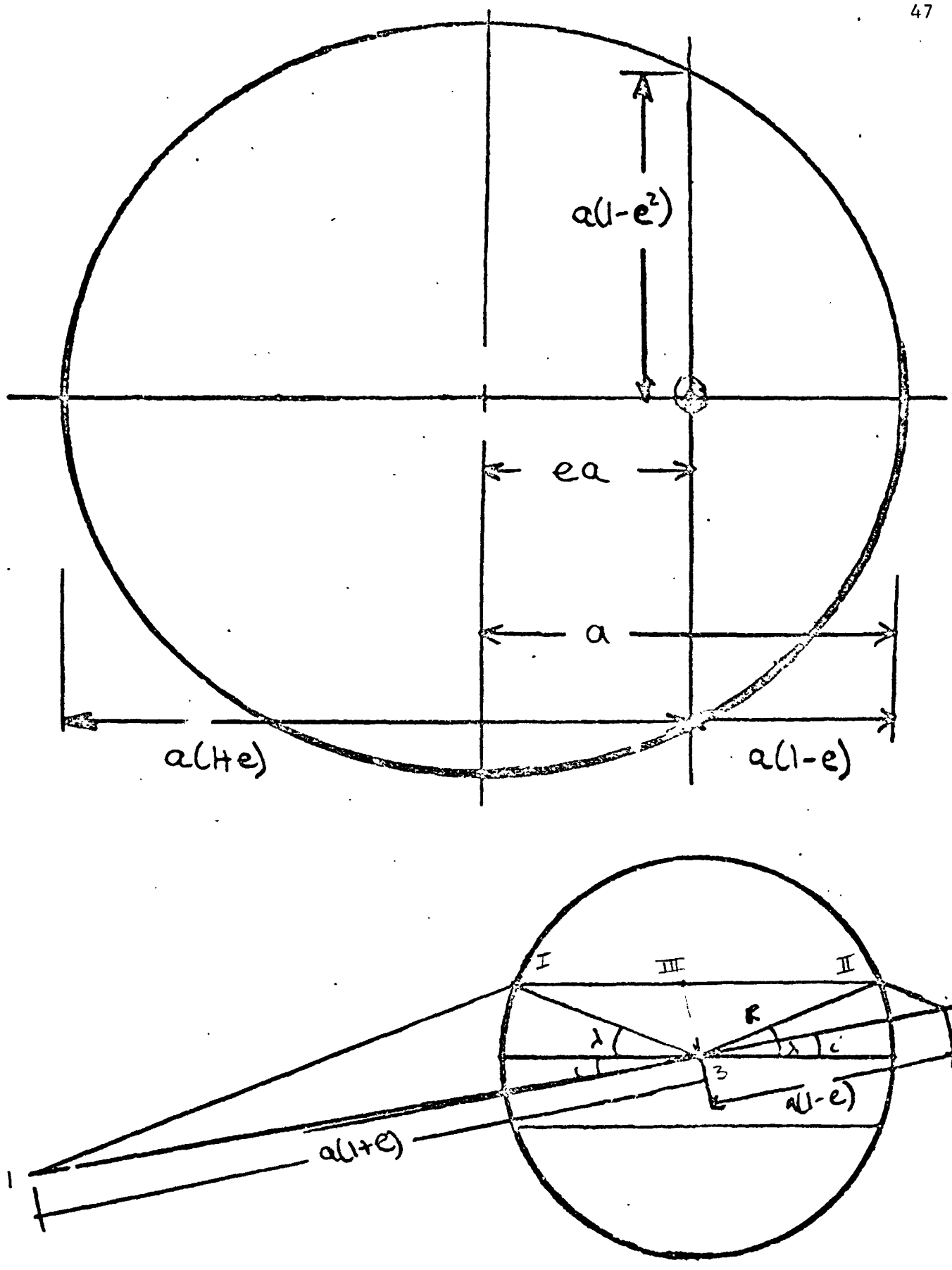

FIG. 13

VISIBILITY GEOMETRY

TABLE I

LIST OF CONSTANTS

SYMBOL	NAME	EQUATION	VALUE	REFERENCE
R	Mars radius	1,2,3,7	3367 km	15
A_{min}	Minimum orbit altitude	9	100 km	-
A_{max}	Maximum orbit altitude	10	6000 km	-
P_{min}	Minimum detectable power	11	$.5 \times 10^{-8}$ watts	9
P_t	Transmitted power of laser	12	5×10^{7} watts	
A_T	Target area on satellite	12,14	2.0×10^{-6} km^2	
θ_t	Transmitted beam divergence	12,14	1.7×10^{-2} rad.	
θ_r	Reflected beam divergence	13,14	$.6 \times 10^{-4}$ rad.	
ϕ_T	Reflector efficiency	14	1.00 rad.	
A_r	Receiver area	13,14	2×10^{-8} km^2	
	Optical efficiency	14	.9	
a	One way atmospheric transmisivity	14	.9	
K	Constant depending on receiver characteristics	15	.4	3
c	Speed of light	15	3×10^{5} km/sec	-
b	Bandwidth	15,16	10^{7} Hz	3
q	Electron charge	16	1.6×10^{-19} coul.	-
n	quantum efficiency	16	.02	4
	Frequency of laser	16	4.32×10^{14} /sec	
h	Planck's constant	16	6.63×10^{-34} joules/sec	
I_d	Receiver dark current	16	8×10^{-14} amps	4
P_B	Background power	16	1×10^{-11} watts	4

TABLE II

RESULTS OF OPTIMIZATION PROGRAM

	Case 1 (constant)	Case 2 (variable)
A	2971.06 km	1921.5 km
	1.16×10^{-4} rad.	5.38×10^{-4} rad.
mse/	24.3	26.15

TABLE III

RESULTS OF VISIBILITY STUDY

	Case 1 (partial visibility)	Case 2 (total visibility	Viking
a (semi-major axis)	15,781 km	23,688 km	20,400
e (eccentricity)	.6649	.7767	.766
i (inclination)	$11^{o}45'25.4"$	$11^{o}45'25.4"$	-20^{o} to +
Periapsis altitude	1921.5 km	1921.5 km	1400 k

constraints. Two cases were investigated. The first assumed that the rover had to be able to see the satellite for the whole orbit. More accurately the rover had to be able to see the orbit so that if the orbiter were in the section visible from that location that rover could communicate with the satellite. The problem of synchronization of the rover and orbiter locations was not considered. The second case assumed that the rover had to see the orbit for only part of the orbit.

The criteria for the first case, total visibility, are seen from Fig.13, to be

$$\alpha(1-e) \geq \frac{R}{\cos(\lambda-i) - \sin(\lambda-i)} \tag{19}$$

and

$$\alpha(1+e) \geq \frac{R}{\cos(\lambda+i) - \sin(\lambda+i)} \tag{20}$$

which are derived using the end points of the orbit, i.e. points I and 1, and II and 2. The criteria for partial visibility can likewise be found using points I and 1, and III and 3. Point III is located so that it is the minimum distance from point 3 on the latitude. These criteria can be written

$$\alpha(1-e) \geq \frac{R}{\cos(\lambda-i) - \sin(\lambda-i)} \tag{21}$$

and

$$\alpha(1-e^2) \geq \frac{R}{\sqrt{1 - \sin^2\lambda\cos^2 i} - \sin\lambda\cos i} \tag{22}$$

Where to guarantee that a solution is possible

$$\lambda + i \leq 45^\circ \tag{23}$$

for the total visibility case. For the partial visibility case

$$\cos i \sin\lambda \leq \sqrt{2}/2 \tag{24}$$

must hold.

Instead of solving that problem as a nonlinear programming problem, it was decided to make some reasonable approximations to arrive at a simplified algebraic solution. First, we assume that we only want to minimize that location error at one point, periapsis. From this approximation we see that

$$\lambda - i = \gamma_{opt} \tag{25}$$

where λ is the latitude of the rover and γopt is the optimal distance that the rover should be from the orbital plane. This also indicates that

$$a(1-e) = R + A_{opt} \tag{26}$$

where A_{opt} is the optimal altitude of the satellite at periapsis. To solve for the orbital inclination i, we must specify the rover latitude λ then the inclination is given from equation (25). For total visibility equations (20) and (26) must be simultaneously solved for a and e. Likewise for partial visibility equations (22) and (26) must be solved to obtain the a and e which correspond to that case.

For λ equal to 30 degrees and using the optimal geometry for the variable $\Delta\tilde{\rho}^2$ case the results of this visibility study is shown in Table III. Also included for comparison in that table are the design parameters for a Viking mission taken from Ref. 14. It is noted that the orbital parameters for the navigation scheme are reasonable when compared to the Viking parameters. Also because the Viking parameters are for an eliptical synchronous orbit, it would be better to use that orbit for the satellite. The use of a synchronous orbit simplifies the problem of timing of the distance measurements to the time when the satellite is visible. The slight loss of accuracy in the location process is most likely worth the simplification of the measurement problem. That this loss would indeed be small is noted in Table II. For the large change in the altitude A the change in the ratio mse/$\Delta\tilde{\rho}^2$ is rather small.

Equation (6) is really only the part of the mse that is a function of the geometry of the relative satellite and rover locations. There is also a term that is constant for any geometry that refers to the error caused in locating the rover that is due to the error in the prediction of the satellite position. This term is derived in Ref. 1 and 2. Thus the mse rover location can be approximated as

$$\text{mse} = 26\,\Delta\tilde{\rho}^2 + 3\,\Delta\tilde{s}^2 \tag{27}$$

In general the $\Delta\tilde{\rho}^2$ is in the order of a few meters. The satellite however can be located to only within a few kilometers. So the dominant error in the location scheme is due to the error in the satellite location $\Delta\tilde{s}^2$. However, even with this large satellite error the error in locating the rover is only about 15 kilometers. Earth based schemes given in Ref. 14 are able to locate the rover to within about 50-60 kilometers showing that the satellite navigation system is still an improvement over earth based systems.

At the present time effort is being devoted to reducing the error that is due to the satellite error. A final report covering all phases of the research into the use of a satellite navigation system is scheduled to be completed in the late spring.

Task C.1.b. Range Measurement and Satellite Tracking - G. Zuraski
Faculty Advisor: Prof. C. N. Shen

A satellite navigation scheme for the Martian rover requires the measurement of the distance between the rover and the satellite in order to locate the rover in a Mars reference frame, Ref. 10. The distance to be measured is of the order of several thousand kilometers and must be measured to within several meters. A laser range finder combined with a retroreflecting surface on the satellite will be shown to meet the requirements of the navigation scheme. Of primary concern is the weight and power requirements of the system. An attempt has been made to include as many factors as possible in the calculation of the power requirements for a given accuracy while at the same time using as simple a system as possible for reliability.

It is also possible to use the same laser range finder for close range obstacle detection, since the geometric power loss resulting from a long range measurement is greater than the reflective power loss from a diffuse target at close range. Problems involved in both close range and long range measurement are being investigated and a mathematical model of the range finding system is being developed.

The measurement procedure is initiated by a trigger pulse from the on-board computer. The trigger pulse causes the laser to fire a single short pulse of light, Fig. 14. A small photodetector mounted on the laser senses the leading edge of the light pulse and starts the counter. The light travels to the target, is reflected, and returns to the light receiver. The light receiver collects light and focuses it on a second photodetector which stops the counter. The counter now contains a number which is proportional to the distance between the range finder and the target. The on-board computer reads out this number and computes the one-way range from the following simple equation:

$$R = \frac{cnT}{2}$$

where

R = Distance to the target (km)
c = Speed of light (km/sec.)
n = Number contained in the counter
T = Period of the counter clock (sec.)

For $T = 10^{-9}$ sec., $c = 3\times10^{8}$ m/sec., and $n = 1.33\times10^{7}$ the range is

$$R = \frac{(3\times10^{8})(1.33\times10^{7})(10^{-9})}{3} = 2000 \text{ km.}$$

Note that the counter must be 8 decades long in order to record n.

The range error is primarily a function of the counter clock period, the pulse width of the laser, the signal-to-noise ratio at the receiver, variation in the speed of light passing through atmosphere, and refraction, A. The range error due to the pulse width of the laser and the signal-to-noise ratio can be derived as follows. The laser pulse width is τ, and has a spectrum of width Δf. Assume the noise is gaussian and occupies the same frequency band Δf. It can now be shown, Ref. 16, that the range error is zero mean gaussian with standard deviations given by:

$$\sqrt{\overline{(R)^2}} = \frac{c}{4\pi B\sqrt{S/N}} \qquad (1)$$

where S/N = Signal-to-noise ratio in energy
B = Second moment of the transmitted spectrum

Note that if the transmitted spectrum is bell shaped, then $2B = f$ and if the spectrum is rectangular, $2B = \Delta f/\sqrt{3}$. Note also that Equation (1) does not hold if the signal-to-noise ratio is sufficiently small. As an example, consider the case where the laser pulse envelope can be approximated by $\frac{\sin 2\pi t/\tau}{2\pi t/\tau}$, where τ is the laser pulse width and t is time. The corresponding spectrum is rectangular of width $\Delta f = 2/\tau$. For $\tau = 10$ nsec, $\Delta f = 2\times10^8$ Hz. Since the spectrum is rectangular, $B = \Delta f/2\sqrt{3}$. For S/N = 10, and $c = 3\times10^8$ m/sec., $\sqrt{(R)^2} = 13$ cm.

The signal-to-noise ratio for a photomultiplier tube can be expressed as, Ref. 17:

$$S/N = \frac{\left[\frac{q\eta P_r}{h\nu}\right]^2 M^2}{b\left[\frac{2kT}{R_{eq}} + 1gM^2\left(\frac{q\eta P_r}{h\nu} + \frac{q\eta P_B}{h\nu} + I_d\right)\right]} \qquad (2)$$

where
q = Electron charge (coul.)
η = Quantum efficiency of photomultiplier
h = Planck's constant (joules-sec.)
ν = Frequency of radiation (sec^{-1})
P_r = Received power (watts)
M = Internal signal multiplication factor
b = Bandwidth (Hz)
k = Boltzman constant
T = Temperature (^oK)
R_{eq} = Equivalent load resistance (ohms)
P_B = Background power falling on the detector (watts)
I_d = Dark current (amps)

A similar expression exists for photodiodes, the difference being that several of the terms have different exponents. The first term in the denominator of Equation (2) represents thermal noise and is generally insignificant in a well designed photomultiplier. The last three terms represent shot noise from the received signal, the background signal, and the dark current. The background signal can be minimized by use of a narrowband light filter. For $b = 10^7$ Hz, $\eta = .02$, $M = 4.7\times10^6$, $\gamma = 4.32\times10^{14}$ Hz, $q = 1.6\times10^{-19}$ coul., $h = 6.63\times10^{-34}$ joule-sec., $I_d = 8\times10^{-14}$ amp, $P_r = .6\times10^{-8}$ watts, negligible background radiation, and shot noise limited operation, S/N = 10. This example is typical of an S-20 photomultiplier, Ref. 17.

The quantization error due to the clock period, T, of the counter can be expressed as:

$$R_{max} = cT$$

Since nanosecond counters are available, this error is small ($\Delta R_{max} = 30$ cm for T = 1 nsec) and will not be considered further.

The velocity of light, c, varies with the properties of the medium. For example, the velocity of light in vacuum and the velocity of light in air at STP agree only to about one part in a thousand, Ref. 18. The velocity of light in a vacuum is known to one part in 10^6. The velocity of light in the Martian atmosphere can be approximated if the atmospheric composition can be determined and the range error can then be estimated as a function of the path length through the atmosphere. More work will be done on this in the future.

The error due to refraction for a horizontal measurement is illustrated in Fig. 15. It can be shown that, Ref. 19

$$\rho = -1/(dm/dh)$$

where

ρ = Radius of curvature
m = Refractive index
h = Height

Also, $2\epsilon = \tau$

where ϵ and τ are shown in Fig. 15

$$\epsilon = -\frac{R_0}{2}\frac{dm}{dh}$$

where R_0 = True distance

The displacement of the spot on the receiving plane is:

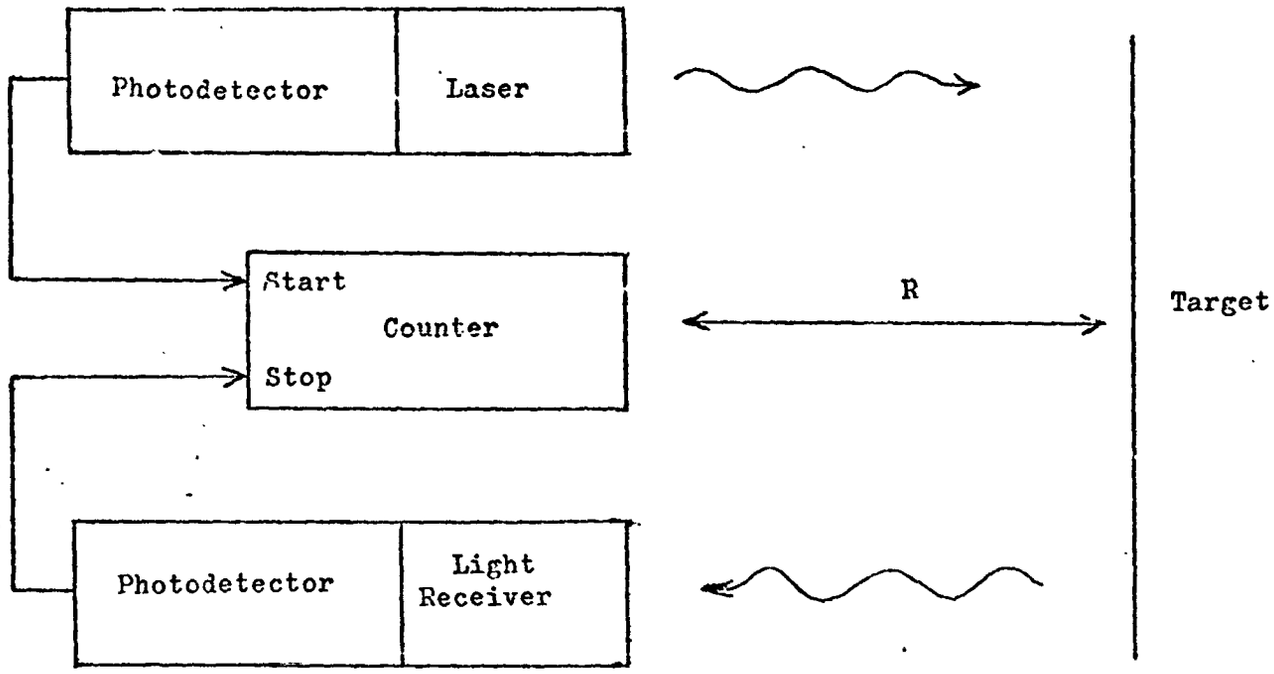

Figure 14 Laser Rangefinder

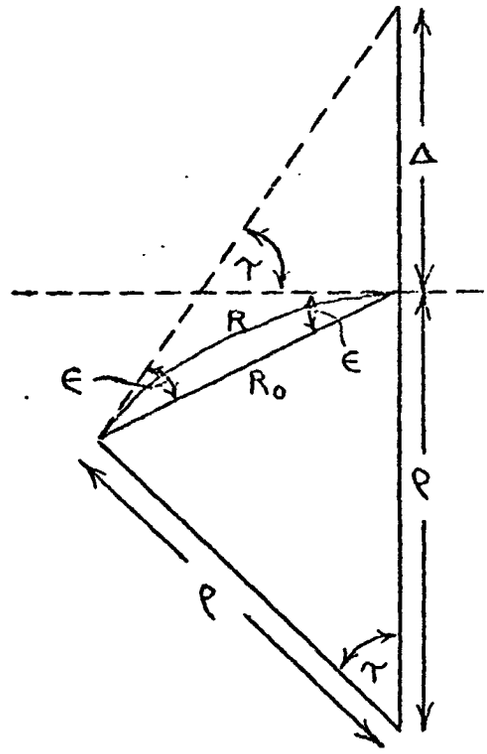

Figure 15 Refraction

ϵ has been measured to be as large as 40 μrad/km on earth, and Δ is typically 1.35 m for a 10 km measurement distance on earth. An estimate of this effect will be carried out for the Martian atmosphere in future work.

The power output required of the laser can be determined from the minimum detectable received power and the power losses along the transmission path. The transmitted power and received power are related by

$$P_r = \frac{\mu \phi_a^2 \phi_T A_r A_T}{\pi^2 \phi_r^2 \phi_t^2 R^4} P_t \qquad (3)$$

where P_r = Power received (watts)
μ = Efficiency of the optics
ϕ_a = One-way atmospheric loss
ϕ_T = Reflective loss
A_r = Receiver area (km^2)
A_T = Target area (km^2)
ϕ_r = Returned beam divergence angle (rad)
ϕ_t = Transmitted beam divergence angle (rad)
P_t = Transmitted power (watts)
R = Range (km)

For $\mu = .9$, $\phi_a^2 = .9$, $A_r = 200\ cm^2$, $\phi_t = 1.7 \times 10^{-2}$ rad., $\phi_r = .6 \times 10^{-4}$ rad., $\phi_T A_T = 2\ m^2$, R = 2000 km:

$$P_r = 1.97 \times 10^{-16} P_t$$

These numbers are typical for measuring the distance to the satellite. Equation 3 was derived on the assumption of a beam of uniform intensity. The output of a single mode laser has a gaussian irradiance distribution which is truncated by the collimating optics.

$$I(r) = \frac{2P \exp(-2r^2/R^2)}{R^2}$$

where r = Radial distance from beam center
P = Laser power
R = Radius at which irradiance falls to e^{-2} times its central value.

If the full beam is transmitted, the full divergence angle in the far field to the e^{-2} irradiance points is:

$$\phi = \frac{2\lambda}{R}$$

where λ = Wavelength of the light.

There is an optimum collimated beam size giving the smallest possible spot at any given distance, Ref. 19. It can also be shown that the largest irradiance results at the center of the received spot for a one-way transmission if the transmitted beam is truncated at the radius where its irradiance has dropped to 8.1% of the maximum value. Due to the motion of the satellite a relativistic effect takes place which results in the return beam being off center. Therefore, it would be desirable to have a flat-topped irradiance distribution. This can be achieved to some extent by choice of the collimating optics. Further work will be done in this area also.

Work done thus far indicates that the range errors in the laser rangefinder are of the order of a meter or less. This is more than adequate for the application considered here. A large portion of the weight of the laser rangefinder is in the power supply capacitors used to fire the laser. As has been shown, the ratio of power transmitted to power received is very great and therefore a high peak transmitted power is required. In order to minimize this power and the weight of the power supply, the beam divergence of the transmitted light must be kept to the minimum necessary to illuminate the satellite. A tracking scheme to locate the satellite within some limits is to be investigated. Shown below is the projected time table.

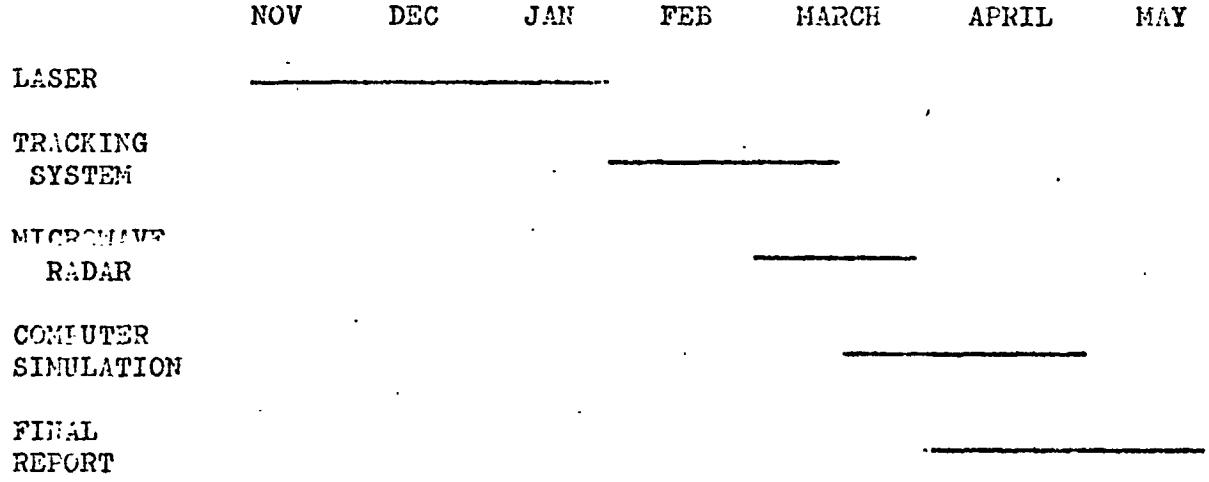

Task C.2. Obstacle Detection Systems

Task C.2.a. Obstacle Detection and Instrumentation - J. Golden
Faculty Advisor: Prof. C. N. Shen

The objective of this task is to develop a short tange obstacle detection system and to define instrumentation requirements for an unmanned Mars rover. Past work, Ref. 9, has described studies of long range navigation (Task C.1.a), medium range terrain sensing and modeling systems as well as a first study of short range terrain and obstacle sensing. As part of this task, an analysis of terrain characteristics was undertaken to provide some rational basis for design of an obstacle detection system. This analysis suggests that mountains and hills, considered as plus obstacles, will tend to be geographically clustered, while craters and other negative obstacles, considered as minus obstacles, will tend to be geographically isolated.

On the basis of this qualitative analysis, it is concluded that a straightforward "walkaround" mode of obstacle detection may well be optimal. System requirements for such a method include 1) constant sensing via discrete measurements and 2) detection of plus- and minus- obstacles at a range of 3 meters. Fig. 16 depicts rover's obstacle detection , with path B illustrating the proposed "walkaround" mode to minimize path length.

Alternatives to the above proposal are 1) an accurate terrain modelling and path selection at short range, and 2) a very short range "emergency stop" mode, possibly in conjunction with one of the other methods. The emphasis of this report is instrumentation for any of the above possible systems.

Instrumentation

A range finder scheme, consisting either of a simple horizontal scan, or a more sophisticated coordinated vertical and horizontal scan (e.g. phased array radar), was considered. The type of scan would be determined from a final decision on the complexity desired, considering the three system alternatives mentioned above. This report begins an analysis of different types of instrumentation, amenable to either instrumentation scheme. Laser, radar and sonar will be investigated, beginning with sonar.

Sonar

The scheme, Ref. 20, will basically operate by transmitting a sound wave of narrow beamwidth forward, and receiving the return pulse some time later. The range then is determined, Ref. 21, by the equation:

$$R = \frac{c\,T}{2} \qquad (1)$$

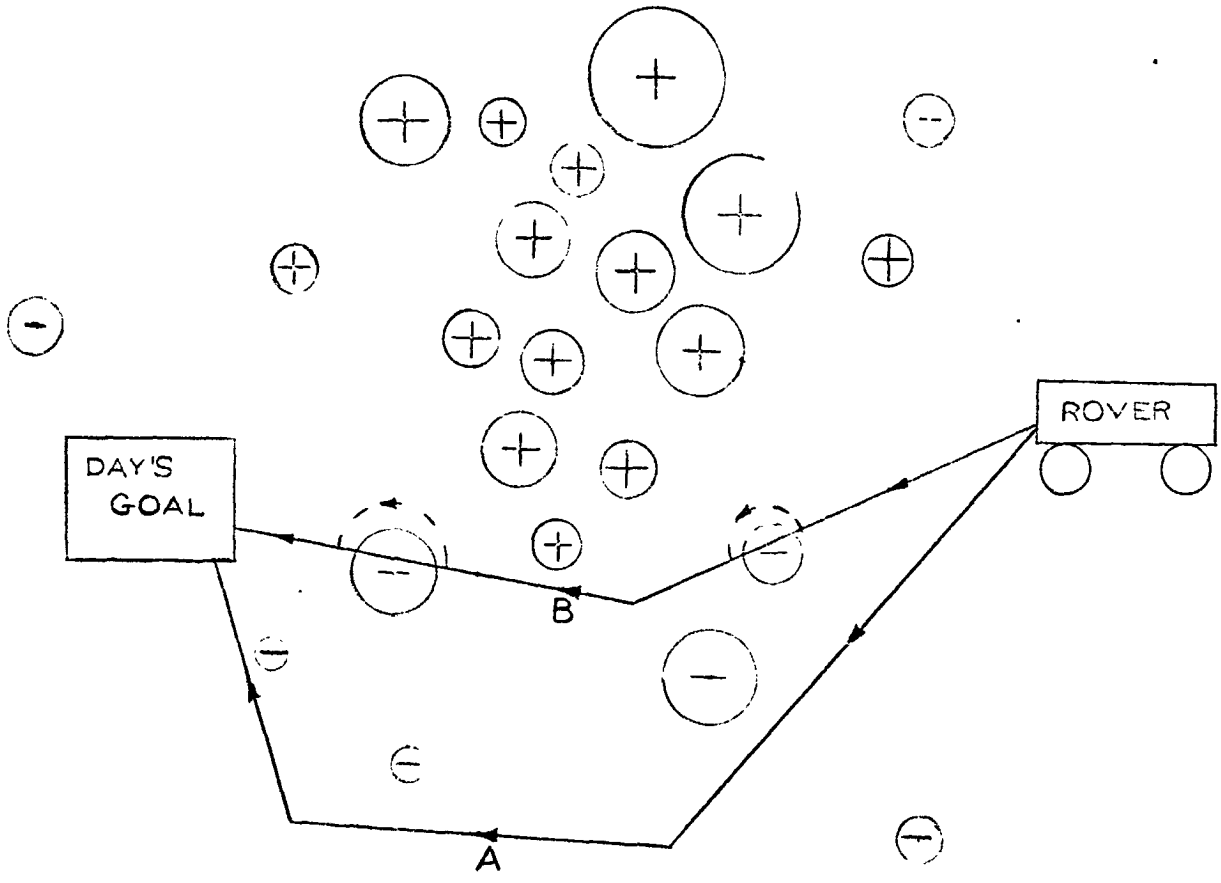

Typical Day's Journey

Figure 16

where
R = range to obstacle
c = speed of sound
T = time of echo, measured by a digital counter

The angle at which the obstacle is located will be determined by the angle at which the sensor is turned at the time of reception. The parameters of range and one angle (or two angles, in the horizontal and vertical scan technique) will suffice to define the location of the obstacle.

Note also that there is an inherent quantization error due to the time increments of the digital counter used, obeying the relation:

$$\Delta R = \frac{c \Delta T}{2} \tag{2}$$

where ΔT = increments of the digital counter
and ΔR = error in range measurement

To investigate this error further, the speed of sound, Ref. 22, on Mars will now be calculated, according to the formula (valid for ideal gases):

$$c = (a B t)^{\frac{1}{2}} \tag{3}$$

where c = speed of sound
a = constant = 1.29 on Mars
B = gas constant = $\frac{35.12 \text{ joule}}{\text{lbm-deg R}}$
t = temperature, absolute = 360 deg R on Mars

The above values were predictions based on a model of the Martian atmosphere composed of 100% CO_2, Ref. 23. With these values, we find:

$$c = \left((1.29)\ \frac{(35.12 \text{ joule})}{(\text{lbm-deg R})}\ \frac{(32 \text{ ft-lbm})}{(\text{sec}^2 \text{ lbf})}\ (360 \text{ deg R})\right)^{\frac{1}{2}}$$

$$= 723 \frac{\text{ft}}{\text{sec}} = 220 \frac{\text{meter}}{\text{sec}}$$

Referring now to the previous equation for quantization error, notice that for a reasonable error (say R = 4 inches), a digital counter with increments of 1 millisecond is required for a sonar system. For a laser or radar system, the increments would have to be 1 nanosecond or less for the same low error, because the speed of light is so much larger. This represents a much more sophisticated counter.

The disparate speeds of sound and light have other ramifications on the choosing of an instrumentation. Considering the range equation (1) and the speed of sound equation (3), a typical measurement at a range of 3 meters takes 27 milliseconds.

Therefore the period associated with the sonar pulse train would have to be about 100 milliseconds. During each horizontal scan, we assume that rover has progressed 1 meter, or less, to insure that the scan doesn't miss many obstacles. Assuming rover moves at 1 meter/second, then, the time associated with each scan is 1 second. For sonar, this means only 10 measurements can be taken per scan, whereas electromagnetic methods would allow about 10 million measurements. It is likely that 10 measurements per scan would be insufficient data to construct an accurate model of the terrain, as required in a complex obstacle detection method, e.g. a coordinated vertical and horizontal scan. For a simple "walkaround" mode, or "emergency stop" mode, 10 measurements would give sufficient data to work with. Therefore sonar is restricted to being used on the less complex navigation methods.

Power considerations are very important, and can be investigated by using the radar range equation, Ref. 21:

$$P_r = \frac{K P_t}{\lambda^2 R^4} \tag{4}$$

where P_r = power received (see Fig. 17)

P_t = power transmitted

λ = wavelength of wave

R = range to obstacle

K = constant

The wavelength of a typical radar or sonar system is close, about 10^{-2} meters, Ref. 24 and 25, but the much smaller wavelength of a laser, 4×10^{-7} meters, Ref. 25, indicates an advantage for laser systems. But preliminary investigations show that the attenuation of a wave by dust particles in the Martian atmosphere is a function of the wavelength, with lower wavelength waves introducing greater attenuation, Ref. 21. In order to accommodate these conflicting trends, the object of future work will be to determine a likely minimum value for power received, based on a typical minimum detectable signal-to-noise ratio, say 10 db. After this, a minimum transmitted power will be determined from the above equation for each type system. Finally, the power requirement will be found from:

$$p_t = \text{efficiency} \times \text{Power Input} \tag{5}$$

where the efficiency will take on values of typical sonar, laser and radar systems. Last, power requirements can be compared and a judgment made.

As a note on sonar systems, the size of the transmitter may prove to be a factor in choosing or scrapping sonar. At the least, special design may have to be made for a suitable transducer. The reason for these complications is the low

acoustic impedance on Mars, i.e., the product of the speed of sound and the density. Consider the intensity of a sound wave in the Martian atmosphere. Its power is given by Ref. 24 as:

$$P_t = \frac{1}{2} \rho c A \omega^2 a^2 \qquad (6)$$

where P_t = power transmitted
ρ = density
c = speed of sound (Ref. to Fig. 18)
A = area of transmitter
ω = frequency of transmitted wave
a = amplitude of vibration

On Mars, the factor ρc is very small, only .1% its value on Earth, Ref. 4. Therefore, to insure sufficient power, the size of the transmitter may prove to be too large, considering the above equation.

To get some estimate of the transmitter size required, the above equation is solved for the required area of the speaker to insure a transmitter power of 10 watts. A frequency of 1 kHz is assumed, and a vibration amplitude of .01 ft. = .003 meter. Equation (6) becomes:

$$10\ W = \frac{1}{2}\ (3.59 \times 10^{-6}\ slug/ft^3)(723\ ft/sec)(2\ \ 1kHz)^2(.01\ ft)^2\ A$$

Solving for A, we find that the transmitter area required is 1.44 ft^2, which is not an unreasonable size.

The actual error equation involves another term besides the quantization error:

$$R = \frac{c \Delta T}{2} + \frac{T \Delta c}{2} \qquad (7)$$

The deviation in the speed of sound is an important factor on Mars because of the substantial wind velocity ~ 57 $\frac{meters}{sec}$, from Ref. 23. The effect of the wind would cause errors in range, according to the above equation. Also, errors in angles would be present, due to refraction of the sound wave. These effects would be large, but could be compensated by installing a wind meter on the rover to approximate, possibly using a Taylor Series, the wind along the path of the sound wave. A computer could then vectorially correct for the effect of the wind.

Calibration of the equipment is recommended to determine the unknown speed of sound, instead of trying to derive accurate atmospheric parameters and using a previous equation to find c. This calibration could be made by aiming the sensor at a point on the rover, a known distance away, then measuring the corresponding time of the echo to determine c, the speed of sound. This calibration method would be superior to an equation

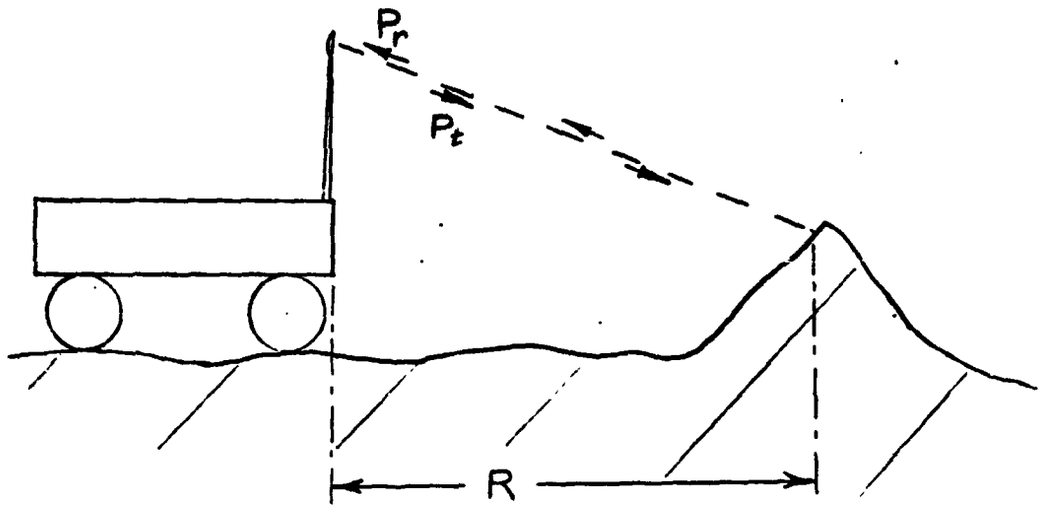

Rover scanning terrain

Figure 17

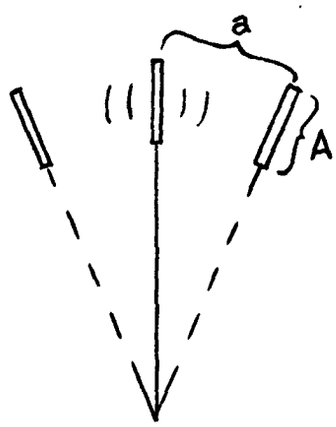

Vibrating reed

(idealization of sonar transmitter)

Figure 18

method, because it would probably be more accurate. Also, by repeatedly calibrating, a good value for c could be found without resorting to its dependence on temperature, pressure, etc.

A final evaluation of a sonar system will be made as investigations are begun on radar and laser, in coming months. One possibility that is being considered, should sonar fail to be optimal for SRN methods because of low accuracy, is to use a sonar system in an "emergency stop" capability. This capability would allow obstacles that somehow sneaked past the SRN, to be detected in time to avoid damage to the rover. Work to be pursued in the future is indicated below.

FUTURE SCHEDULE

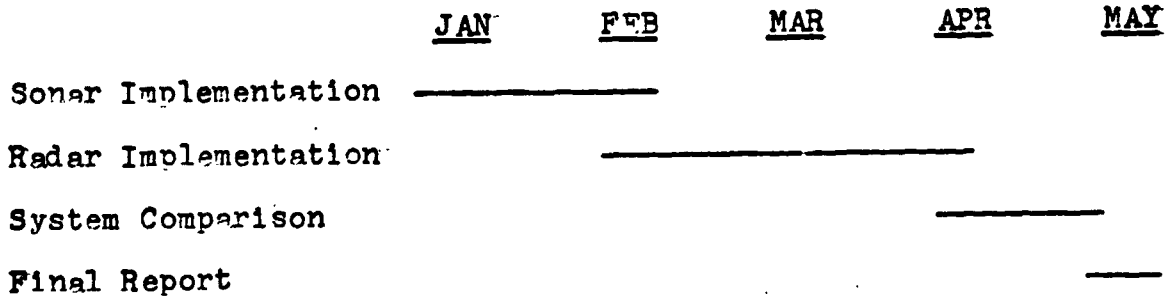

Task C.2.b. Obstacle Detection System - William Mounce
Faculty Advisor: Prof. C. N. Shen

An autonomous Martian roving vehicle must have the ability to detect and avoid obstacles dangerous to its safety such as boulders, craters, and crevaces, as it moves across the surface of the planet. The detection system would be concerned with the range 3 meters to 30 meters in front of the vehicle and should operate continuously so as to avoid frequent data stops which waste mission time. The system must also conform to the size, weight, power, and computer space limitations of a feasible space vehicle while insuring vehicle safety.

As a precurser to the study of this problem, all available reports on past work in the area of navigation were studied to determine what proposals had been considered, what problems were encountered, and what type system environment was most likely. This last area included consideration of systems already needed by the rover for possible double usage, such as use of the on-board television camera for obstacle detection, and resulted in the discovery of a possible solution to another part of the navigation problem; the use of the rover's high gain communications antenna direction to update the reference direction of the rover's gyro-compass, Ref. 26. Because of its potential value as either a primary or a back-up system, a brief study was initiated to determine the value of future study into the scheme. A system which accurately aligned the antenna, Ref. 27, on a tone sent from earth would

combine this direction with the local vertical and the position of the earth to determine a reference direction. The reference corrections would take place at rover science stops when the antenna must be pointed at earth anyway, and could refer to either astronomical data or rover generated earth position data from a known rover position. This system has a long way to go before it reaches final form, but it is definitely an area of future interest.

On the obstacle detection problem the past work consisted of studies in two areas: a short range optical obstacle detection, and a terrain modeling and path selection algorithm scheme for the longer range problem of avoiding hills and large depressions, Ref. 28. An attempt was made by Rautio, Ref. 29, to adopt this longer range scheme to the short range problem but several difficulties were encountered: the gradient output of the algorithm was very inaccurate when dealing with fractions of meters, the system was overly sensitive to elevation angle and ranging errors, a prohibitive amount of computer memory was necessary to adequately define the terrain, and the rover had to be stationary to provide a fixed data base, Ref. 29. These studies showed the need for a completely different approach to the short range problem.

The physical constraints under which any detection system must operate are not specified yet, but two preliminary designs are available which will probably be close to the final rover, Ref. 26 and 29:

Rover Speed	13.9 cm/sec			
" Width	-2 meters			
" Length	-3 meters			
Sensor Height	2-3 meters			
Step Height Max.	43 cm	R.P.I. Rover	40.64 cm	NASA Rover
Crevace Max	86 cm		81.28 cm	

The last two parameters are based solely on wheel dimensions and do not include the ability of the NASA vehicle to "push" itself up over some obstacles. These parameters set a limit on sensor resolutions, thus forming the main basis for design.

A possible system which avoids the problems encountered in the previous studies would employ a highly directional range finder, probably a laser, which would sweep the area in front of the rover at a fixed distance with a split beam which hits the surface at two points, as in Fig. 19. The fixed range gives the system simplicity by precluding the need for a complicated vertical scan pattern necessary to insure that no obstacle disappears between adjacent beams. Each split pulse of the range finder would have two returns separated by a time lag determined by the beam elevation angle and the nature of the terrain. The comparison of the return times will give sufficient indication of the slope of the terrain such that,

if a discontinuity such as a boulder or crater were present, the variation from the time difference of the return from a flat plane would signal an obstacle, as shown by Fig. 20. The angular distance between the two elements of the split beam in the vertical plane is determined by either the desired step height detected or crevace width detected; whichever gives the most desirable performance. The horizontal sweep, as shown in Fig. 21, should be as fast as practical so that the area in front of the rover is carefully searched, but it must be at least fast enough so that there is overlapping coverage in spite of the rover's forward motion so that no terrain is missed if the rover rolls up over a small rise.

A preliminary design of this system which swept the terrain 7 meters from the vehicle using a sensor 3 meters above ground and a horizontal beam spacing of .75 cm gave the following results:

Beam Elevation:	lower 70.5° / upper 72°	$\Delta\theta = 1.5°$
Beam Length	lower 9.018 m / upper 9.726 m	$\Delta\ell = .708$m
Flat Plane t:	4.72 n sec.	
Threshold :	4.6 n sec.	
Step Detection:	25 cm.	

The horizontal spacing was set at 75 cm so that no crevaces could escape between the beam elements, but if the sweep rate in the horizontal plane is sufficiently fast, this restriction may be relaxed and the beam split could be set by the step height detection desired.

Once a discontinuity is detected, a flag set on that azimuth in the computer memory would define it as a dangerous direction and the rover would start turning away in a direction determined by the obstacle location and the desired heading. The horizontal sweep must be sufficiently wide so that the rover can swing around an obstacle without leaving the area scanned by the detector. If the obstacle is too large to avoid by a small shift in direction, the rover must stop, reverse at an angle such that the sensor scan is within the previously scanned region, and then proceed off in a new direction, "feeling" its way around the obstacle, Ref. 30.

The main advantage of this system is its continuity; the comparison scheme allows operation in spite of vehicle motion. The amount of added instrumentation should not be large and little computer space is necessary compared with the large memory requirements of a terrain mapping scheme.

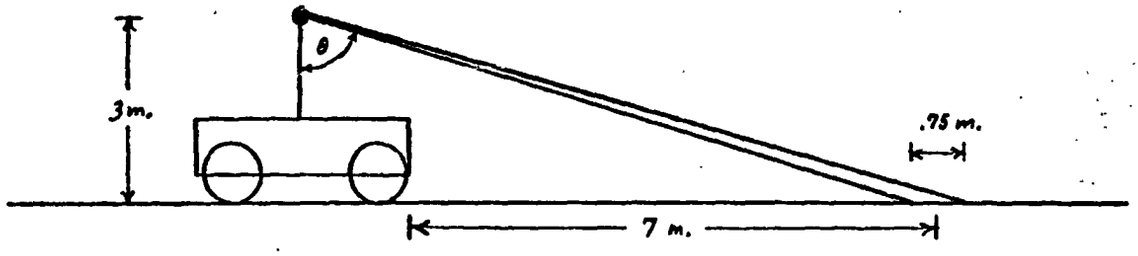

Fig. 19 - Preliminary Design

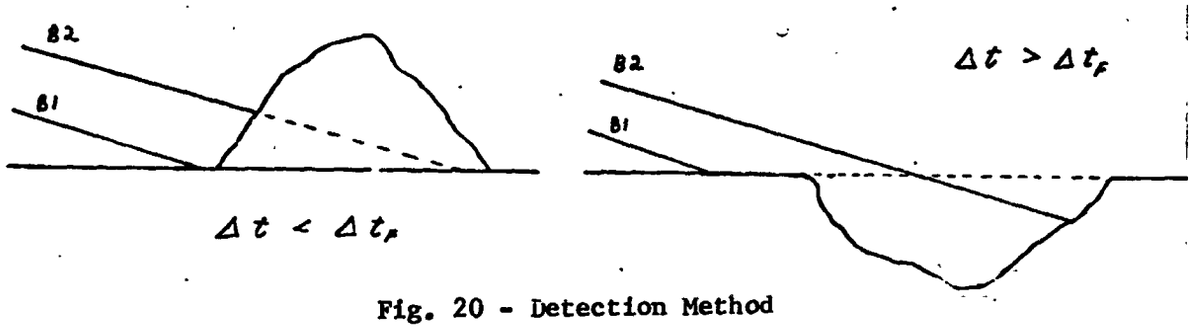

Fig. 20 - Detection Method

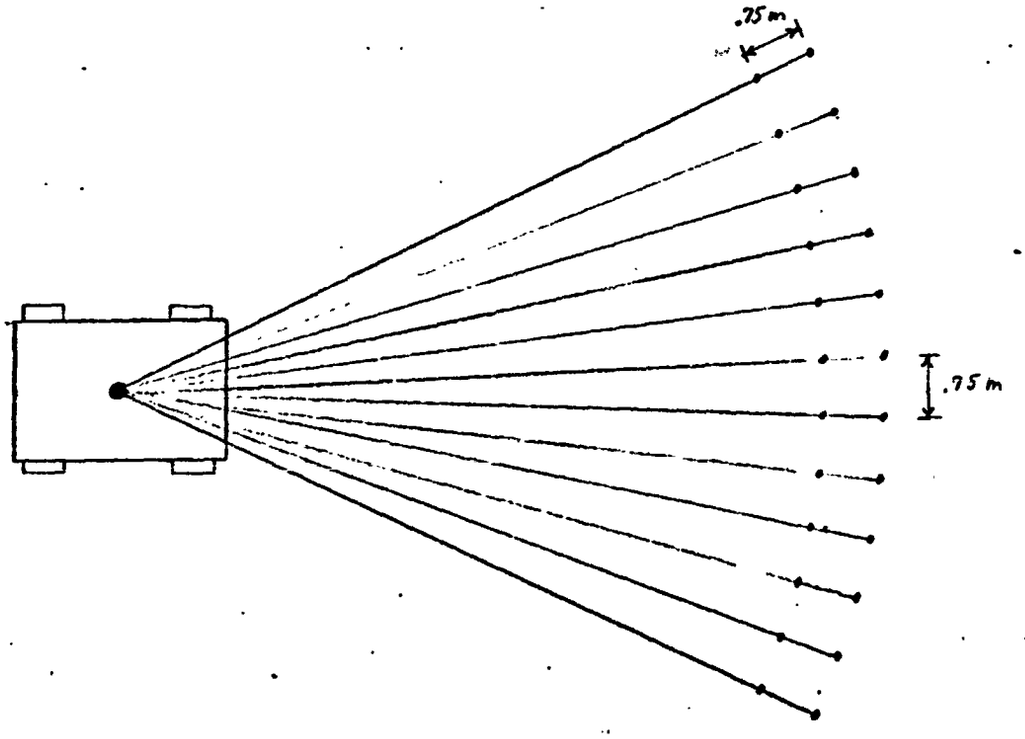

Fig. 21 - Scan Pattern

The schedule of future work will include choice of optimum scan distance and beam split, determination of the best scan rate, solution of the received response problem, refinement of the path decision algorithm, and choice of laser instrumentation, the last of which hopefully including some laboratory testing of the system.

PROJECT TIMETABLE

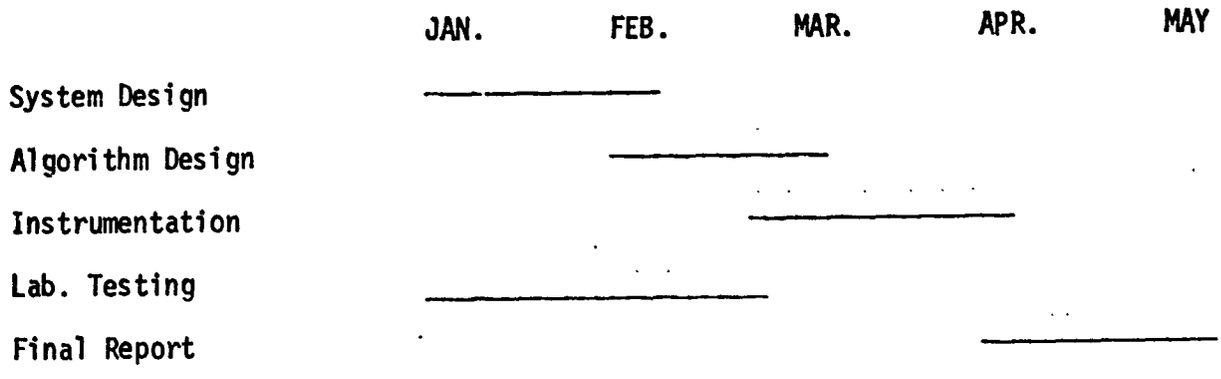

Task C.3. Terrain Modeling and Path Selection System Evaluation -
S. Boheim, W. Purdon
Faculty Advisor: Prof. D. K. Frederick

Previous efforts concerning this area of investigation have concentrated upon the development of a terrain modeling system, including analysis of the effects of sensor error on the model, and upon studies of path selection algorithm characteristics. One study did involve the integration of terrain modeling and path selection systems for the purpose of algorithm performance evaluation, Ref. 28. However, these works have been mainly applicable to a long range obstacle detection system, e.g., 50 to 1500 meters, and have no included quantitative criteria for performance evaluation.

The objective of the present effort is twofold. The first is the development of a computer package which will provide the capability of dynamically simulating a wide variety of sensor, terrain modeling, and path selection algorithm combinations. The second is the generation of criteria for the quantitative evaluation and comparison of the system's performance. It is anticipated that the development of a realistic simulation capability is a necessary condition for the establishment of meaningful performance criteria.

Attention will be directed at middle-range, assumed to be 3 to 30 meters, applications as distinct from short range applications using a tactile sensor and the previously studied long-range system.

The progress in the two areas of study is discussed below, followed by a statement of future work and a timetable.

Task C.3.a. Computer Simulation Package

The computer simulation package is to be a self-contained unit. Not only will it simulate the functions of a terrain sensor and modeler, contain a path-selection algorithm, and simulate the vehicle's motion dynamics, but it will also include a mathematical description of a terrain and associated features, and it will execute the evaluation of system performance using the criteria established for this purpose, Task C.3.b. The inclusion of the latter two items in the package should reduce error-prone handwork and will extend considerably the scope of the simulation's evaluation capabilities.

There are two major considerations to be taken into account during the computer package design. First, the flexibility and realism of the simulation are of primary importance. For example, the substitution of alternate path-selection algorithms and sensor schemes based upon conclusions from simulated runs must be conducted with a minimum of reprogramming. Inputing of terrain data must be flexible enough to allow for the evaluation of system performance over a variety of terrain types. Furthermore, the simulation results must be realistic.

As a second consideration, it must be possible to incorporate non-ideal features which will tend to degrade performance. Such additions will enhance the realism of the simulation and improve result reliability. Examples of non-ideal features are: vehicle bounce, slope of terrain at vehicle location, and sensor-reading uncertainty.

The areas of program development in which the efforts have been made to date are discussed below.

Program Structure

In establishing the computer simulation package structure, the approach taken has been to separate logical functions into individual blocks as much as possible. As for the path-selection system itself, the logical functions were divided according to: 1) the sensor operation simulation, 2) the terrain modeling process, using data from the sensor, and 3) the path selection algorithm, which utilizes information from the model to make path-selection decisions. Further, the simulation structure will also include a vehicle dynamics block to represent vehicle's motion.

As stated earlier, the computer package includes a simulated terrain, from which the sensor will obtain its terrain data, and a system evaluation capability, in addition to the simulated path-selection control system. The structure of the package is shown in Fig. 22. Excluding the display functions, which are used for operator visual display of the terrain or model, there are six major blocks.

At this point in time, development has proceeded to flowcharting and some software implementation of the terrain

PROGRAM STRUCTURE

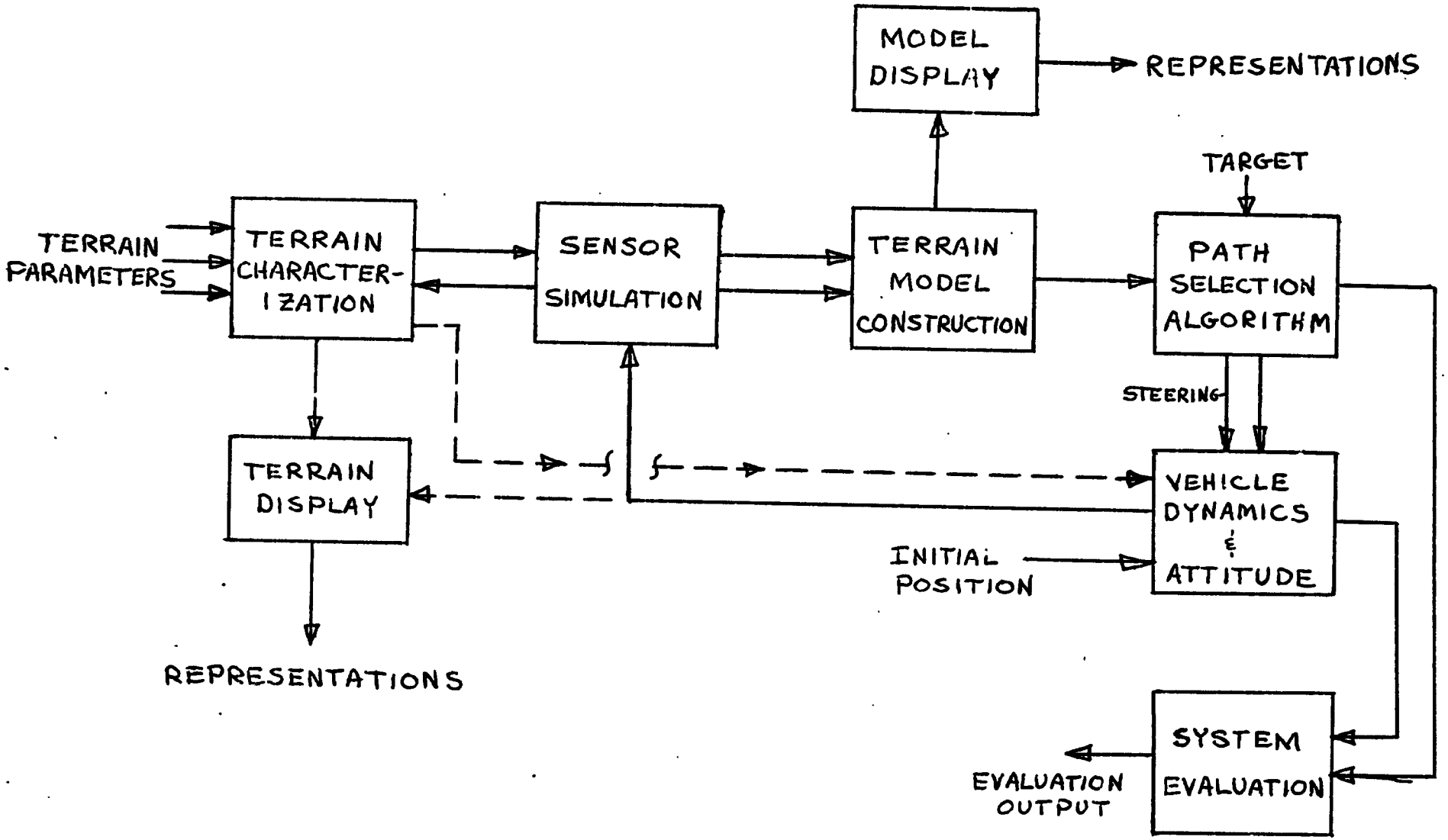

FIGURE 22

characterization and sensor simulation blocks. The objective is to get a simplified system into operation first. Then, sophistication of the system will follow by the addition of refinements and more complex schemes.

Terrain Characterization Block

The initial investigation for the design of this block involved studies of various mathematical approaches to terrain description. The approach settled upon involves utilizing a polynomial (in two independent variables) representation and building Gaussian distributions upon this base. These descriptions are used to convey low frequency features. In addition, a special features input will allow for boulders and crevasses (high frequency components). The computer simulation block will read in data conveying each of the mathematical characterization of the terrain, and will store that information. The block also accepts an input which allows the operator to choose a mathematical terrain characterization type (polynomial, Gaussian, special, combinations of these, etc.) to be used in a simulation run. Once the simulation of a path-selection process begins, the sensor simulation block returns the value of the altitude at that point on the surface, using all of the terrain features specified.

The software development of this block has been completed for a polynomial type terrain description. After the initial development of the entire system has been completed, refinements will involve inclusion of the Gaussian feature and special feature segments.

Sensor Simulation Block

The scheme chosen for an initial development of this block involves a laser beam scanner with zero beamwidth. The vehicle is assumed to be stationary for each scan and there is a uniform time (T) between scans. A single beam is used and discrete samples are taken during each scan. The beam has a fixed attitude with respect to the local vertical.

The block simulates the motion of the beam scan and the impingement of the beam on the terrain. Values for the x and y coordinates along the beam are supplied to the terrain characterization block which in turn generates a value of the altitude (z) of the terrain at the point x,y. This z value is compared with the altitude (z^*) of the beam at the same x,y coordinates above. The process is continued until z^* is sufficiently close to z, Fig. 23. Then this z is taken to be the altitude of the terrain at the point of beam impingement, and the distance from the sensor to the impingement point (range) is calculated.

The output of the block will include the aximuth, elevation and range from the senor to each of the points of impingement

GEOMETRY OF BEAM IMPINGEMENT CALCULATION

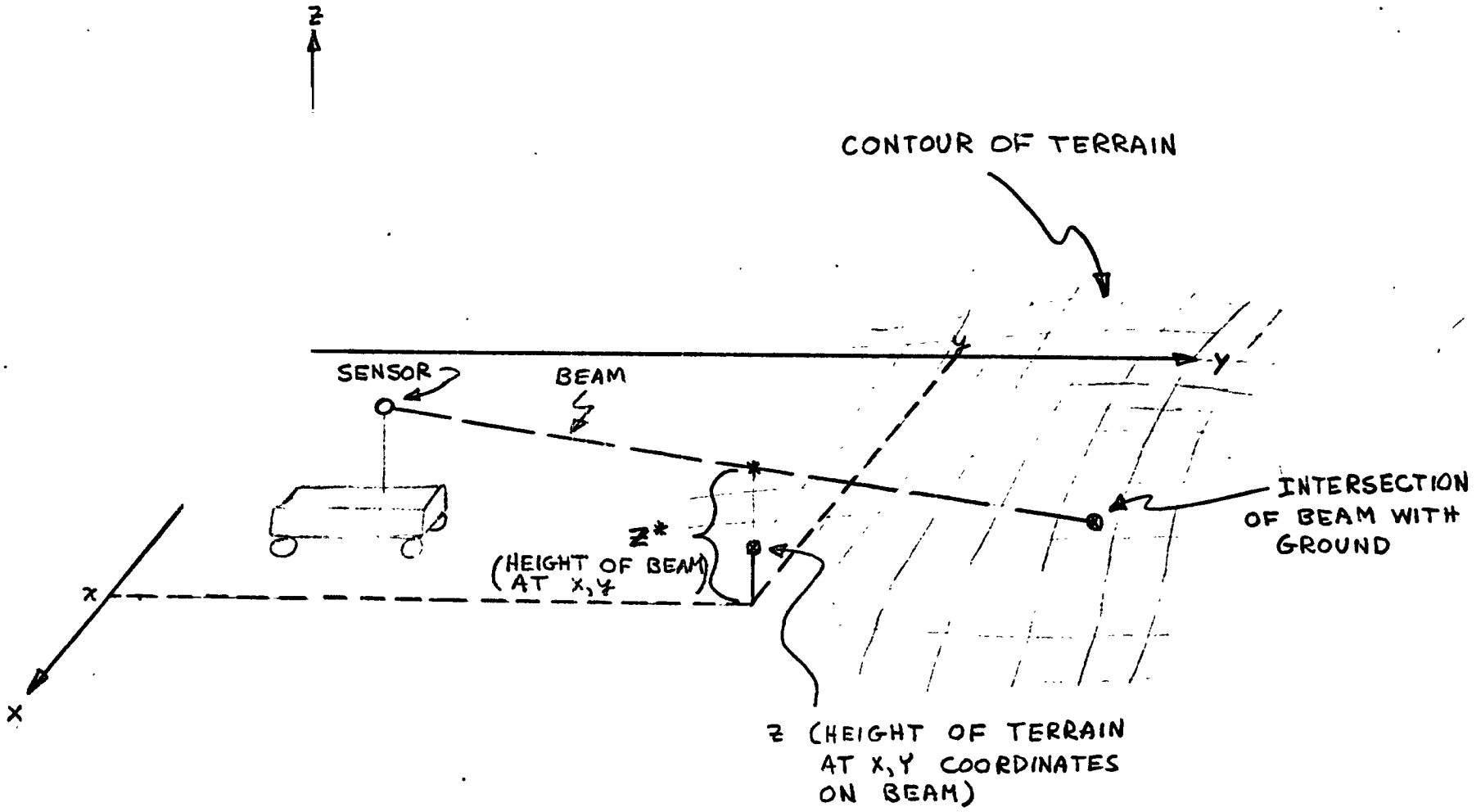

FIGURE 23

along the beam scan. In addition, random uncertainty or error in the measurement of range will be included at a later date.

Subsequent developments will include program sophistications involving memory storage of separate scans, sensor scan degradation due to vehicle attitude, and scan results related to the vehicle's forward motion.

Vehicle Dynamics Block

The purpose of this block is to simulate the motion of the vehicle and to provide the system evaluation block with the necessary information for analysis of the vehicle's motion. In its simplest form, the vehicle dynamics block would use the outputs of the path selection algorithm (i.e., steering commands) and of the terrain characterization block to determine the exact velocity of the vehicle (e.g., steep slopes slow the vehicle down). In its more complex forms, the vehicle dynamics block will include such items as representative dynamic equations of the vehicle and the influence of the tactile sensor, bouncing of the vehicle, etc. Its output will include such information as the velocity and the direction of the vehicle at the next mid-range-sensor scan time, as well as the information mentioned earlier that is being passed to the systems evaluation block.

Task C.3.b. System Evaluation

To develop an effective means for evaluating the performance of the vehicle for various sensor schemes and/or path selection algorithms, both quantitative and heuristic methods of evaluation will be employed.

Quantitative Evaluation

It is desired to describe mathematically as many important features of the total system as possible so as to minimize any discrepancies due to human mis-analysis of the heuristic evaluation results. The following formula was postulated so that important characteristics (features) of a system and their relative importance can be stated analytically:

$$D = \sum_{i=1}^{3} W_i F_i$$

where D - is the degree of effectiveness or measure of desirability of the system,

F_i - are indexes that represent the important characteristics, or features, of the system,

W_i - represent the weights of the corresponding indexes.

Numerically, the indexes are numbers ranging between zero (worst case) and 1.0 (optimum value), the weights range between zero (least important) and 1.0 (most important), and the degree of effectiveness ranges between zero (least desirable) and 1.0 (most desirable). Hence, the sum of the weights must equal 1.0.

If the weights and index are appropriately chosen, then the system that generates the highest value of D, when the above formula is applied, would be the most desirable system. Assuming that the index chosen adequately describe the system, there still remains the selection of the values for the weights. An initial guess followed by a small-scale iterative training procedure will be used. A small number of sensor and path selection algorithm combinations will be inserted into the overall software package, where simulations can be run. The weights will be adjusted until the value of D is proportional to the attractiveness of performance of each of these training combinations. These new weights can then be used to evaluate the performance of other systems.

The actual mechanics of each index must now be considered. Tentatively, it has been decided that three indexes sufficiently describe vehicle performance, and, if certain conditions are set, the number of indexes may be reduced to two. The three indexes are:

1. Path Length - If D_m is the distance between the starting point and the target, and D_e+D_m is the length of the path chosen by the vehicle, then the index $F_1 = \frac{D_m}{D_e+D_m}$ is defined.

2. Battery Energy - If the total time taken by the vehicle to reach its target is called T_e+T_m, and the time that the vehicle uses its batteries is called T_b, then the index

$$F_2 = \frac{T_e+T_m-T_b}{T_e+T_m} \quad \text{is defined.}$$

3. Run Time - If D_m is the distance between the vehicle and the target, and the maximum velocity of the vehicle is V_m, then the minimum time required to reach the target is $D_m/V_m=T_m$. If T_e+T_m is the total time taken by the vehicle to reach its target, then the index

$$F_3 = \frac{T_m}{T_e+T_m} \quad \text{is defined.}$$

The first index penalizes long and/or wandering paths, while the second penalizes the selection of paths that contain steep slopes, forcing the vehicle to rely on its batteries as well as its radiactive thermal generators (RTGS). If the

vehicle must slow down for other reasons besides steep slopes (e.g., tactile sensor contact), then the system will be penalized for this loss of time.

Heuristic Evaluation

Some important characteristics of a system are not easily described in quantitative form, and yet these characteristics seem to require some sort of evaluation. The following two features fit into this non-quantitative category:

1. Safety of Path Selected - Although the safety of the vehicle is of primary importance, it is difficult to analytically describe the inherent danger to the vehicle present in a selected path. What is hoped to be an indication of safety will be implemented by counting the number of times the tactile sensor indicates the vehicle is about to encounter an obstacle.

2. Correct Performance - Situations may arise where the vehicle is called upon to 'not succeed'. For example, if the target is surrounded by an untraversable crevasse, then it would be better for the vehicle to get 'close', rather than attempt to reach the exact target location. This feature is a purely heuristic characteristic, and any evaluation in this area would be performed by humans.

Future Work and Timetable

The dates included in the following are tentative, and the timetable is designed such that it is flexible enough to sustain changes when made.

Initial Simulation Package - This should be completed by February 1. It will contain all the blocks shown in Fig. 22, but will minimize the complexity of each. For example, only a polynomial description will be used in the terrain characterization block, a simplified sensor scheme will be employed, and vehicle bounce will be ignored in this initial package.

Refined Simulation Package - This should be completed by March 1. It will provide refinements in the initial simulation package so that more realistic and/or complete computer simulations may be made. Some of these refinements will include bouncing of the vehicle, sensor measurement errors, and vehicle location errors.

Software Implementation - This should be completed by April 1. By this time, detailed information on all sensor schemes and path selection algorithms to be evaluated will be available and programmed for use in the refined simulation package. Both past and present work in these two areas will be used as sources.

Cumulative Report - This should be completed by late May. Combinations of the various available sensor schemes and path selection algorithms will have been evaluated under different terrain conditions. From these results, information should be obtained which would indicate general desirable characteristics for sensor and path selection algorithm combinations.

Task D. Chromatographic Systems Analyses

One important phase of the initial missions to Mars is the search for organic matter and living organisms on the martian surface. The present concept for attaining this objective consists of subjecting samples of the atmosphere and surface material to certain chemical and biologically-related reactions and thereafter analyzing the products produced, probably in a combination gas chromatograph/mass spectrometer. The gas chromatograph is proposed for separating complex mixtures evolved from the chemical and biological experiments into small groups of similar chemical species. Chemical analysis of these groups would be accomplished in the mass spectrometer.

Most of the previous effort has involved the systems analysis of the gas chromatograph using simulation (1,2). This technique uses mathematical models, which incorporate fundamental parameters evaluated from reported experiments, to explore various concepts and to direct further experimental research.

The objectives of the task have been extended to include preliminary studies of the entire chemical analysis system. In particular, a systematic evaluation of the effects of the chromatograph parameters (carrier gas flow rate, column dimensions, temperature, and particle size) upon system requirements has been started. System topics to be considered include carrier gas generation and removal, sample size and component detectability limits, and limitations imposed by and upon the mass spectrometer.

The task problems are being attacked by a five-member team, each of whom is pursuing a specific assignment:

1. Overall system aspects

    a. Mass spectrometer system characteristics.
    b. Carrier gas generation and removal.
    c. Chromatograph model evaluation using multicomponent chemical systems.
    d. Improvement of the mathematical model of the chromatograph.
    e. Estimation of chromatograph column parameters which appear as constants in the mathematical models.

Task D.1. GC/MS System Concepts

a. Mass Spectrometer System Characteristics - M.P. Badawy
b. Carrier Gas Generation and Removal - C.W. Jarva
Faculty Advisor: Professor P. K. Lashmet

The overall concept of the chemical analysis system is shown

schematically in Fig. 24. The idea of the combined gas chromatograph/mass spectrometer for use in detecting life on other planets has been described by others, Ref. 33, 34, 35. The design of such a system to function in a hostile atmosphere represents a formidable problem which is suitably handled by system modeling and simulation by compter. For simulation to be effective, it is necessary to uniquely describe the important characteristics of the entire system by a minimum number of variables and equations. The development of the governing relations for the system components excluding the gas chromatograph is the initial objective of this subtask.

It is the purpose of the mass spectrometer to provide mass spectra from three different inputs: effluents from the gas chromatograph; direct samples from the life-determing experiments; and samples of the atmosphere. Functional requirements for the Viking mass spectrometer have been defined previously, Ref. 35, 36, 37, and typical specifications appear in Table IV.

Small mass spectrometers suitable for adaptation to the Mars roving lander have been under development, Ref. 33, 36, 38, 39, and prior work is being reviewed to quantitatively represent the various characteristics and limitations of the instrument. Specific topics include the following:

1. Scan rate as affected by the scan method.
2. Resolution.
3. Operating pressure (vacuum) and methods of attaining it.
4. Accelerating potential.
5. Protective devices.
6. System weight and volume.
7. Power requirements.
8. Detection devices for producing output signals.

From the literature, it is evident that the instrument must be multifunctional. For example, McMurray and Green, Ref. 40, report that fast scan rates are not required for high resolution mass spectra whereas low resolution data from fast scan rates may be satisfactory in certain instances. Miniaturization and the resulting problems with the power supply and voltage level are not trivial considerations, judging from the reported catastrophic failure of one instrument under development, Ref. 38. These studies and development programs provide physical limitations of the equipment, a necessary input for proper system analysis. In addition, prior work on mathematically modeling the mass spectrometer, Ref. 34, 41, is being considered as a possible base for the desired system model.

By June 1972, the current studies and literature review should yield qualitative characteristics and quantitative representations of the mass spectrometer suitable for overall systems studies. In addition to the system studies, future work will consider data output characteristics and analysis of mass spectral data based on previous extensive investigations, Ref. 42, 43 and 44.

Carrier gas, which is relatively inert with respect to the samples being analyzed and which must be in supply for an as yet undetermined

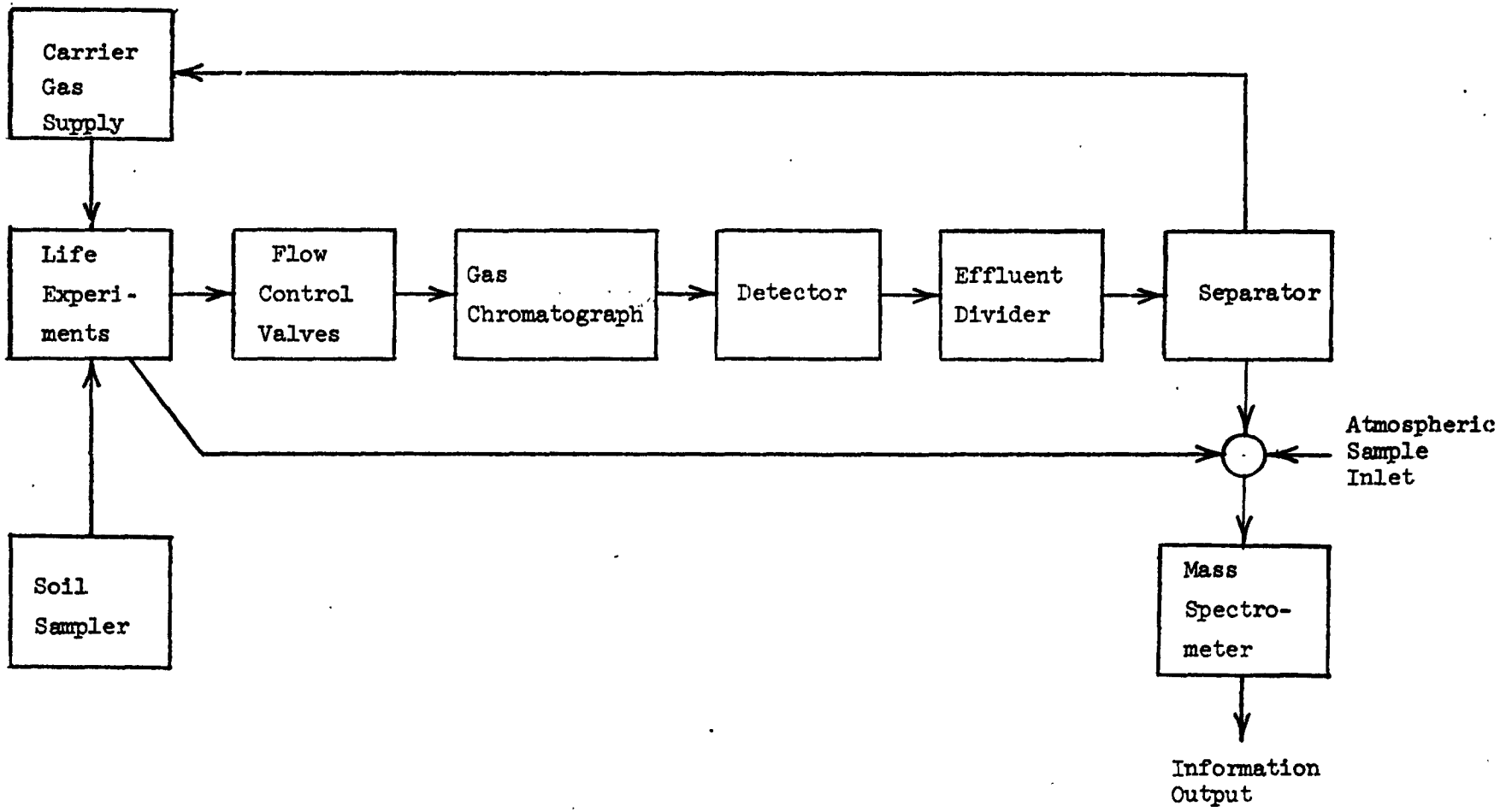

Figure 24

BLOCK DIAGRAM OF GAS CHROMATOGRAPH - MASS SPECTROMETER SUBSYSTEM

TABLE IV

TYPICAL DESIGN SPECIFICATIONS:
MINIATURIZED MASS SPECTROMETER

Mass range	12-200 atomic mass units (AMU)
Mass resolution	$(M/\Delta M)_{10\%\ \text{valley}} = 140$; 12-140 AMU
	$(M/\Delta M)_{20\%\ \text{valley}} = 200$; 140-200 AMU
Sensitivity	2.5×10^{-8} amp/(nanogram/sec) at 200 AMU
Minimum detectable output current	1.0×10^{-11} amp
Dynamic range (maximum peak/minimum peak)	10^5
Maximum ion source pressure	10^{-4} torr
Mass scan rate	53 seconds for 12-200 AMU

time, is required to propel minute samples through the column of the gas chromatograph, Ref. 31. On arriving at the mass spectrometer, which operates at a low pressure (10^{-4} torr), the major portion of this carrier gas must be separated from the sample and must be removed from the system. Thus the systems for generating, separating, and removing the carrier gas are important to overall system design and operation.

The quantity of carrier gas available on the lander depends upon the frequency and time of operation of the chromatograph. For short periods of operation, simple high-pressure gas storage with discharge to the atmosphere after separation from the samples prior to entering the mass spectrometer may be adequate. For more frequent or longer periods of operation, a recycling or regeneration technique appears advantageous. Mechanical pumps and chemical pumps, Ref. 45, offer a possible solution.

Because the operating pressure of the mass spectrometer is about 10^{-7} times the pressure expected in the chromatograph, Ref. 46, a carrier gas removal system must be considered. To maintain an adequate amount of sample for analysis by the mass spectrometer, a technique for concentrating the sample and removing the carrier gas must be provided, Ref. 45, 46, 47. Among the most promising separators, if hydrogen is to be used as a carrier gas, is the palladium-silver alloy membrane which is permeable to hydrogen and a barrier to other chemicals, Ref. 45, 48, 49. In such a system, a pressure gradient is required across the membrane to maintain hydrogen flow, Ref. 50. This might be accomplished by reacting the effluent hydrogen with oxygen and removing the resulting water vapor by adsorption or by ejection to the atmosphere, Ref. 45. Use of the palladium-silver alloy as the cathode and anode in a fuel cell offers an interesting possibility. Hydrogen for carrier gas usage may be generated by water electrolysis and then be recovered via membrane diffusion and reaction with hydroxyl ions in the fuel cell electrolyle as water which can then be re-electrolyzed, Ref. 45, 51.

Although these systems are promising, problems arise because of the structural breakdown of the palladium during temperature and pressure recycling, Ref. 52. Furthermore, contamination by halogens and other chemicals reduce the effectiveness of the membranes, Ref. 51. Other separating techniques such as semipermeable silicone rubber membranes and supersonic (Rjyage) separators have been proposed and their characteristics are being review.

By June 1972, the current studies and literature review should yield the gross characteristics and limitations of possible carrier gas generation and removal systems suitable for the roving vehicle. These results will provide a basis for conducting overall system studies.

Task D.2 Chromatographic Model Evaluation Using Multicomponent Chemical Systems - P. S. Keba
Faculty Advisor: Professor P. K. Lashmet

A mathematical model composed of a system of partial differential

equations was developed earlier to represent the chromatographic column behavior, Ref. 31. Solutions to linearized approximations of the differential equations obtained by classical techniques have been reported, Ref. 53, 54. Because of their complexity, the equations were solved by assuming the sample to be injected as an impulse. Using data obtained from a specially constructed chromatographic test facilty, Ref. 55, Benoit showed that convolution of the input data with the theoretical impulse response gave a reasonable representation for a single component in the system, Ref. 32. It is the objective of this subtask to experimentally verify the mathematical model for multicomponent chemical systems using superposition of single component data. Specifically the simplified equilibrium adsorption model, Ref. 54, is bein considered:

$$Y(\theta) = \sqrt{\beta Pe/4\pi\theta^3}\ \exp\left[-(Pe/4\beta\theta)(\theta-\beta)^2\right]$$

where

β = $1 + (1/mR_0)$

θ = dimensionless time = vt/L

v = carrier gas velocity

t = time

L = column length

Pe = the Peclet number, a dimensionless measure of sample diffusion in the carrier gas

mR_0 = a thermodynamic parameter, peculiar to the specific chemical system considered

Y = composition response to a unit impulse

This model assumes the gas at each point to be in equilibrium with the solid adsorbent; i.e., the column is very long. The Peclet number is predictable since it depends only upon the system configuration and fluid mechanics. The thermodynamic parameter mR_0 is specific to the system used and is determined from the system data using a curve fitting technique.

Prior to experimentation, modifications to the test facility were made to provide more accurate measurement of the carrier gas flow rate and the gas pressure within the chromatographic column. In addition, the single component data of Benoit, Ref. 32, are being recalculated because of a less uncertain correlation for the Peclet number (See Task D.4).

Initial studies of multicomponent chemical systems will involve binary systems and the equilibrium adsorption model. The binary system pentane-heptane as representative of a heavy organic system is being considered first. Later experiments may involve a system of light gases such as ethylene, carbon monoxide, nitrogen, etc. The characteristics

of three different chromatographic columns which will be used in the experiments are given in Table V.

The two primary variables in these studies are composition and temperature with experimental data being taken over the range of 30 to 200 deg. C. The thermodynamic parameter mR_0 may change a factor of 20 over this temperature range, this being a suitable variation for evaluating the model. Variation in sample composition will provide quantitative information about detectability limits as the composition changes from an excess of one component to an excess of the other.

After obtaining and evaluating binary system data, a preliminary computational analysis of the effects of the chromatograph parameters such as carrier gas flow rate, column dimensions, temperature, etc. upon system performance will be initiated. Results from computer simulation using the equilibrium adsorption model will provide background information for the projected system optimization studies.

By June 1972, it is expected that the validity and limitation of superpositioning single component information to obtain multicomponent behavior will be defined. Additionally, initial subsystem studies are expected to have commenced.

Task D.3. Chromatograph Model Improvement - P. T. Woodrow
Faculty Advisor: Professor

In previous work, Benoit, Ref. 32, showed that under certain conditions, as yet undefined, the equilibrium adsorption model represented fairly well single component data provided the input pulse is considered through a convolution procedure. In other instances, however, agreement between the theoretical prediction and experimental data was not as satisfactory. Dispersion in the gas composition exiting the chromatographic column was observed greater than that predicted by the model. It is the objective of this subtask to investigate methods for improving the predictive capability of the model.

A less restrictive solution to the system of partial differential equations was reported earlier, Ref. 56, and was adapted for use in the chromatographic system studies, Ref. 53. This solution does not assume equilibrium adsorption and introduces a dimensionless mass transfer parameter N_{tOG}. This model, which involves the integral of a first-order modified Bessel function and complicated exponentials and which represents the response to an impulse sample injection, was developed before the data reduction program and convolution procedure outlined in Task D.2 were available. Although preliminary analysis showed the model to be animprovement over the equilibrium adsorption model, Ref. 53. it was not evaluated with experimental data.

Initial attempts to evaluate the model using the convolution procedure showed calculations to be unstable for various values of the parameters Pe, N_{tOG}, and mR_0. The numerical calculations for this model have been reprogrammed using different numerical techniques, and previous computational problems appear solved.

TABLE V

COLUMN CHARACTERISTICS

Designation	Chromosorb 102	Molecular Sieve 5A	Carbowax 1500/ Chromosorb P
Composition	Microporous styrene divinyl - benzene polymers	Synthetic zeolite	Polyethylene glycol (20% by weight) on diatomaceous earth
Temperature range	to 250°C	to 325°C	to 225°C
Application	Separation of low molecular weight highly polar substances	Separation of light gases	Separation of high boiling, polar compounds

Length - 100 cm; inside diameter - 0.22 cm; particle size - 0.025/0.018 cm

The new program is being used in two ways:

1. With the aid of the general data reduction program, Ref. 32, this second order model is being evaluated with experimental data. This study will determine whether or not use of this more complicated model to represent system performance is warranted.

2. The moment analysis as outlined by Voytus, Ref. 54, and Taylor, Ref. 53, is being verified. It is believed that these results may be further used to improve the efficiency of generating system information.

The results of this evaluation are still preliminary, but they do indicate the more complicated model yields a better predicition of the output chromatogram. A technical report summarizing this evaluation should be available in March 1972.

As this more complicated model may not predict the shape of the output chromatograph especially in the case of porous particles, the mechanism of intraparticle diffusion, which was previously neglected, will be considered. This mass transport mechanism accounts for the capacitance and flow resitance of the column particles for the adsorbing components. Consideration of this diffusion further complicates the mathematical models, and a workable, analytical solution may not be obtained. If this is the case, direct numerical techniques will be employed. The resulting mathematical model will subsequently be evaluated with the experimental data to establish the importance of this mechanism. Preliminary results are expected by May 1972, but a final evaluation will probably not be available before December 1972.

Task D.4. Transport Parameter Estimation - P. K. Lashmet

Mathematical representation of the chromatograph requires a priori estimates of the transport parameters Pe and N_{tOG} as well as other properties which depend upon the complexity of the mathematical model. This task has as its objective the development of suitably accurate methods for estimating the above two parameters.

The Peclet number, which is a dimensionless measure of diffusion of the sample in the direction of carrier gas flow, is defined as

$$Pe = v\ L/D$$

where

v = mean length of the carrier gas

L = length of chromatographic column

D = effective diffusion or dispersion coefficient

This Peclet number is a function of the fluid mechanics of the system as well as the physical properties of the chemical sample and carrier

gas. As a first approximation, the dimensionless Reynolds number Re and Schmidt number Sc represent these effects:

$$Re = d\ v\rho\ /\mu$$

$$Sc = \mu / \rho\ D_M$$

where

d = diameter of particle

ρ = carrier gas density

μ = carrier gas viscosity

D_M = molecular diffusivity of sample in carrier gas

Prior attempts to compute the Peclet number from theoretical considerations and other measured transport properties of the system were not completely successful, Ref. 57. In the meantime, numerous sets of experimental Peclet number data, both published and unpublished, have been obtained. Also a correlation based on two additional sets of data, Ref. 58, appears adequate for the present studies. Further work on this subject will include an evaluation of the correlation using other available data and an estimate of the uncertainty in predicting the Peclet number.

Prediction of the number of transfer units N_{tOG} was discussed earlier, Ref. 31. A correlation possibly providing less uncertainty in the prediction, Ref. 59, is being evaluated. Preliminary results suggest little problems in adequately predicting N_{tOG} for this project.

These prediction techniques are being computerized to reduce the data reduction effort. Both prediction methods require values of the Schmidt number Sc, and a separate estimating procedure based on the theoretical work of Bird, Hirschfelder and Curtiss, Ref. 60, and using measured physical properties has been developed and is operational.

The work on this task will be completed in the near future and a technical report detailing the activity should be available by June 1972.

In overall summary, the major effort in predicting behavior appears to have reached its peak and the resulting mathematical models should be available for system studies in the near future. The task has initiated studies on other components of the analytical system, and in the future, the behavior of the overall system will receive more emphasis.

REFERENCES

1. Rayfield, W.P., "Design and Analysis of an Unmanned Martian Roving Vehicle," Doctoral Dissertation, Rensselaer Polytechnic Institute, Troy, New York. Expected date of publication May 1972.

2. Rodamaker, M.C., "Design and Analysis of a Local Vertical Sensor for Use in an Unmanned Martian Roving Vehicle," Master's Project Report, Rensselaer Polytechnic Institute, Troy, N.Y., June 1971.

3. "SPACE Program Summary," Volume III, Summary 35-55, JPL, Pasadena, California.

4. Simon, R.L., "Design of a Toroidal Wheel for a Martian Roving Vehicle," Technical Report MP-21, Rensselaer Polytechnic Institute, Troy, N.Y., June 1971.

5. Pavarini, Baker and Goldberg, "An Optimal Systems Design Process for a Mars Roving Vehicle," RPI Technical Report MP-24, Rensselaer Polytechnic Institute, November 1971.

6. Fiacco, Anthony V. and McCormick, Garth P., "Programming Under Nonlinear Constraints by Unconstrained Minimization: A Primal-Dual Method," The Research Analysis Corporation, RAC-TP-96, Bethesda, Md., Sept. 1963.

7. Fiacco, Anthony V. and McCormick, Garth P., "The Sequential Unconstrained Minimization Technique for Nonlinear Programming, A Primal-Dual Method," Management Science, 10(2): 360-366 (1964).

8. Fiacco, Anthony V., and McCormick, Garth P., Nonlinear Programming: Sequential Unconstrained Minimization Techniques, New York: Wiley, 1968.

9. Frederick, D.K. et al, "Analysis and Design of a Capsule Landing System and Surface Vehicle Control System for Mars Exploration," A Progress Report for July 1, 1970 to June 30, 1971, RPI Technical Report MP-23, Rensselaer Polytechnic Institute, Troy, N.Y., July 1971.

10. Janosko, R.E. and Shen, C.N., "A Simplified Satellite Navigation System for an Autonomous Mars Roving Vehicle," Rensselaer Polytechnic Institute, Troy, New York.

11. Watkins, M.C., "Laser Tracking/Ranging Measuring System," Proceedings SPIE Laser Range Instrumentation Seminar, El Paso, Texas, October 1967.

12. Quelle, F.W., "Alternatives to Q-spoiled Ruby Range Finders," Proceedings SPIE Laser Range Instrumentation Seminar, El Paso, Texas, October 1967.

13. Battin, Richard H., Astronautical Guidance, McGraw-Hill Book Co., New York, N.Y., 1969.

14. Polson, R.H., Blackshear, W.T. and Anderson, S.G., "Orbit and Position Determination for Mars Orbiters and Landers," AIAA Paper No. 70-160, 1970.

15. Michaux, C.M., "Handbook of the Physical Properties of Mars, NASA SP-3030, 1967.

16. Carpentier, M.H., Radars: New Concepts, Gordon and Breach Science Publishers, 1968.

17. Quelle, F.W., Jr., "Alternatives to Q-Spoiled Ruby Rangefinders," Proceedings SPIE Laser Range Instrumentation Seminar, El Paso, Texas, October 1967.

18. Ditchburn, R.W., Light, Interscience Publishers Inc., New York, 1953.

19. Ross, Monte, Laser Applications, Academic Press, New York, 1971.

20. Summary Technical Report of the National Defense Research Committee, Basic Methods for the Calibration of Sonar Equipment, Washington, D.C., 1946.

21. "Radar," Encyclopedia Brittanica (1968), Vol. 18, p. 994, 1005, 1006.

22. Whitaker, Stephen, Introduction to Fluid Mechanics, Prentice-Hall, Inc. Englewood Cliffs, New Jersey, 1968, pp. 402, 404.

23. Stone, Irving, "Atmosphere Data to Alter Voyager Design," Aviation Week and Space Technology, Vol. 83, Nov. 22, 1965, p. 69.

24. Horton, J.W., Fundamentals of Sonar, United States Naval Institute, Annapolis, Maryland, 1957, p. 20, 326.

25. Halliday and Resnick, Physics, Wiley and Sons, Inc., New York, 1962, p. 993.

26. Moore, J. and Burke, J., "An Exploratory Investigation of a 1979 Mars Roving Vehicle Mission," JPL Document No. 760-58, Dec. 1, 1970.

27. Parker, G., "Techniques for Autonomously Pointing an Antenna at Earth from Mars," Journal of Spacecrafts and Rockets, Sept. 1969.

28. Pavarini, C. and Chrysler, J.H., "Terrain Modeling and Path Selection by an Autonomous Martian Exploration Vehicle," RPI Technical Report MP-14, Rensselaer Polytechnic Institute, Troy, N.Y., June 1970.

29. Rautio, A., "An Analysis of the Effect of Sensor Errors on a Long-Range Terrain Modeling System and a Study of Short-Range Terrain Modeling for an Autonomous Roving Vehicle," RPI Master's Project Report, Rensselaer Polytechnic Institute, Troy, N.Y., June 1971.

30. Kirk, D. and Lim, L., "A Pathfinding Algorithm for an Autonomous Roving Vehicle," NASA Contract No. NAS7-100, 1970.

31. Sliva, T.F., "Chromatographic Systems Analysis: First-Order Model Evaluation," RPI Technical Report MP-1, Rensselaer Polytechnic Institute, Troy, New York, September 1968.

32. Benoit, G.L., "Reduction of Chromatographic Data and Evaluation of a GC Model," RPI Technical Report MP-22, Rensselaer Polytechnic Institute, Troy, New York, June 1971.

33. Bentley, K.E., Giffen, C.E., Whitten, D.G., and Wilhite, W.F., "Detection of Life-Related Compounds on Planetary Surfaces by Gas Chromatography - Mass Spectrometry Techniques," Tech. Rept. 32-713, Jet Propulsion Lab., Pasadena, California, August 1965.

34. "Gas Chromatograph/Mass Spectrometer," JPL Space Programs Summary 37-61, v. I, pp. 22-28, Jet Propulsion Lab., Pasadena, California, January 31, 1970.

35. Viking Management, "1973 Viking Voyage to Mars," Astronaut. Aeronaut. 7 (11), 30-59 (Nov. 1969).

36. Engineering Model GC/MS Design Review: Mass Spectrometer Subsystem, pp. 12-65, Jet Propulsion Lab., Pasadena, California, January 27, 1971.

37. Moore, J.W., "Computer System Requirements for an Autonomous Martian Roving Vehicle," Paper 69-980, Am. Inst. Aeronaut. Astronaut., New York, 1969.

38. Hanson, W.B., "OGO-F-06 Ion Mass Spectrometer. Final Report, March 1966 - June 1970," Report NASA-CR-111146, Natl. Aeronaut. Space Admin., Washington, D.C., Aug. 1970.

39. Johnson, F.S., "High-Sensitivity Miniaturized Magnetic Sector Mass Spectrometer for the ALSEP Program. Final Report," Report NASA-CR-114774, Natl. Aeronaut. Space Admin., Washington, D. C., June 1970.

40. McMurray, W.J., Greene, B.N., and Lipsky, S.R., "Fast Scan High Resolution Mass Spectrometer. I. Operating Parameters and Its Tandem Use with Gas Chromatography," Anal. Chem., 38, 1194-1204 (1966).

41. McDowell, C.A., "Mass Spectrometry," pp. 201-271, McGraw-Hill, New York 1963.

42. Gill, J.M. and Hartmann, C.H., "Characteristics of Ion Detectors and Gas Chromatography Electrometers," J. Gas. Chromatog., 5, 605-611 (1967).

43. McCoy, R.D., Porter, G.T., and Ayers, B.O., "Data Presentation from a Mass Spectrometer/Chromatograph System," Amer. Lab., 3 (9), 17-25 (Sept. 1971).

44. Noonan, D.J., and March, E.W., "Performance Characteristics of a New GC Data System," Amer. Lab., 3 (6), 55-61, (June 1971).

45. Engineering Model GC/MS Design Review: Gas Chromatograph Subsystem, pp. 6-1 to 6-29, Jet Propulsion Lab., Pasadena, Cal., Jan. 28, 1971.

46. "Dynamic Response of a Gas Chromatograph-Mass Spectrometer Combination," JPL Space Programs Summary 37-62, v. I, pp. 28-33, Jet Propulsion Lab., Pasadena, Cal., March 31, 1970.

47. McFadden, W.H., "Introduction of Gas-Chromatographic Samples to a Mass Spectrometer," Separ. Sci., 1, 723-746 (1966).

48. Wise, E.M., "Palladium Recovery, Properties and Uses," pp. 149-156, Academic Press, New York, 1968.

49. Lovelock, J.E., Charlton, K.W., and Simmonds, P.G., "The Palladium Transmodulator: A New Component for the Gas Chromatograph," Anal. Chem., 41, 1048-1952 (1969).

50. Lucero, D.P. and Haley, F.C., "Sample Enrichment Techniques for a Gas Chromatograph/Mass Spectrometer Analysis System," J. Gas Chromatog., 6, 477-482 (1968).

51. Lovelock, J.E., Simmonds, P.G., and Shoemake, G.R., "The Palladium Generator-Separator: A Combined Electrolytic Source and Sink for Hydrogen in Closed Circuit Gas Chromatography," Anal. Chem., 42, 969-973 (1970).

52. Lewis, F.A., "The Palladium Hydrogen System," pp. 47-49, Academic Press, New York, 1967.

53. Taylor, P.N., "Chromatographic Systems Analysis: Second-Order Model Development," M. Eng. Report, Rensselaer Polytechnic Institute, Troy, New York, June 1970.

54. Voytus, W.A., "Chromatographic Systems Analysis: Moment Analysis of the Equilibrium Adsorption Model," RPI Technical Report MP-9, Rensselaer Polytechnic Institute, Troy, New York, Aug. 1969.

55. Baer, S.R., and Benoit, G.L., "Chromatographic Test Facility," RPI Technical Report MP-19, Rensselaer Polytechnic Institute, Troy, New York, March 1971.

56. Lapidus, L., and Amundson, N.R., "Mathematics of Adsorption in Beds, VI. The Effect of Longitudinal Diffusion in Ion Exchange and Chromatographic Columns," J. Phys. Chem., 56, 984-988 (1952).

57. Reichman, D.A., "Chromatographic Systems Analysis: Dispersion Parameter Evaluation," M. Eng. Report, Rensselaer Polytechnic Institute, Troy, New York, September 1969.

58. Gunn, D.J., "Theory of Axial and Radial Dispersion in Packed Beds," Trans. Inst. Chem. Eng., 47, T351-T359 (1969).

59. Wakao, Noriski, Oshima, Takashi, and Yagi, Sakae, "Mass Transfer from Packed Beds of Particles to a Fluid," Kagaku Kogaku, 22, 780-785 (1958).

60. Bird, R.B., Hirschfelder, J.O., and Curtiss, C.F., "Theoretical Calculations of the Equation of State and Transport Properties of Gases and Liquids," Trans. ASME, 76, 1011-1038 (1954).